STRUCTURE - FUNCTION INTERRELATIONSHIPS OF TRYPTOPHAN SYNTHASE

Stanley *GOLDSTEIN*

A thesis submitted to the
Faculty of Science, University
of the Witwatersrand, in ful-
filment of the requirements for
the degree of Doctor of Philosophy.

Johannesburg, 1985

I declare that this thesis is my own, unaided work. It is being submitted for the degree of Doctor of Philosophy in the University of the Witwatersrand, Johannesburg. It has not been submitted before for any degree or examination in any other University

S. Goldstein

June 1986

ABSTRACT

The assembly mechanism of the apo-tryptophan synthase complex of *E. coli* was investigated in the presence of rhodamine-isothiocyanate (RITC) and anilino-naphthalene-sulphonate (ANS) fluorescence dyes, as well as bromo-phenol-blue (BPB) absorbance dye, using a stopped-flow apparatus. Full enzyme activity of the tryptophan synthase complex is achieved in two steps involving the binding of α-subunit and pyrodoxal-5'-phosphate (PLP) ligands to the $apo\beta_2$-dimer to form the $\alpha_2\beta_2(PLP)_2$-complex. The first step of activation, which is the formation of $\alpha_2 apo\beta_2$-complex, is investigated here.

Equilibrium dialysis measurements were used to obtain the thermodynamic binding parameters for the $\alpha_2 apo\beta_2$-complex. In sodium-pyrophosphate buffer pH 7.5 two α-subunits bind cooperatively to $apo\beta_2$-dimer but in potassium-phosphate buffer pH 7.5 the binding is either non-cooperative or negatively cooperative.

The intrinsic protein absorbance and fluorescence changes resulting from assembly of subunits into the $\alpha_2 apo\beta_2$-complex are small. Larger signal changes are obtained by performing the subunit assembly in the presence of BPB absorbance and ANS and RITC fluorescence dyes. In low concentrations these dyes were found not to affect the rate or extent of assembly to any significant degree.

Fluorescence titrations of ANS and absorbance titrations of BPB show that these dyes bind reversibly to the α-subunit, the $apo\beta_2$-subunit and the $\alpha_2 apo\beta_2$-complex. Large fluorescence or absorbance changes are obtained when excess α-subunit is mixed with $apo\beta_2$-subunit

in the presence of ANS or BPB. The signal changes observed were used to monitor the course of $\alpha_2 apo\beta_2$-complex assembly. However, when excess $apo\beta_2$-subunit was mixed with α-subunit the fluorescence of the RITC dye, covalently bound to α-subunit, was monitored.

Using a stopped-flow apparatus, excess $apo\beta_2$-subunit was rapidly mixed with α-subunit and the fluorescence of the RITC dye was monitored. Addition of α-subunit was shown to proceed in two steps: an initial αβ-protomer is formed which subsequently isomerises to the equilibrium state.

Mixing excess α-subunit with $apo\beta_2$-subunit, in the presence of ANS or BPB dyes, produced more complex signal changes. Here addition of α-subunit proceeds in three steps; addition of two α-subunits to form the $\alpha_1\beta_2^*$ and $\alpha_2\beta_2$ intermediates with subsequent isomerisation to the equilibrium state.

Since both the partially saturated $\alpha\beta_2$-complex and the saturated $\alpha_2\beta_2$-complex undergo similar isomerisation reactions, the two αβ-protomers within the $\alpha_2\beta_2$-complex behave independently.

ACKNOWLEDGEMENTS

I wish to thank Dr J S Davis for providing the facilities for this work and for his supervision and discussions relating to this research project.

I am also grateful to Mrs V Phillips for her encouragement and technical skill which was always at my disposal.

I would like to thank Mrs G E MacLachlan for typing this thesis.

TABLE OF CONTENTS

CONTENTS (continued)

CONTENTS (Continued)

1. INTRODUCTION

1.1 Structure of *E. coli* Tryptophan Synthase

Tryptophan synthase [L-serine hydro-lyase (adding indoleglycerol-phosphate) EC 4.2.1.20] is a multimeric enzyme catalyzing the terminal reaction in the biosynthesis of tryptophan (reaction 3 in Table 1). The presence of tryptophan synthase in bacteria and yeasts has been reviewed by Crawford (1975). Tryptophan synthase from *E. coli* consists of two α-subunits and one β_2-dimer which combine to form the tetrameric $\alpha_2\beta_2$-complex. Yanofsky & Crawford (1972) have reviewed the structure and reactive properties of the native enzyme and Miles (1979) has reviewed the structure, function and subunit interactions of the tryptophan synthase-complex.

The α-subunit has a molecular weight of 28 727 with 268 amino acid residues of known sequence but lacks any tryptophan residues (Yanofsky *et al.*, 1981). The α-subunit is normally monomeric and does not form dimers or higher order multimers (Jackson & Yanofsky, 1969).

The cofactor, pyridoxal-5'-phosphate (PLP) which is essential for reactions 2 and 3 (see Table 1), is bound through a Schiff base linkage to an ε-amino group of a lysine residue within the active site of the β_2-dimer (Fluri *et al.*, 1971). The β_2-dimer has a molecular weight of 85 976 with 397 residues of known sequence (Yanofsky *et al.*, 1981). Each β-chain has two tryptophan residues which accounts for the higher absorption at 280 nm than that of the α-subunit. Although the β_2-subunit exhibits dissociation into monomers, it exists predominantly as a dimer in both the holo (+PLP) and apo(-PLP) forms (Hathaway, 1972).

TABLE 1

Reactions catalysed by tryptophan synthase

and its subunits

TABLE 1

Reaction		Catalysed by
1.	indole-3-glycerol-phosphate ⟶ indole + D-glyceraldehyde-3-phosphate	α , $\alpha_2\beta_2$
2.	indole + L-serine $\xrightarrow{PLP}$ L-tryptophan + H_2O	β_2, $\alpha_2\beta_2$
3.	indole-3-glycerol-phosphate + L-serine $\xrightarrow{PLP}$ L-tryptophan + D-glyceraldehyde-3-phosphate + H_2O	$\alpha_2\beta_2$

Tryptophan synthase displays mutual activation of subunits whereby the individual α-subunit and β_2-subunit activities are markedly enhanced by the binding of the second subunit (see reactions 1 and 2 in Table 1). This phenomenon has prompted many workers to study the conformational states and functional roles of the separate and complexed subunits in order to understand this mutual activation process.

1.2 Properties of Tryptophan Synthase and its Subunits

1.2.1 The α-subunit

The α-subunit which normally exists as a monomer, may be induced to form dimers that -complex with and stimulate the β_2-subunit to full activity. This dimerisation is achieved at high α-subunit concentrations in the presence of urea and is not physiologically important (Jackson & Yanofsky, 1969). The partial reaction catalysed by the α-subunit (see reaction 1 in Table 1) proceeds a hundred times faster when the α-subunit is in the $\alpha_2\beta_2$-complex (Yanofsky & Crawford, 1972). The mechanism of the reverse of this reaction (indole+D-glyceraldehyde-3-phosphate + indole-3-glycerolphosphate) is *similar whether catalysed by the α-subunit alone or by the* $\alpha_2\beta_2$-complex (Weischet & Kirschner, 1976a,b). However, the affinities for certain ligands are altered when the α-subunit is in the $\alpha_2\beta_2$-complex.

Ligand Binding Properties of the α-subunit

The α-subunit binds 1 mole of indole at its active site (K_d = 18 mM) and 1 mole at a second site (K_d = 1.5 mM), whereas the $\alpha_2\beta_2$-complex binds indole weakly to as many as 40 sites (K_d = 30 mM) and strongly to 1 or 2 sites (K_d = 1.2 mM) (Weischet & Kirschner, 1976b). Indole-3-propanol-phosphate has been found to be a competitive inhibitor of indole-3-glycerol-phosphate and binds to the α-subunit with a lower affinity than to the $\alpha_2\beta_2$-complex (Kirschner *et al.*, 1975). These altered binding properties, together with temperature-jump studies of indole-3-propanol-phosphate binding to the α-subunit, indicate that the α-subunit must exist in at least three distinct conformations (Kirschner & Wiskocil, 1972).

Further indirect support for this hypothesis derives from the reactivity of N-ethyl-maleimide with the α-subunit. Protection against reaction is effected by indole-3-propanol-phosphate binding (Hardman & Yanofsky, 1965) while sensitisation is effected by indole binding (Freedberg & Hardman, 1971). These effects are probably achieved by stabilisation of different conformations of the α-subunit by the respective ligands (Kirschner & Wiskocil, 1972).

Unfolding of the α-subunit

The binding of the holoβ_2-subunit to the α-subunit protects the α-chain from extensive degradation by trypsin, yielding instead, an active nicked α-subunit derivative. The protection of cleavage sites may be due to either the masking of the α-subunit by the

β_2-subunit or the conformational transitions in the α-protein subsequent to holoβ_2-subunit binding (Miles & Higgins, 1978). The nicked α-subunit derivative can be dissociated into two fragments (α-1 and α-2) by treatment with urea. Upon removal of the urea those two fragments refold into the active α-subunit derivative and are therefore thought to represent separate folding domains of the α-subunit (Higgins *et al.*, 1979).

The intact α-subunit may be unfolded by high concentrations of urea or guanidine-hydrochloride. The urea induced unfolding proceeds through two intermediates (denoted by I_1 and I_2) to two unfolded forms (denoted by U_1 and U_2) with the intermediates inter-converting via the cis-trans isomerisation of a proline residue (Matthews & Crisanti, 1981).

The guanidine-hydrochloride induced unfolding of the intact α-subunit involves an intermediate with only one of the separately folding domains of the α-chain in an unfolded form as shown below.

Native form	→	Intermediate	→	unfolded form
α-1, α-2 intact		α-1 intact α-2 unfolded		α-1, α-2 unfolded

These separately folding domains of the intact α-subunit correspond to the α-1 and α-2 folding domains of the nicked α-subunit (Yutani *et al.*,1980; Miles *et al.*, 1982). Lane & Kirschner (1983c) used the existence of these two autonomously folding domains to pictorially represent the α-subunit as consisting of two globular unequal sized spheres.

1.2.2 The β_2-subunit

The physiological reaction catalysed by the holoβ_2-subunit (see reaction 2 in Table 1) proceeds fifty times faster when complexed with the α-subunit. In addition several non-physiological reactions which are catalysed by the holoβ_2-subunit are inhibited by the addition of the α-subunit (Yanofsky & Crawford, 1972).

The two molecules of PLP are bound through a Schiff base linkage to the ε-amino group of lysine which may be reduced to a single covalent bond with sodium-borohydride (Wilson & Crawford, 1965). Removal of bound PLP requires lengthy dialysis against tris-HCl buffer, brief dialysis against β-mercapto-ethanol and L-serine or brief treatment with hydroxylamine (Miles, 1979). Conversion of the holoβ_2-subunit to the apoβ_2-subunit decreases the solubility of the protein in ammonium sulphate solutions (Adachi & Miles, 1974) but without loss of the antigenic determinants of the β_2-subunit (Zalkin *et al.*, 1980) Therefore the tertiary structures of the holoβ_2-subunit and apoβ_2-subunit appear to be similar.

Removal of the bound PLP from the $\alpha_2$holoβ_2-complex cannot be achieved by either of the three methods above. Treatment with hydroxylamine, for example leads to a pyridoxal-phosphate oxime, which is tightly bound to the $\alpha_2\beta_2$-complex, requiring treatment with 1M-KSCN for removal (Miles & Moriguchi, 1977).

Ligand binding to the β_2-subunit

Studies of ligand binding to the β_2-subunit alone and to the $\alpha_2$holoβ_2-

complex have been used to contrast the different conformations accessible to the β_2-subunit.

The Binding of L-serine to the β_2-subunit

Temperature-jump studies of the absorbance changes occurring during the binding of L-serine to the holoβ_2-subunit have been performed by Faeder & Hammes (1970). The binding mechanism proposed by the authors is given in Equation 1.

$$\begin{array}{ccc} E + \text{serine} & \rightleftharpoons & E\text{-serine} \\ \rightleftharpoons & & \rightleftharpoons \\ E' + \text{serine} & \rightleftharpoons & E'\text{-serine} \end{array} \rightleftharpoons E''\text{-serine} \qquad (1)$$

where E, E', E" represent three different holoβ_2-subunit isomers.

In the presence of α-subunit, one conformation of the holoβ_2-subunit is destabilised and the E' conformation is no longer populated. *This suggests that a pre-equilibrium between the two states of the* holoβ_2-subunit (E and E') is shifted towards one state (E) upon forming the $\alpha_2$holoβ_2-complex. The mechanism for L-serine binding is then modified as shown below.

$$\alpha_2\text{holo}\beta_2 + \text{serine} \rightleftharpoons \alpha_2\text{holo}\beta_2 \sim \text{serine} \rightleftharpoons \alpha_2\text{holo}\beta_2''\text{-serine}$$

complex have been used to contrast the different conformations accessible to the β_2-subunit.

The Binding of L-serine to the β_2-subunit

Temperature-jump studies of the absorbance changes occurring during the binding of L-serine to the holoβ_2-subunit have been performed by Faeder & Hammes (1970). The binding mechanism proposed by the authors is given in Equation 1.

$$\begin{array}{ccc} E + \text{serine} & \rightleftharpoons & E\text{-serine} \\ \uparrow\downarrow & & \uparrow\downarrow \\ E' + \text{serine} & \rightleftharpoons & E'\text{-serine} \end{array} \rightleftharpoons E''\text{-serine} \qquad (1)$$

where E, E', E" represent three different holoβ_2-subunit isomers.

In the presence of α-subunit, one conformation of the holoβ_2-subunit is destabilised and the E' conformation is no longer populated. This suggests that a *pre-equilibrium* between the two states of the holoβ_2-subunit (E and E') is shifted towards one state (E) upon forming the $\alpha_2$holoβ_2-complex. The mechanism for L-serine binding is then modified as shown below.

$$\alpha_2\text{holo}\beta_2 + \text{serine} \rightleftharpoons \alpha_2\text{holo}\beta_2 \sim \text{serine} \rightleftharpoons \alpha_2\text{holo}\beta_2''\text{-serine}$$

Lane & Kirschner (1981, 1983a,b) monitored the fluorescence changes during the binding of L-serine to the holoβ_2-subunit and the $\alpha_2$holoβ_2-complex and the subsequent reaction with indole to form L-tryptophan.

The mechanism of the reaction catalysed by the holoβ_2-subunit is shown in Equation 2 and the mechanism of the reaction catalysed by the $\alpha_2$holoβ_2-complex is shown in Equation 3.

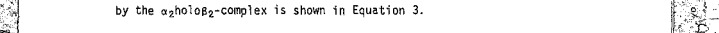

Equation 2

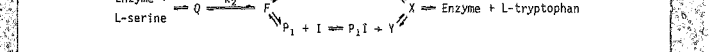

Equation 3

(where I represents indole and A_1, A_2, F, P, PI, Y, Q, W, Y and X all represent intermediates in the overall mechanism.
The intermediate A_2 (in Equation 2) probably corresponds to the intermediate Q (in Equation 3). The values k_2 and k_2 refer to the forward rate constants for the reactions shown).

The conversion of A_2 to F by the holoβ_2-subunit (see Equation 2) is rate limiting and probably represents a deprotonation step which requires a basic group (B:) as a catalyst as shown below.

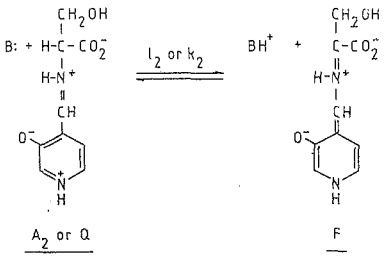

This deprotonation step ℓ_2 for holoβ_2-subunit, has a rate constant of approximately 0.6 s^{-1} and is five hundred fold slower than k_2 for $\alpha_2$holoβ_2-complex which has a rate constant of 300 s^{-1}. Thus the major effect of the α-subunit on the activity of the holoβ_2-subunit is to accelerate this proton abstraction step.

The Binding of PLP and Analogues to the apoβ_2-subunit

Pyridoxine-5'-phosphate (PNP) and N-phosphopyridoxyl-L-serine (PPS) are analogues of PLP which do not form aldimines with lysine side chains but do bind to the apoβ_2-subunit at the PLP binding site.

The $\alpha_2$apoβ_2-complex binds PNP, PPS and PLP non-cooperatively to two sites of equal affinity (Bartholmes *et al.*, 1976; Tschopp & Kirschner, 1980a). Both PNP and PPS bind to the $\alpha_2$apoβ_2-complex in a single rapid step consistent with Equation 4.

$$E + L \rightleftharpoons EL \qquad (4)$$

where E represents free enzyme binding sites and L represents free ligand.

In contrast, PNP and PPS bind cooperatively to two identical sites on the apoβ_2-subunit. The kinetics of binding is characterised by two distinct steps consistent with Mechanism 5 (Tschopp & Kirschner, 1980b).

$$E + L \rightleftharpoons (EL) \rightleftharpoons EL^* \rightleftharpoons EL^{**} \qquad (5)$$

where E represents the ß-protomer, (EL) and EL* are enzyme-ligand complexes and EL** is an isomer of EL*.

The binding of PNS, PPS and PLP to the apoβ_2-subunit is consistent with the model of Monod, Wyman and Changeux as shown in Equation 6 (Tschopp & Kirschner, 1980b).

$$\begin{array}{ccc} 2L + T_o & \rightleftharpoons & 2L + R_o \\ \uparrow\downarrow & & \uparrow\downarrow \\ L + T_1 & \rightleftharpoons & L + R_1 \\ \uparrow\downarrow & & \uparrow\downarrow \\ T_2 & \rightleftharpoons & R_2 \end{array} \qquad (6)$$

here L represents free ligand and T and R represent low affinity and high affinity states of the apoβ_2-subunit for the ligand, respectively.

In the absence of ligand the [To]/[Ro] ratio is approximately 200 but on addition of excess ligand, T_z is formed before any appreciable conformational transition of T to R forms can occur. The T_2 form then isomerises to the R_2 form of the enzyme-ligand complex.

Comparison of Equations 4 and 5 shows that the binding of the α-subunit to the apoβ$_2$-subunit eliminates protein conformational transitions when the ligand is PNP or PPS. Thus the α-subunit appears to stabilise a high affinity state of the cofactor binding site similar to, but not identical to, the R form of the holoβ$_2$-subunit.

The binding of PLP to the apoβ$_2$-subunit and the $\alpha_2$apoβ$_2$-complex, both leading to an internal aldimine with a lysine group, is characterised by two distinct steps (see (a) and (b) in Equation 7) consistent with Mechanism 7 (Bartholmes *et al.*, 1980).

$$E + L \rightleftharpoons (EL) \rightleftharpoons EL^* \rightleftharpoons EL^{**} \qquad (7)$$

(a) (b)

Reduction of the aldimine formed between the lysine ε-amino group and the PLP occurs at the same rate as the generation of EL* and explains the difference between the binding of PLP and the binding of PNP or PPS to the apoβ$_2$-subunit. Formation of active enzyme occurs at the same rate as the generation of EL**. Therefore part (b)of Equation 7 could represent a slow conformational change of the protein to yield active enzyme. Similar rates are obtained with the apoβ$_2$-subunit and the $\alpha_2$apoβ$_2$-complex, even though the activity of the resultant enzyme is very low in the former case.

This suggests that the same process is involved regardless of whether the PLP binding sites interact (apoβ_2-subunit) or are independent ($\alpha_2$apoβ_2-complex).

The model of Monod, Wyman and Changeux predicts that the half saturated β_2-subunit should exist in two forms (T_1, R_1). A hybrid apo$\beta\beta$*-dimer containing one functional protomer *and one reduced PLP moity*, has been prepared by partial reduction of the holoβ_2-subunit (Balk *et al.*, 1981a). Two distinct steps are apparent for the PLP binding to this hybrid apo$\beta\beta$*-*subunit. The faster process corresponds* to the R_1 to R_2 transition and accounts for 85% of the total amplitude of reaction (see Mechanism 6). The remaining 15% of the amplitude *of the reaction coresponds* to the T_1 to T_2 transition. Therefore the hybrid apo$\beta\beta$*-subunit may represent a half staturated apoβ_2-subunit and supports the proposed model of Monod, Wyman and Changeux.

The binding of PLP to the apoβ_2-subunit and the $\alpha_2$apoβ_2-complex does not vary the circular dichroism spectrum of the proteins in the far ultraviolet region. This indicates that the secondary structure in the active centre of the enzyme is conserved during cofactor binding (Balk *et al.*, 1981b).

However, the circular dichroism spectrum of the proteins in the near ultraviolet region is significantly altered *upon cofactor binding*. This alteration is due to a summation of the effects of aromatic side chains and the formation of the internal aldimine.

Two distinct steps are apparent when following the circular dichroism

increase at 415 nm upon mixing PLP and the $\alpha_2 apo\beta_2$-complex. The faster step corresponds to that shown by the fluorescence detection of the PLP binding to the $\alpha_2 apo\beta_2$-complex while the slower step is much slower than the formation of active enzyme as shown by Bartholmes *et al.* (1980). This circular dichroism spectral change is probably due to a slow orientation of the cofactor and enzyme when in its resting state (Balk *et al.*, 1981b).

Dissociation and Proteolysis of the β_2-subunit

The $apo\beta_2$-dimer can be dissociated into randomly coiled monomers by incubating with high concentrations of urea or guanidine-hydrochloride (*Groha et al.*, 1978). After removal of the denaturing agents, renaturation in the presence of PLP leads to 90% recovery of the enzymatic activity by the mechanism shown in Equation 8.

$$2M + 2M^* \rightleftharpoons D_2^* \rightarrow \text{active holo}\beta_2\text{-subunit.} \qquad (8)$$

where M represents monomer and D represents dimer.

The recovery of activity occurs in a rate determining unimolecular reaction corresponding to the conversion of D_2^* to $holo\beta_2$-subunit.

The $holo\beta_2$-subunit can be "nicked" by treatment with trypsin to produce a stable non-covalent complex of two non-overlapping fragments denoted by $(F_1F_2)_2$ (Högberg-Raibaud & Goldberg, 1977). The two fragments (molecular weight of F_1 is 29 000 and that of F_2 is 12 000)

may be dissociated and denatured in 6 M urea. Both fragments can refold independently to conformations which resemble the structure of the fragments in the nicked protein. The isolated F_1 and F_2 fragments therefore appear as intermediate structures in the folding of the β_2-subunit.

In contrast, tryptic proteolysis of the $\alpha_2$holoβ_2-complex yields an active "nicked" α'_2holoβ_2-protein with cleavage taking place in the α-chain (Miles & Higgins, 1978). Therefore the association of the α and β_2-subunits prevents (a) the cleavage of the β_2-subunit into two fragments with loss of activity and (b) the complete degradation of the α-subunit with the loss of α-subunit activity.

1.2.3 *The $\alpha_2\beta_2$-complex*

Crude extracts of, or purified $\alpha_2$holoβ_2-complex, in tris-HCℓ buffer sediment in sucrose density gradients as two peaks. The first peak detected by enzymatic activity assays, corresponds to β_2-subunit ($S_{20,w}$ = 5.1). Addition of PLP to the buffer promotes partial association of the subunits while addition of both PLP and L-serine results in *full association* ($S_{20,w}$ = *6.4*). *(Creighton & Yanofsky,* 1966).

The sedimentation as fully associated $\alpha_2$holoβ_2-complex depends on rotor speed and therefore on hydrostatic pressure. Increasing the rotor speed from 39 000 rpm to 50 000 rpm interferes with complex formation at 5°C, even in the presence of PLP and L-serine. This effect is reversed by *increasing the temperature from* 5°C to 20°C

or by low concentrations of a non-polar solvent. Therefore hydrophobic bonding plays an important role in forming the tryptophan synthase complex. Monovalent and divalent cations also interfere with subunit association, indicating the possibility that ionic bonds are also involved (Dicamelli *et al.*, 1973)

The α-β affinity has been measured with enzymatic activity assays (Creighton & Yanofsky, 1966), equilibrium dialysis (Bartholmes & Teuscher, 1979) and microcalorimetry (Wiesinger *et al.*, 1979).

The apparent dissociation constant for the α- and holoβ_2-subunits varies from 0.25 μM (measured with reaction 1 in Table 1) to 0.38 nM (measured with reaction 3 in Table 1). In the latter case, the higher degree of association is probably due to the presence of PLP and L-serine in the assay medium. Under these assay conditions, the two α-subunit binding sites of the holoβ_2-subunit behave independently since the αholoβ_2-complex has exactly half the activity of the $\alpha_2$holoβ_2-complex (Creighton & Yanofsky, 1966).

The binding affinity of the α-subunit and the apoβ_2-subunit to form a stable $\alpha_2$apoβ_2-complex has been measured by equilibrium dialysis and analytical ultracentrifugation in a pyrophosphate buffer (Bartholmes & Teuscher, 1979). The α-subunit binding is cooperative and weaker than the binding to the holoβ_2-subunit.

The overall assembly of the $\alpha_2$holoβ_2-complex is given in Equation 9.

$$(1) \qquad 2\alpha + 2PLP + \beta_2 \rightleftharpoons 2\alpha + \beta_2(PLP)_2 \qquad (2)$$

$$\Big\Vert \qquad\qquad\qquad \Big\Vert \qquad (9)$$

$$(3) \qquad \alpha_2\beta_2 + 2\ PLP \rightleftharpoons \alpha_2\beta_2(PLP)_2 \qquad (4)$$

Since reactions (1) to (2) and (1) to (3) are cooperative and reaction (3) to (4) is non-cooperative, the β_2-subunit must exist in at least three conformations; the apoβ_2-subunit conformation, the holoβ_2-subunit conformation and the conformation of the β_2-subunit in the $\alpha_2$apoβ_2-complex.

The measured values of the Hill coefficient and the total Gibbs free energy change (ΔG) are identical for the cooperative binding processes; α_2+apoβ_2 and PLP + apoβ_2 (Bartholmes *et al.*, 1976). This suggests that in the presence of either the α-subunit or PLP, the apoβ_2-subunit undergoes a similar concerted transition (Bartholmes & Teuscher, 1979).

Microcalorimetry confirms the results obtained from the equilibrium dialysis experiments and quantifies the number of protons taken up during the subunit association reaction as shown in Equation 10.

$$2\alpha + \beta_2 + nH^+ \rightleftharpoons \alpha_2\beta_2\,(H^+)_n \qquad (10)$$

with n = 0.75 at 25°C in the presence or absence of PLP

and n = 2 in the absence of PLP or n = 1 in the presence of PLP at 35°C.

The kinetics of the α-subunit binding to the holoβ_2-subunit may be followed at 288 nm and 405 nm as shown by difference spectra of bound versus unbound subunits (Kirschner *et al.*, 1975). Three exponential processes are observed after mixing α-subunit and holoβ_2-subunit in a stopped-flow instrument. The intermediate process rate constant rises towards a plateau value with increasing α-subunit concentrations. This suggests that the assembly reaction involves a binding step followed by an isomerisation step. It is this isomerisation which must occur before enzyme activity can be expressed.

A recent kinetic study, monitoring the fluorescence of the PLP coenzyme, shows that the α-subunit is bound with negative cooperativity to holoβ_2-subunit in phosphate buffer (Lane *et al.*, 1984). Addition of each α-subunit leads to formation of an initial αβ-protomer which isomerises to an equilibrium state. The data fit a sequential assembly mechanism consisting of seven protein species as shown below.

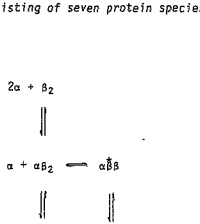

Negative cooperativity results from the weaker initial binding of a second α-subunit to the $\alpha\beta_2$-intermediate, possibly due to steric hinderance within the $\alpha_2\beta_2$-complex. The isomerisation reactions

are responsible for attaining full enzyme activity and involve synchronous conformational changes of both the α- and β-protomers.

Small angle X-ray scattering studies have predicted the molecular sizes and most probable shapes for the α-subunit, the holoβ_2-subunit and the $\alpha_2$holoβ_2-complex (Wilhelm *et al.*, 1983). A correlation with various intramolecular and intermolecular distances indicate the tertiary and quaternary structural changes occurring during $\alpha_2$holoβ_2-complex assembly (Lane & Kirschner, 1983c). The α-protomer and holoβ-protomer consist of two autonomously folding domains which associate to form an intermediate-complex closely resembling the summation of the individual α-subunits and the holoβ_2-subunits. An isomerisation, probably involving the rearrangement of the autonomously folding domains, then follows to give the final $\alpha_2$holoβ_2-complex.

Analysis of the structural domains of the equilibrium $\alpha_2$holoβ_2-complex has been achieved with neutron small angle scattering studies (Ibel *et al.*, 1985) and show that the holoβ_2-subunit changes to a more compact form in the $\alpha_2$holoβ_2-complex. However the α-subunits do not exhibit any detectable structural change. Measurements of the distances between the α-subunits in the $\alpha_2$holoβ_2-complex exclude the interpretation of steric hinderance to account for the observation of negative cooperativity (Lane *et al.*, 1984) during assembly of the tryptophan synthase complex.

1.3 Purification of Tryptophan Synthase and its Subunits

1.3.1 Purification of the α-subunit

The mutant *E. coli* strain BB produces high levels of a wild type α-subunit and only low levels of an altered β_2-subunit when grown under derepressing conditions. Henning *et al.* (1962) purified α-protein by a manganese-chloride and acid precipitation step followed by DEAE-cellulose chromatography. Crystallisation of the protein resulted in an overall yield of 24% and a specific activity of 4700 *units* mg^{-1} (*the definition* of units and assay methods are given in Section 2.3).

An improved and reproducible chromatographic method, using DEAE-cellulose, hydroxylapatite and Sephadex G-100, has been developed by Kirschner *et al.* (1975). Crystalline material of 5 500 units mg^{-1} was obtained in a 32% yield.

Recently strains of *E. coli* have been developed with deletions starting in the leader region of the tryptophan operon and terminating in a structural gene of the operon (Miles, 1979). The *E. coli* trp R^- Δ trpLD102/F'Δ trpLD102 strain produces wild type tryptophan synthase constitutively. Crystalline $\alpha_2\beta_2$-complex, with a specific activity of 1920 units mg^{-1} of complex, was obtained by Adachi *et al.* (1974) in a 60% yield.

An improved and reproducible method, developed by Tschopp & Kirschner (1980a), resulted in a 54% yield of $\alpha_2\beta_2$-complex with a specific activity of 2175 units mg^{-1} of complex. The resultant $\alpha_2\beta_2$-complex has been separated into individual subunits by treatment with hydroxylamine and potassium-isothiocyanate (Miles & Moriguchi, 1977)

or by treatment with acid (to destroy the β_2-subunit) or by heating (to destroy the α-subunit) (Tschopp & Kirschner, 1980a).

1.3.2 Purification of the β_2-subunit

The *E. coli* trpA2/F'trpA2 strain produces high levels of wild type β_2-subunit with very low levels of an inactive altered α-protein, when grown under derepressing conditions.

Wilson & Crawford (1965) purified β_2-subunit from this strain with a specific activity of 2700 units mg^{-1} and a 30% yield. The method involved two heat treatments which may lead to an unstable altered enzyme since other workers have reported a range of lower activities using this method : 1600 to 2000 units mg^{-1} (Faeder & Hammes, 1970) and 1500 units mg^{-1} (Miles, 1970). This led Adachi & Miles (1974) to develop a more efficient and less damaging method, based upon the different solubilities of the apoβ_2-subunits and holoβ_2-subunits in ammonium sulphate solutions. Crystals of the apoβ_2-subunit were obtained in an 84% yield with a specific activity of 3250 units mg^{-1}. Barthołmes *et al.* (1976) improved upon this method by using the differential solubilities of the apoβ_2-subunits and the holoβ_2-subunits in a partially purified preparation rather than a crude extract. A specific activity of 4100 units mg^{-1} and a yield of 45% was obtained for the material purified by this improved method.

As mentioned above, the β_2-subunit has also been obtained from purified tryptophan synthase after heat treatment.

1.4 Fluorescence Energy Transfer

Fluorescence energy transfer between protein bound donor and acceptor fluorescent dyes provides measurements of the distances between the dyes. The light absorbed by the donor may be transferred non-radiatively to the acceptor over distances of 1.5 to 7 nm. The efficiency of this energy transfer is related to (a) the distances between the dyes, (b) the necessary spectral overlap of the donor emission and acceptor absorption, (c) correct relative orientation of dye molecules and (d) suitable singlet fluorescence lifetimes.

Suitable pairs of dyes are given in a review by Fairclough & Cantor (1978).

Both the static and the dynamic properties of protein complexes have been studied with the fluorescence energy transfer technique. The dansyl-ligand has been used as donor with fluorescein or rhodamine B as acceptor to measure interprotein distances in complexes of trypsin and trypsin inhibitors (Gennis *et al.*, 1972). The rate of subunit exchange in actin polymers has been quantified in kinetic experiments with fluorescein as donor and eosin as acceptor (Wang & Taylor, 1981).

The fluorescein (donor) labelled tubulin and rhodamine (acceptor) labelled tubilin have been assembled into microtubules. As the assembly progressed, the intersubunit distances decreased causing the energy transfer efficiencies to increase. Thus a record of the extent of assembly was obtained (Becker *et al.*, 1975).

Specific loci within the active sites of the α-subunits and β_2-subunits of tryptophan synthase have been labelled with various dyes. The distances between these loci have been measured to estimate the distances between the loci within the $\alpha_2$holoβ_2-complex (Lane & Kirschner (1983c).

1.5 Non-Covalently Bound Fluorescent Probes

The fluorescence of the ANS molecule is dependent upon the environment in which the molecule is constrained. It has a low fluorescence in aqueous buffers but exhibits a blue shift in fluorescence maximum and a large increase in fluorescence yield when bound to non-polar sites on membranes or proteins. The interaction of ANS with proteins has been quantified by fluorescence titrations for bovine serum albumin (Daniel & Weber, 1966) apomyoglobin (Stryer, 1965) and the apoβ_2-subunit of tryptophan synthase (Seifert *et al.*, 1984).

Displacement of the bound ANS molecules by ligands that compete for the same ANS binding sites, causes a decrease in the fluorescence signals. Thus ANS may be used as a reporter group to monitor ligand binding reactions in which the intrinsic protein-ligand signals are too small for observation. Examples of this are, the thermodynamic study of the nucleotide binding of an aldolase protein (Kasprzak & Kochman, 1981) and the cofactor binding and conformational transitions of glutamate dehydrogenase (Dodd & Radda, 1969).

1.6 Summary

Both the α- and β_2-subunits of tryptophan synthase have been shown to be flexible proteins exhibiting mutual stabilisation of conformations by assembly into the $\alpha_2\beta_2$-complex. This assembly may occur with PLP binding to the apoβ_2-subunit preceding the α-subunit binding or with the α-subunit binding preceding the PLP binding.

The holoβ_2-subunit is stabilised in a conformation that is similar to, but not identical with, the conformation stabilised in the $\alpha_2$apoβ_2-complex (Tschopp & Kirschner, 1980b). Therefore the conformational transitions from the apoβ_2-state to the holoβ_2-state must be similar to those initiated by α-subunit binding to the apoβ_2-subunit.

Direct observation of these conformational transitions would indicate (a) the mechanism whereby both PLP and α-subunit stabilise the same conformational state of the β_2-subunit although they must necessarily bind to different regions of the β_2-subunit and (b) whether both the α- and β_2-subunit exhibit conformational transitions upon forming the $\alpha_2$apoβ_2-complex.

The small amplitudes obtained from direct observation of the α-subunit and apoβ_2-subunit reactions, necessitated the development of techniques to monitor the protein assembly using signals derived from artificial probes present during protein assembly.

2. EXPERIMENTAL MATERIALS AND METHODS

2.1 Materials

2.1.1 Chemicals

All chemicals for the growing of bacterial strains were obtained from Saarchem, Johannesburg, South Africa. Ammonium sulphate for biochemical work and rhodamine B isothiocyanate were obtained from E. Merck AG, Darmstadt, Germany. Chromatographic materials were products of Pharmacia, Uppsala, Sweden. The fluorescein isothiocyanate, anilino-naphthalene-sulphonate and bromophenol-blue probes were obtained from the Sigma Chemical Company, St. Louis Missouri, *USA. All other chemicals were of the highest purity available from* E. Merck or British Drug Houses, Poole, Dorset, England.

2.1.2 Biological Materials

Mutant strains of *E.coli* K12 (trpB8 and trp A2/F'A2) were kindly donated by Dr I P Crawford (Scripps Clinic and Research Foundation, *La Jolla, California, USA) and served as sources of* α-subunits and β_2-subunits respectively.

Native $\alpha_2\beta_2$-complex was purified from the mutant strain *E.coli* w3110 trpR$^-$cysB$^-$$\Delta$trpLD102trpB$^+$trpA$^+$/F'colVBcysB$^+$ ΔtrpLD102trpB$^+$trpA$^+$ (abbreviated name : *E.coli* trp R$^-\Delta$trpLD102/F' ΔtrpLD102) which was a generous gift from Dr E W Miles (National Institutes of Health, Bethesda, *Maryland, USA).*

2. EXPERIMENTAL MATERIALS AND METHODS

2.1 Materials

2.1.1 Chemicals

All chemicals for the growing of bacterial strains were obtained from Saarchem, Johannesburg, South Africa. Ammonium sulphate for biochemical work and rhodamine B isothiocyanate were obtained from E. Merck AG, Darmstadt, Germany. Chromatographic materials were products of Pharmacia, Uppsala, Sweden. The fluorescein isothiocyanate, anilino-naphthalene-sulphonate and bromophenol-blue probes were obtained from the Sigma Chemical Company, St. Louis Missouri, *USA. All other chemicals were of the highest purity available from* E. Merck or British Drug Houses, Poole, Dorset, England.

2.1.2 Biological Materials

Mutant strains of *E.coli* K12 (trpB8 and trp A2/F'A2) were kindly donated by Dr I P Crawford (Scripps Clinic and Research Foundation, *La Jolla, California, USA) and served as sources of* α-subunits and β_2-subunits respectively.

Native $\alpha_2\beta_2$-complex was purified from the mutant strain *E.coli* w3110 trpR$^-$cysB$^-$$\Delta$trpLD102trpB$^+$trpA$^+$/F'colVBcysB$^+$ ΔtrpLD102trpB$^+$trpA$^+$ (abbreviated name : *E.coli* trp R$^-\Delta$trpLD102/F' ΔtrpLD102) which was a generous gift from Dr E W Miles (National Institutes of Health, Bethesda, *Maryland, USA*).

2.1.3 Buffers

The buffer hereafter referred to as the standard buffer contained the reagents listed below

0.2 mM	EDTA
0.2 mM	dithiothreitol
0.1 M	potassium-phosphate buffer pH 7.5

2.2 Protein Estimation

Concentrations of protein in crude extracts were determined by the method of Lowry *et al.* (1951) using bovine serum albumin as standard. Concentrations of purified subunits of tryptophan synthase were obtained from the specific absorbance values and molecular weights given in Table 2.

2.3 Enzyme Activity Assays

One unit of activity in the indole to tryptophan reaction (See Table 1) is defined as the disappearance of 0.1 μmole of indole in 20 minutes at 37°C. The β_2-subunit activity was measured in the presence of α-subunit at a concentration twenty times that of the β_2-subunit. The α-subunit activity was measured in the presence of β_2-subunit at a concentration twice that of the α-subunit.

The subunits were diluted with a buffer containing the reagents listed below (Adachi & Miles, 1974).

TABLE 2

Specific absorbance and molecular weights of tryptophan synthase subunits

References

(a) Adachi *et al.* (1974)

(b) Henning *et al.* (1962)

(c) Hathaway & Crawford (1970)

TABLE 2

Subunit	$A^{1\%}_{1\ cm}$	Molecular Weight
α	4.4 at 278 nm[a]	29 500[b]
apoβ_2	5.8 at 280 nm[c]	89 000[c]
holoβ_2	6.5 at 280 nm[c]	89 000[c]
holo$\alpha_2\beta_2$	6.05 at 278 nm[a]	147 000[c]

20	μM	pyridoxal phosphate
0.2	mM	dithiothreitol
5	mM	EDTA
0.5	mg/mℓ	bovine serum albumin
100	mM	potassium phosphate buffer pH 7.8

The reaction was initiated by adding a 0.05 mℓ aliquot of enzyme, containing both α-subunit and β_2-subunit at the required concentrations, to 0.2 mℓ of assay medium at 37°C. After 20 minutes a 3 mℓ aliquot of indole reagent (Miles, 1970) was added to the assay solution and the absorbance at 540 nm was measured after standing for 5 minutes. A standard curve of absorbance versus indole concentration was drawn by adding 3 mℓ of indole reagent to 0.25 mℓ of a solution containing indole at concentrations ranging from 0 to 0.4 mM. The enzyme activity was then calculated from the quantity of the indole consumed during the 20 minutes of reaction which was obtained from the standard curve. The assay medium contained the reagents listed below.

5	mM	EDTA
0.25	mM	dithiothreitol
0.375	mM	pyridoxal phosphate
0.5	mM	indole
50	mM	*L-serine*
0.625	mg/mℓ	bovine serum albumin
125	mM	Tris-HCℓ buffer pH 7.8 at 37°C.

2.4 Bacterial Growth Procedures

The minimal medium used for bacterial growth was sterilized by autoclaving at 121°C for 15 minutes and contained the reagents listed below.

0.8	mM	$MgSO_4$
10	mM	citric acid
60	mM	K_2HPO_4
17	mM	$NaNH_4HPO_4$

2.4.1 Storage of Bacterial Strains

The *E. coli* strains trp A2/F'A2 and trp B8 were stored on nutrient agar slants at 4°C. Strains were periodically screened by growing them on minimal medium agar plates supplemented with 0.5% (w/v) D-glucose in the presence or absence of 5 μg/mℓ L-tryptophan. Subculturing of bacterial colonies which grew on plates containing tryptophan ensured the integrity of the strains.

The *E. coli* strain trp R-ΔLD102/F'ΔLD102 was stored on Luria broth agar slants at 4°C. Screening was performed on minimal medium agar plates supplemented with the reagents given below.

0.5%	(w/v)	D-glucose
5	μg/mℓ	indole
50	μg/mℓ	5-methyl (D,L) tryptophan

The strain was maintained since it produces tryptophan synthase constitutively and is therefore able to grow on these plates by converting the indole present on these plates into L-tryptophan for incorporation into proteins. Other contaminating bacterial strains which have unaltered trp operons cannot grow on these plates because 50 µg/mℓ 5-methyl(D,L) tryptophan represses the trp operon preventing L-tryptophan synthesis. The 5-methyl(D,L) tryptophan cannot be utilised by the enzymes involved in protein synthesis and the contaminating bacteria are therefore prevented from growing because of L-tryptophan depletion.

2.4.2 Growth of Bacterial Strains

Overnight nutrient broth cultures of *E. coli* strains (40 mℓ) were used to innoculate 72 ℓ (four 18 ℓ glass containers with sintered glass bubblers) of minimal medium supplemented with 0.05% (w/v) acid hydrolysed casein and 0.5% (w/v) D-glucose. Media for the trpA2/F'A2 and trp BB strains also contained indole at derepressing concentrations (5 µg/mℓ) while the trpR⁻ΔLD102/F'ΔLD102 strain required the addition of 15 µg/mℓ of L-tryptophan.

The bacterial growth was monitored by withdrawing samples and measuring their turbidities at 540 nm after appropriate dilution with water. Growths were terminated after 16 to 18 hours of growth at 37°C.

The cells were harvested by centrifugation through a Beckman JCF-Z continuous flow rotor at 18 000 rpm at 400 mℓ min^{-1}. The cells

The strain was maintained since it produces tryptophan synthase constitutively and is therefore able to grow on these plates by converting the indole present on these plates into L-tryptophan for incorporation into proteins. Other contaminating bacterial strains which have unaltered trp operons cannot grow on these plates because 50 µg/mℓ 5-methyl(D,L) tryptophan represses the trp operon preventing L-tryptophan synthesis. The 5-methyl(D,L) tryptophan cannot be utilised by the enzymes involved in protein synthesis and the contaminating bacteria are therefore prevented from growing because of L-tryptophan depletion.

2.4.2 Growth of Bacterial Strains

Overnight nutrient broth cultures of *E. coli* strains (40 mℓ) were used to innoculate 72 ℓ (four 18 ℓ glass containers with sintered glass bubblers) of minimal medium supplemented with 0.05% (w/v) acid hydrolysed casein and 0.5% (w/v) D-glucose. Media for the *trpA2/F'A2* and *trp B8 strains* also contained indole at derepressing concentrations (5 µg/mℓ) while the trpR$^-$ΔLD102/F'ΔLD102 strain required the addition of 15 µg/mℓ of L-tryptophan.

The bacterial growth was monitored by withdrawing samples and measuring their turbidities at 540 nm after appropriate dilution with water. Growths were terminated after 16 to 18 hours of growth at 37°C.

The cells were harvested by centrifugation through a Beckman JCF-Z continuous flow rotor at 18 000 rpm at 400 mℓ min^{-1}. The cells

were then suspended in 0.13 M - NaCℓ and centrifuged before being stored at -70°C.

2.5 Purification of Tryptophan Synthase Subunits

The required quantity of bacteria were thawed in the specified buffers at 4°C and the cells were disrupted by sonication of 50 mℓ aliquots for 10 minutes using a Model 20 MSE sonicator (20 KHz). The temperature of the suspension was kept below 10°C by cooling with an ice-salt mixture.

2.5.1 Purification of the α-subunit

The α-subunit was purified from 900 g of *E. coli* trp 88 according to the method of Kirschner *et al.* (1975).

The purified α-subunit was dialysed against water and crystallised by the method of Henning *et al.* (1962). The crystals were stored at 4°C in a solution containing the reagents listed below.

2 mM	dithiothreitol
55%	saturation of ammonium sulphate (at 0°C)
10 mM	potassium phosphate buffer pH 7.8

(Note that all ammonium sulphate solutions were prepared by adding solid ammonium sulphate to solutions according to the tables given by Di Jeso (1968).)

2.5.2 Purification of the β_2-subunit

The β_2-subunit was purified from *E. coli* trpA2/F'A2 by two different methods as described below.

First Method : Method of Bartholmes *et al.* (1976)

The β_2-subunit was purified by a scaling down of this method for 250 g wet weight of *E. coli* trpA2/F'A2. Three separate purifications resulted in β_2-subunit with specific activities of 1800, 2040 and 1830 units mg^{-1} respectively.

Second Method : Modification of the Methods of Wilson & Crawford (1965) and Adachi & Miles (1974)

The crude extract of β_2-subunit was subjected to the first heat step and protamine sulphate treatmert as described by Wilson & Crawford (1965). The supernatant was then made 5 mM in NH_2OH (by adding NH_2OH from a 0.5 M stock solution at pH 7.5). Powdered ammonium sulphate was added to achieve a concentration of 35% saturation (Calculated for a temperature of 0°C). After stirring for 45 minutes at 4°C, the suspension was centrifuged at 12 000 g for 30 minutes. The precipitate was suspended in a buffer containing the reagents listed below, to give a final concentration of $2x10^4$ units $m\ell^{-1}$.

0.2 mM PLP

1 mM dithiothreitol

0.5 mM phenylmethane sulphonyl fluoride (A stock solution of this reagent in ethanol was prepared and the required quantity of stock solution was added to the buffer just before the buffer was to be used).

100 mM potassium phosphate buffer pH 7.8

This enzyme solution was dialysed against the above buffer for 4 hours and then dialysed for 12 hours against this buffer supplemented with ammonium sulphate at 18.5% saturation (calculated at a temperature of 0°C). The suspension was centrifuged at 15 000 g for 30 minutes and the supernatant was clarified by centrifugation at 80 000 g for 3 hours (Beckman 60 Ti rotor).

The supernatant was dialysed for 16 hours against a buffer containing the reagents listed below.

5 mM NH_2OH

5 mM EDTA

1 mM dithiothreitol

0.5 mM phenylmethanesulphonyl fluoride (added from an ethanol stock solution as described above)

18.5% saturation of ammonium sulphate (calculated for a temperature of 0°C)

100 mM potassium phosphate buffer pH 7.8

The suspension was then centrifuged at 12 000 g for 30 minutes. The precipitate was very slowly and carefully dissolved by the addition of small amounts of precipitate to a buffer containing the reagents listed below

2 mM dithiothreitol
100 mM potassium phosphate buffer pH 7.8

The buffer was stirred slowly at 25°C during the dissolving process and further additions of precipitate were only made once the previous addition was fully dissolved.

A buffer temperature of 25°C was required since attempts to dissolve the apoβ_2-subunit at 5°C resulted in a maximum concentration of dissolved protein of 1.5 mg $m\ell^{-1}$. Small additions of precipitated protein prevented clumping of the protein and reduced the time required for the dissolving process.

The protein solution, which contained 10 mg $m\ell^{-1}$ of apoβ_2-subunit, was clarified by centrifugation at room temperature and then placed in a polystyrene ice-bucket. By placing the ice-bucket in a 4°C cold room, the protein solution was cooled to 4°C over a period of about 8 hours. This slow cooling of the protein solution was found to enhance the crystallisation of the apoβ_2-subunit.

The required quantity of powdered ammonium sulphate (Di Jeso, 1968) was added to the apoβ_2-subunit suspension to increase the ammonium sulphate saturation by 1%. These additions were carried out twice

TABLE 3

Purification of the apoB_2-subunit from 200 g of *E. coli* trpA2/F'trpA2 by a modification of the methods of Adachi & Miles (1974) and Wilson & Crawford (1965). The results represent an average of four purifications .

TABLE 3

Step	Volume (mℓ)	Protein (mg/mℓ)	Activity (units/mℓ)	Total protein (mg)	Total activity (units)	Specific activity (units/mg)	Purification	Yield (%)
Crude extract	490	38.4	3 140	18 800	1540×10^3	82	1	100
1st heating step	460	21.7	2 914	9 970	1340×10^3	134	1.6	87
Protamine sulphate treatment	470	21.0	2 958	9 890	1390×10^3	140	1.7	90
Ammonium sulphate precipitation	50	43.5	21 200	2 170	1060×10^3	483	5.9	69
1st Ammonium sulphate dialysis	42	26.2	21 000	1 100	880×10^3	802	9.8	57
2nd ammonium sulphate dialysis	46	10.4	16 283	480	749×10^3	1 520	18.5	49
Crystals	16	20.0	39 600	320	634×10^3	1 970	24.0	41

a day for two days. The crystals obtained were stored at 4°C in a buffer containing the reagents listed below.

2 mM dithriothreitol
0.5 mM phenylmethanesulphonyl fluoride
26% saturation of ammonium sulphate (calculated at 0°C)
100 mM potassium phosphate buffer pH 7.8

Table 3 contains a summary of the purification procedure described above.

2.5.3 Purification of Native Tryptophan Synthase and Dissociation into Subunits

The $\alpha_2\beta_2$-complex was purified by the method of Tschopp & Kirschner (1980a). Dissociation of the α_2*holo*β_2-*complex was achieved by a* modification of the method of Miles & Moriguchi (1977) as described below.

The enzyme (1.3 g in 50 mℓ) was dialysed overnight against a buffer containing the following reagents.

1 mM *EDTA*
0.5 mM dithiothreitol
40 mM Bicine buffer pH 7.8 at 4°C

The dialysed enzyme solution was made 1 M with respect to KSCN and 10 mM with respect to NH_2OH. The mixture was incubated at 22°C

for 10 minutes and then loaded on to a column (4.4 x 150 cm) packed with Sephadex G-100. The protein was eluted at 4°C with the buffer described above. Crystallisation of the α-subunit and apoβ$_2$-subunit was performed as described under sections 2.5.1 and 2.5.2 respectively.

2.6 Equilibrium Dialysis

Equilibrium dialysis was performed in pairs of Perspex cells (0.4 mℓ volume) separated by Sartorius SM11533 membranes. These membranes are permeable to proteins with molecular weights below 70 000. Equilibrium dialysis experiments with PLP and ANS were also performed with Sartorius SM 11533 membranes since the large pore size of this membrane allowed rapid transfer of the ligands between chambers.

Samples were dialysed by loading one chamber with protein and the opposite chamber with liquid.

2.6.1 PLP Binding to the Apoβ$_2$-subunit

The binding to PLP to the apoβ$_2$-subunit was performed as described by Bartholmes *et al.* (1976) except that the concentrations of free and bound PLP were measured by Bonavita's method (Storvick *et al.*, 1964). Samples of 0.1 mℓ were withdrawn after 12 hours of dialysis at room temperature (about 24°C) and diluted with buffer to 3 mℓ. Aliquots of 0.1 mℓ of a buffer containing the reagents listed below were added to the diluted samples and the samples were then incubated for 30 minutes at 35°C.

0.03 M KCN

0.2 M sodium phosphate buffer pH 7.4

The pH of the incubated samples was adjusted with HCl to between 3 and 4 and the fluorescence measured on a Perkin-Elmer model 204 fluorimeter (excitation wavelength was 325 nm and the emission was measured at 415 nm). The PLP concentrations were obtained from a calibration curve obtained by preparing solutions with known PLP concentrations and treating the PLP solutions in a manner similar to the samples from the equilibrium dialysis experiments.

2.6.2 ANS Binding to the apoβ_2-subunit

ANS binding to the apoβ_2-subunit was measured at room temperature (about 24°C). Concentrations of ANS were measured spectrophotometrically using the molar absorptivity of 4.95 x 10^3 M^{-1} cm^{-1} at 355 nm (Daniel & Weber, 1966).

2.6.3 α-subunit Binding to the Apoβ_2-subunit

After dialysis at room temperature for 20 hours, samples were withdrawn from both chambers. The α-subunit activity was measured in the standard indole to tryptophan assay and the α-subunit concentration was calculated from its specific activity.

2.6.4 *Curve Fitting*

The data for non-cooperative binding was plotted according to the Scatchard equation:-

$$\nu/[L] = K_a(n-\nu)$$

where ν = moles of ligand bound per mole of protein

$[L]$ = concentration of free ligand

n = number of intrinsically identical sites

and K_a = microscopic association constant of the individual sites for ligand.

Curves were fitted to the data by the least squares procedure of Wilkinson (1961).

2.7 Spectrophotometric and Fluorimetric Spectra and Titrations

2.7.1 Difference Spectra

Difference spectra were recorded on a Pye-Unicam SP8-100 spectrophotometer equipped with water jacketed cell holders at 24°C. Two cuvettes in the reference beam contained α-subunit and β_2-subunit respectively or protein and ligand respectively. One of the two sample cuvettes contained a mixture of the α-subunit and β_2-subunit or proteins plus ligand at the same concentrations as in the reference cuvettes.

2.7.2 Titrations of the Proteins with Ligands

A single cuvette containing dye (the ligand) at a specific concentration was placed in the sample beam of the spectrophotometer or fluorimeter (Perkin-Elmer Model 204) equipped with water jacketed cell holders at 24°C. Aliquots of a concentrated stock solution of protein containing dye (at the same concentration as that originally in the cuvette) were added to the cuvette.

Curve fitting was performed by the method described in Section 2.6.4.

2.8 Fluorescence Energy Transfer Experiments

2.8.1 Labelling of Subunits

Labelling of proteins was carried out in 0.1 M-potassium-phosphate

buffer pH 8.2 supplemented with 20 μM-PLP for the labelling of the β_2-subunit. The FITC and RITC dyes were dissolved in this buffer by the addition of KOH until a pH of 9.5 was obtained. Various concentrations of dye were reacted with the α-subunit (3 to 4 mg $m\ell^{-1}$ for 5 to 60 minutes and with the holoβ_2-subunit (2 to 3 mg) $m\ell^{-1}$ for 15 minutes at 25°C.

The reaction was terminated by passing the mixtures through a Sephadex G-25 column equilibrated with the desired buffers. The labelled α-RITC complex exhibited a fluorescence char upon dilution with buffer which indicated the presence of two $s_{...}$ ies of labelled α-subunit. It was thought that the two species present were monomers of α-subunit and dimers of α-subunit. Removal of the presumed α-subunit dimers was achieved by filtration through a Sephadex G-100 column.

Concentrations of the labelled proteins were estimated from the protein absorbances at 278 nm corrected for the small absorption of the dye at 278 nm. Bound dye concentrations were obtained from absorbance measurements and the molar absorptivities of the FITC and RITC dyes given by Gennis *et al.* (1972).

2.8.2 Fluorescence Energy Transfe...

The α-subunit was labelled by reaction with RITC at a concentration six times that of the α-subunit for 10 minutes at 25°C or with FITC at a concentration ten times that of the α-subunit for 10 minutes at 25°C. The holoβ_2-subunit was labelled by reaction with FITC at a concentration twice that of the holoβ_2-subunit for 15 minutes at 25°C.

Emission wavelength scans of dissociated and assembled proteins were recorded at 24°C at equal concentrations of subunits. Difference spectra were obtained by subtraction.

2.9 Pressure-jump and Stopped-flow Experiments

2.9.1 Pressure-jump Apparatus

The pressure-jump apparatus was similar to that described by Davis & Gutfreund (1976) and the data storage system was similar to that described by Davis (1981a,b). The light source for intrinsic fluorescence measurements was a 200 W Xenon arc bulb powered by a 250 W Xenon arc power supply (Applied Photophysics, London, W1, U.K.). Sample emission was measured after passing through WG320, OG590 or GG435 optical filters (JENAer Glaswerke, Schott & Gen, Mainz).

2.9.2 Stopped-flow Apparatus

Experiments were performed with the stopped-flow apparatus described by Bagshaw *et al.* (1972), fitted with a 2 mm path optical cell, used in conjunction with the peripheral optics and electronics of the pressure-jump apparatus. The light source used was a 12V-100 W quartz halogen bulb and sample excitation was achieved with a monochromator entrance slit of 5 mm and an exit slit of 20 nm band width.

The stopped-flow apparatus dead time was measured with the 2,6 dichlorophenolindophenol-ascorbic acid system (Tonomura *et al.*, 1978) and was approximately 3 ms. All stopped-flow experiments were performed at room temperature which varied from 22°C to 27°C.

2.9.3 Extraction of Rate Constants from Experimental Curves

The data from three to five relaxations or transients at each protein concentration were averaged. Rate constants were obtained from linear least squares lines fitted to the exponential curves of the averaged data.

3. RESULTS

3.1 Purification of Tryptophan Synthase Subunits

Purification of the native $\alpha_2$holoβ_2-complex and subsequent dissociation of this complex provided the most convenient route for obtaining tryptophan synthase subunits. The reasons for this are twofold. Firstly, both tryptophan synthase subunits could be purified from a single strain of bacteria and secondly, the overall yields of both subunits obtained per litre of bacterial growth medium were greater than when the subunits were purified from two different bacterial strains.

Crystals of the purified subunits (Fig. 1) were subjected to SDS polyacrylamide gel electrophoresis on 7.5% gels according to the method of Weber & Osborn (1969). Densitometer scans of the crystalline material are given in Figure 2.

The scans of the subunits shown in Figure 2 indicate that the purity of the subunits is far greater than that suggested by the ratios of the specific activities obtained to the maximum specific activities for the subunits. The α-subunit prepared by Kirschner *et al.* (1975) had a specific activity of 5500 units mg^{-1} while the β_2-subunit prepared by Bartholmes *et al.* (1976) had a specific activity of 4100 units mg^{-1}. The ratios of specific activities are given below.

α-subunit	3300/5500	=	0.60
β_2-subunit	2100/4100	=	0.51

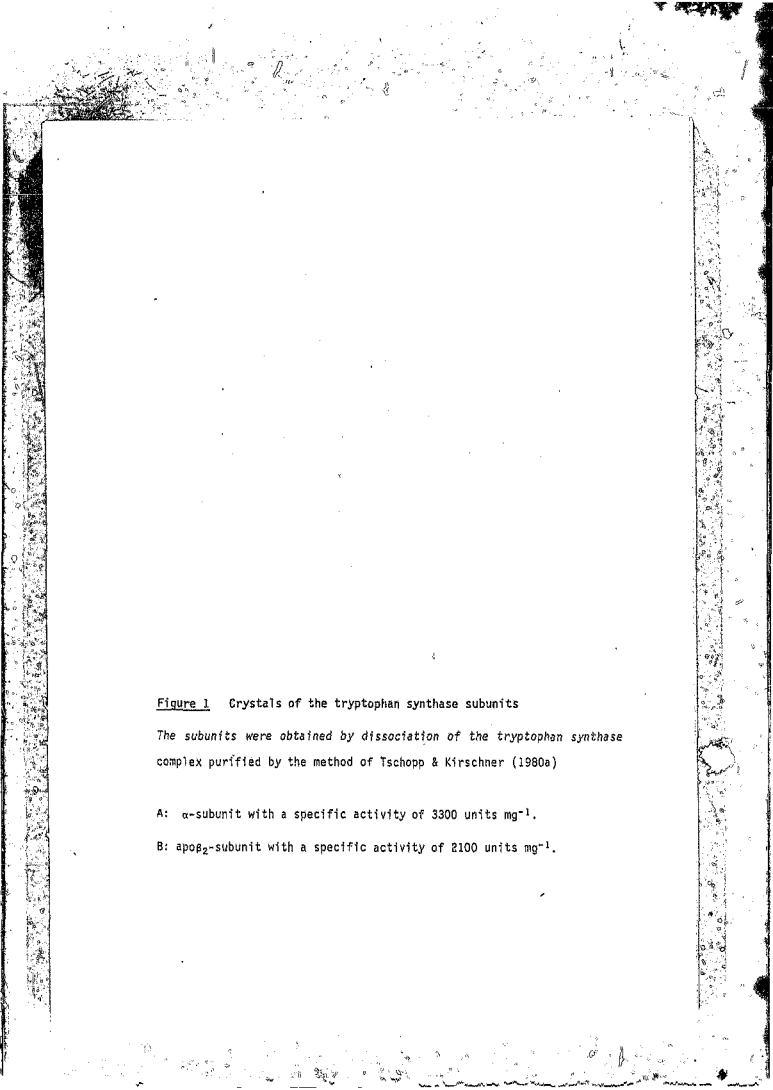

Figure 1 Crystals of the tryptophan synthase subunits

The subunits were obtained by dissociation of the tryptophan synthase complex purified by the method of Tschopp & Kirschner (1980a)

A: α-subunit with a specific activity of 3300 units mg^{-1}.

B: apoβ_2-subunit with a specific activity of 2100 units mg^{-1}.

FIGURE 1A

FIGURE 1B

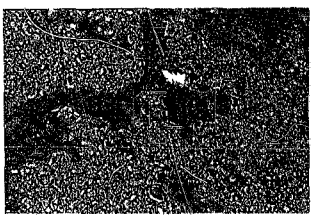

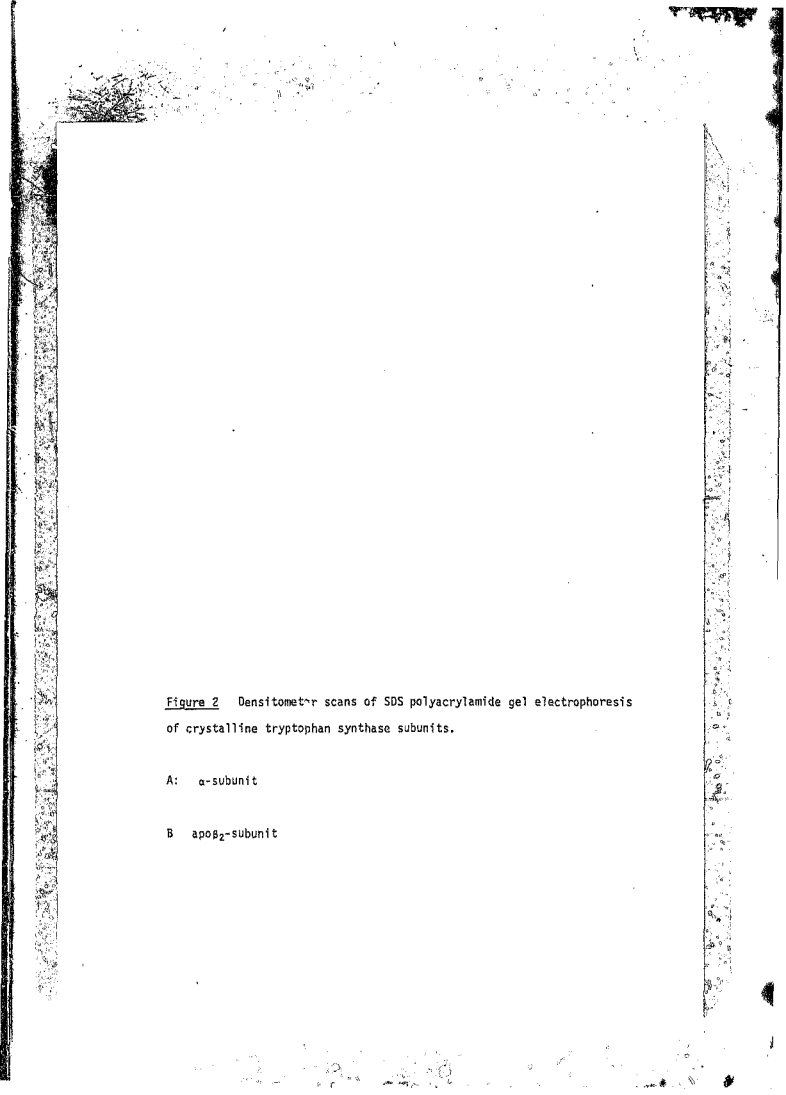

Figure 2 Densitometer scans of SDS polyacrylamide gel electrophoresis of crystalline tryptophan synthase subunits.

A: α-subunit

B apog_2-subunit

FIGURE 2

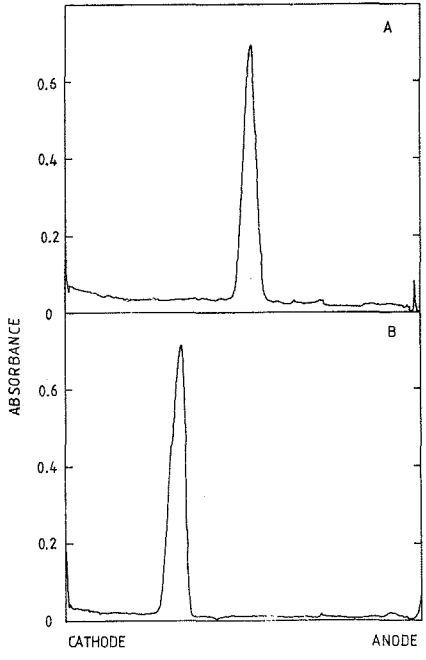

3.2 Binding of PLP to the Apoβ_2-Subunit by Equilibrium Dialysis

Binding of PLP to the apoβ_2-subunit was measured in order to ascertain whether the lower specific activity material prepared here is vastly different from high specific activity apoβ_2-subunit with respect to PLP binding.

Figure 3 represents a Scatchard plot of the PLP binding to the apoβ_2-subunit. There is a good correlation between the experimental points and the solid curve which was plotted using the Adair parameters reported by Bartholmes *et al.* (1976). This indicates that the lower activity apoβ_2-subunit prepared here displays the same PLP binding properties as the high specific activity apoβ_2-subunit of Bartholmes *et al.* (1976).

3.3 Binding of the α-Subunit to the Apoβ_2-Subunit by Equilibrium Dialysis

Binding of the α-subunit to the apoβ_2-subunit, in various solvents, was investigated for two reasons. The first being that kinetic studies in standard buffer precluded a cooperative binding mechanism which has been reported by Bartholmes & Teuscher (1979) (see Section 3.5.3.4). The second reason was to compare the lower specific activity subunits prepared here with those prepared by Bartholmes & Teuscher (1979).

Subunit association was measured by equilibrium dialysis and Scatchard plots of the results are given in Figure 4. The relevant thermodynamic constants for the subunit association are presented in Table 4.

Non-cooperative subunit binding occurs in bicine with lower affinity than in phosphate or pyrophosphate. This phenomenon is not merely due to ionic strength differences because the inclusion of 0.2 M-KCℓ in the bicine buffer does not affect subunit association (see Figure 4B). Pyrophosphate converts the binding to a cooperative mechanism with binding affinity intermediate between that of bicine and phosphate.

The scatter of the data in the Scatchard plot for subunit association in phosphate (see Figure 4A) is fairly large and may be due to partial dissociation of the apoβ_2-dimer into apoβ_1-monomers at the low concentrations used here (Hathaway & Crawford, 1970). With the data available from these experiments and without evidence to the contrary a non-cooperative mechanism has been assumed. The linearity of the relevant plot is reasonable but certainly a concave curve would also fit the data. Such a curve would indicate the presence of negative cooperativity or two dissimilar sites on the apoβ_2-dimer. Certainly the data exclude the possibility of a convex curve and therefore exclude positive cooperativity.

Since the mechanism of α-subunit binding in pyrophosphate is different from that in bicine, the pyrophosphate ion must affect the molecular conformation of the apoβ_2-subunit. In addition, the observation that different binding mechanisms operate in pyrophosphate and phosphate, implies that the phosphate ion affects the molecular conformation of the apoβ_2-subunit in a different manner to that of the pyrophosphate ion. The difference in subunit binding affinities in bicine and phosphate suggests that the molecular conformation of the α-subunit may also be altered by the phosphate ion.

Figure 3 Scatchard plot of the binding of PLP to 14.7 μM-apoB_{2}-subunit.

The solid curve has been plotted using the Adair parameters determined by Bartholmes *et al.* (1976) of $\psi_1 = 2.3 \times 10^5\ M^{-1}$ and $\psi_2 = 5.0 \times 10^{11}\ M^{-2}$.

The Adair Equation is given below:

$$v = \frac{2(k_1[L] + k_1k_2[L]^2)}{1+2k_1[L] + k_1k_2[L]^2}$$

where V is the number of moles of ligand bound per mole of apoB_{2}-subunit,

[L] is the concentration of free ligand

and k_1 and k_2 are the association constants for the binding of the first and second ligands to the two sites of the apoB_{2}-subunit.

Note that with the nomenclature used here the parameters determined by Bartholmes *et al.* (1976) are given by the following relations.

$k_1 = \psi_1/2$ and $k_1k_2 = \psi_2$.

FIGURE 3

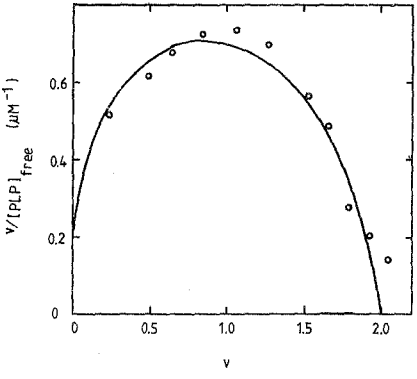

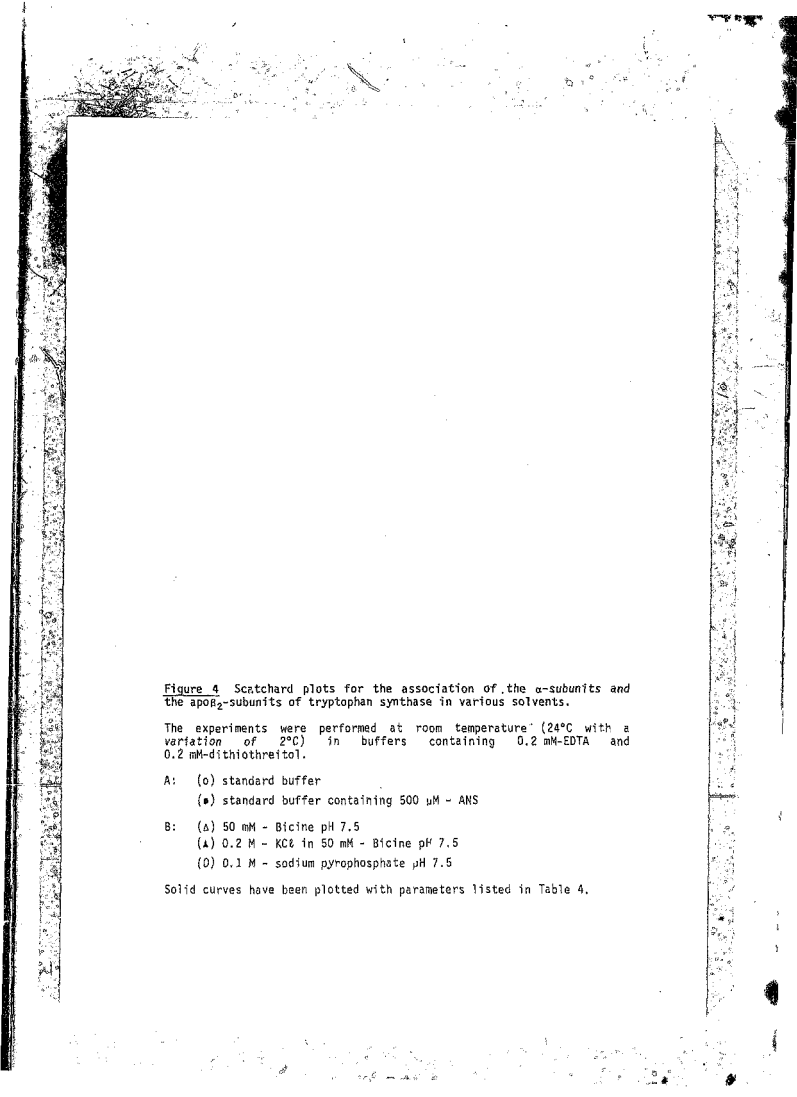

Figure 4 Scatchard plots for the association of the α-subunits and the apoβ$_2$-subunits of tryptophan synthase in various solvents.

The experiments were performed at room temperature (24°C with a variation of 2°C) in buffers containing 0.2 mM-EDTA and 0.2 mM-dithiothreitol.

A: (o) standard buffer
(•) standard buffer containing 500 μM - ANS

B: (Δ) 50 mM - Bicine pH 7.5
(▲) 0.2 M - KCℓ in 50 mM - Bicine pH 7.5
(◇) 0.1 M - sodium pyrophosphate pH 7.5

Solid curves have been plotted with parameters listed in Table 4.

FIGURE 4A

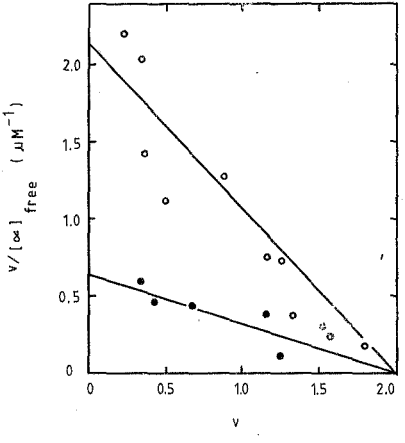

FIGURE 4B

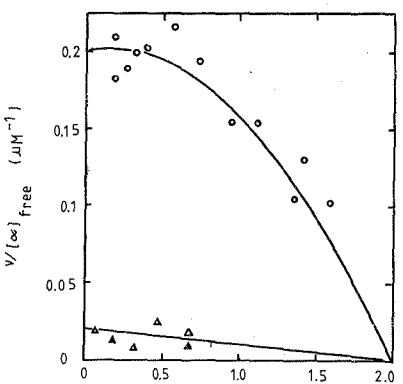

TABLE 4 Thermodynamic constants for the association of α-subunits and apoβ_2-subunits of tryptophan synthase in various solvents

(a) The analysis of the non-cooperative binding was by the method of Wilkinson (1961) as described in Section 2.6.1.

(b) The data for the cooperative binding was fitted to the Adair Equation as described in Section 3.2.

TABLE 4

Buffer	Type of Binding	Dissociation constants (uM)	Number of sites
Bicine	non-cooperative[a]	100	2
Sodium pyrophosphate	cooperative	K_1=10 K_2= 4	2
Potassium phosphate	non-cooperative[a]	0.93	2
500 uM-ANS in potassium phospate	non-cooperative[a]	3.1	2

3.4 Methods for Observing Subunit Assembly

3.4.1 Difference Spectra of Assembled Subunits

Difference spectra of α-subunit bound to both the apo and holo forms of the β_2-subunit were recorded to estimate the absorbance change accompanying subunit assembly.

The difference spectrum for the $\alpha_2apo\beta_2$-complex in Figure 5 has a maximum absorbance increase of 0.013 units at 286 nm. The concentration of bound α-subunit in the $\alpha_1apo\beta_2$-complex form and in the $\alpha_2apo\beta_2$-complex form has been calculated as $[\alpha]_{bound} = 8.9$ μM using the dissociation constant given in Table 4. Therefore, assembly of 2 μM-α-subunit into 1 μM-$\alpha_2apo\beta_2$-complex provides an absorbance change of 0.003 units at 286 nm.

The difference spectrum for the $\alpha_2holo\beta_2$-complex in Figure 6 has a maximum absorbance increase of 0.043 units at 410 nm. The concentration of bound α-subunit in the $\alpha_1holo\beta_2$-complex form and in the $\alpha_2holo\beta_2$-complex form has been calculated as $[\alpha]_{bound} = 15$ μM using the apparent association constant of 3.2×10^7 M^{-1} as determined by Creighton & Yanofsky (1966). Therefore, assembly of 2 μM-α-subunit into 1 μM-$\alpha_2holo\beta_2$-complex provides an absorbance change of 0.0057 units at 410 nm.

Assembly of the $\alpha_2holo\beta_2$-complex provides an absorbance change at 410 nm nearly twice that of the assembly of the $\alpha_2apo\beta_2$-complex followed at 286 nm. In addition, the assembly of the holo-complex has the advantage that the α-subunit does not absorb in the 410 nm range.

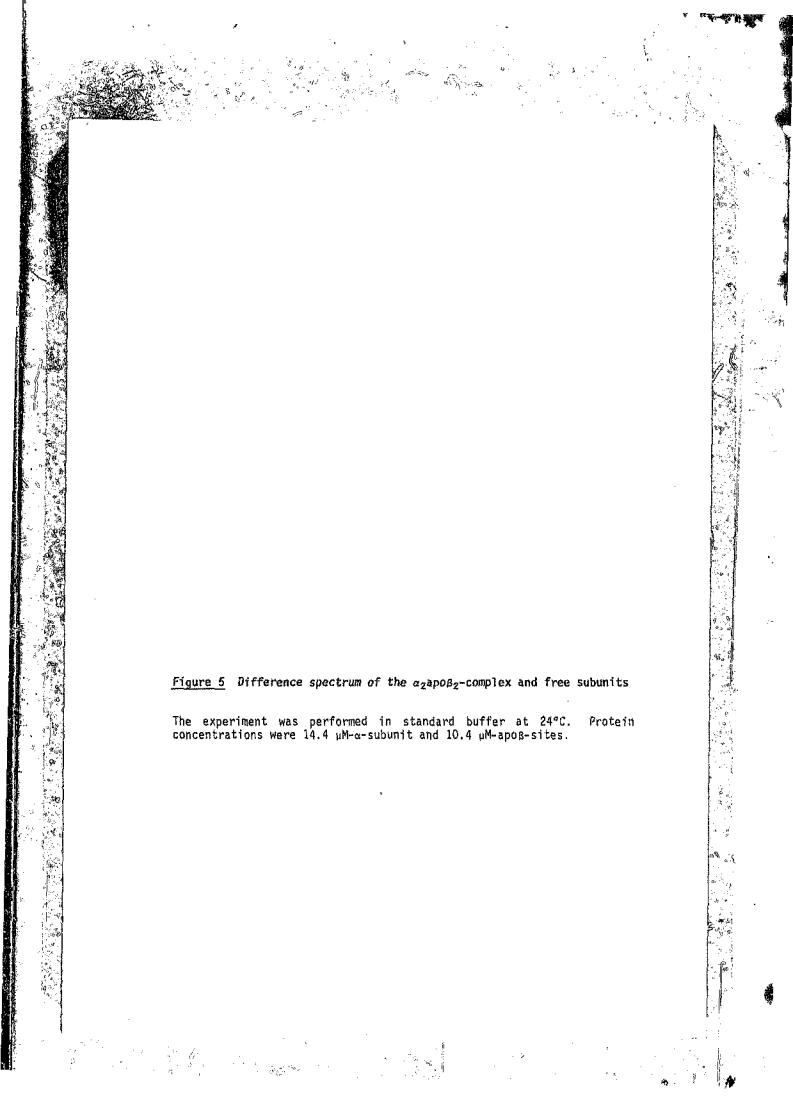

Figure 5 *Difference spectrum of the $\alpha_2 apo\beta_2$-complex and free subunits*

The experiment was performed in standard buffer at 24°C. Protein concentrations were 14.4 μM-α-subunit and 10.4 μM-apoβ-sites.

FIGURE 5

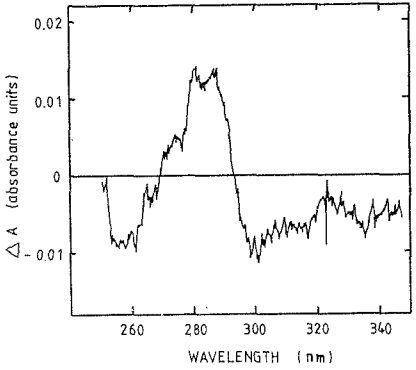
0.02
0.01
0
- 0.01
△ A (absorbance units)
260
280
300
320
340
WAVELENGTH (nm)

Figure 6 Difference spectrum of the $\alpha_2$holoβ_2-complex and free subunits

The experiment was performed with protein concentrations of 17.4 μM-α-subunit and 15.2 μM-holoβ-sites in a buffer containing the reagents listed below.

0.2 mM EDTA

0.2 mM dithiothreitol

20 μM PLP

25 mM Bicine buffer pH 7.5 at 24°C.

FIGURE 6

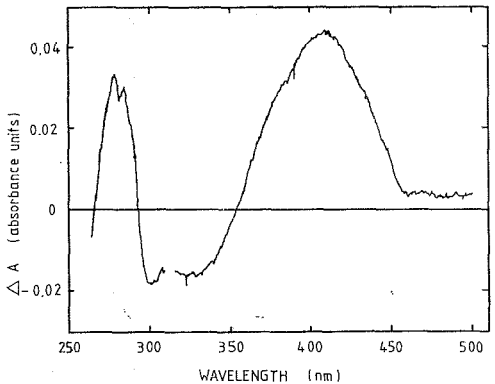
0.04
0.02
0
-0.02
△A (absorbance units)
250
300
350
400
450
500
WAVELENGTH (nm)

FIGURE 6

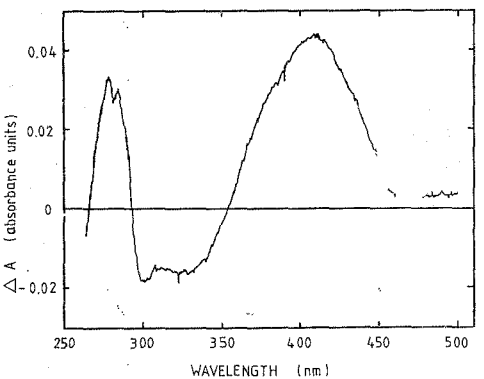
0.04
0.02
0
-0.02
△ A (absorbance units)
250
300
350
400
450
500
WAVELENGTH (nm)

Therefore, in kinetic experiments the α-subunit concentration could be varied without raising the total background absorbance of the unassembled subunits.

For the assembly of the apo-complex, increasing the α-subunit concentration would increase the total background absorbance of the unassembled subunits due to the intrinsic absorbance of the α-subunit at 286 nm. The smaller absorbance change due to subunit assembly must then be measured against a larger background signal requiring higher signal amplification. For this reason various dyes were investigated as to their suitability for use as probes of subunit assembly in the absence of PLP.

3.4.2 Probes Covalently Bound to Subunits

Fluorescence energy transfer between FITC and RITC dyes would be expected to increase when the subunits, to which the dyes are bound, assemble into the $\alpha_2\beta_2$-complex. This fluorescence energy transfer would only be observable if a number of requirements are satisfied. One of these requirements is that the FITC and RITC moeities must not inhibit subunit assembly. It was therefore necessary to standardise the subunit labelling procedures in order that they maintain their maximum specific activities.

3.4.2.1 Labelling of Subunits with FITC and RITC

Both FITC and RITC contain the isothiocyanate functional group which reacts with uncharged amine groups on lysine side chains and the free N-terminus of the protein.

Tryptophan synthase subunits were reacted with increasing concentrations of FITC and RITC and the concentrations of bound dyes and specific activities of subunits were determined (Figure 7). The α-subunit maintained its maximum specific activity as the extent of dye labelling was increased. In contrast the holoβ_2-subunit lost over half of its specific activity as the extent of labelling was increased.

The large difference between the α-subunit binding curves (Figure 7A) for FITC and RITC suggests that the α-subunit binds a proportion of the RITC dye in a different manner to the binding of the FITC dye. Chromatography of α-subunit labelled with a dye to protein concentration ratio of 6:1 indicated the presence of two different forms of RITC labelled α-subunit (Figure 8).

The first peak in Figure 8 eluted at a position close to the arrow and therefore exhibits elution behaviour of a globular protein with a molecular weight of about 68 000. All of the α-subunit activity, loaded on to the column was recovered in the second peak of Figure 8 (fractions 10 to 28), with the first peak having no detectable enzyme activity. Although further experiments were not performed, the material present in the first peak might be highly labelled inactive dimers of the α-subunit present in very low concentrations.

The extent of labelling the α-subunit present in the second peak of Figure 8 was investigated as shown in Figure 9. After removal of the material eluted in the first peak from a Sepahdex G-100 column, the remaining α-subunit exhibits a maximum ratio of bound RITC to α-subunit concentration of between 1.5 and 2. This extent of labelling matches that of labelling the α-subunit with the FITC dye (Figure 7A).

Figure 7 The extent of labelling the α-subunit and holoβ_2-subunit with FITC and RITC

A. labelling of the α-subunit with FITC(o) and RITC(●)

B. labelling of the holoβ_2-subunit with FITC(o) and RITC(●)

Left hand axis (———) n is the ratio of the concentration of bound dye to the concentration of α-subunits or holoβ_1-protomers.

Right hand axis (------) Specific activity of enzyme after labelling.

Horizontal axis. The ratio of the concentration of dye to the concentration of α-subunits or holoβ_1-protomers in the reaction mixture.

FIGURE 7A

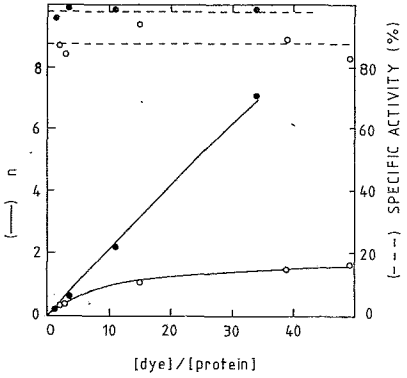
(——) n
(- - -) SPECIFIC ACTIVITY (%)
0
2
4
6
8
0
20
40
60
80
0
10
20
30
40
[dye]/[protein]

FIGURE 7A

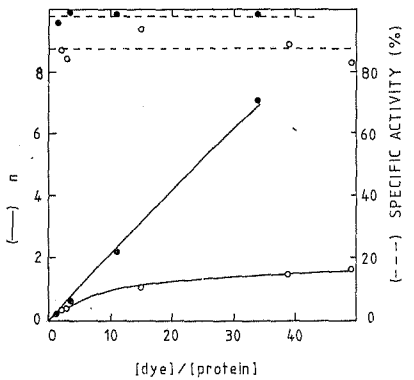
(——) n
(- - -) SPECIFIC ACTIVITY (%)
[dye]/[protein]
0
2
4
6
8
0
20
40
60
80
0
10
20
30
40

FIGURE 7B

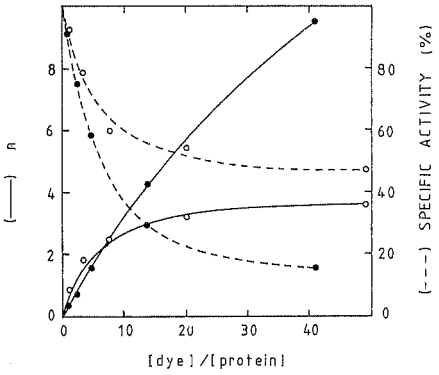
n
(——)
(- - -) SPECIFIC ACTIVITY (%)
0
2
4
6
8
0
20
40
60
80
0
10
20
30
40
[dye] /[protein]

Figure 8 Elution profile of *RITC labelled α-subunit passed through* a Sephadex G-100 column

Separation of 1.5 mℓ of RITC labelled α-subunit (2 mg/mℓ) on a Sephadex G-100 column (1.6 x 30 cm) with standard buffer at room temperature. The arrow indicates the position of elution of bovine serum albumin with a molecular weight of 68 000, separated under identical conditions.

FIGURE 8

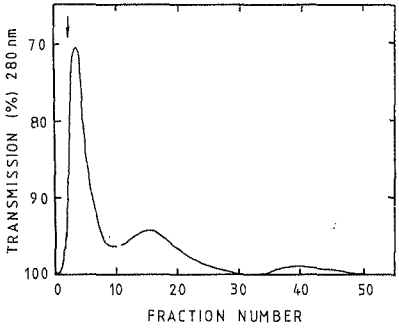
TRANSMISSION (%) 280 nm
70
80
90
100
0
10
20
30
40
50
FRACTION NUMBER

Figure 9 Extent of labelling the α-subunit with RITC

α-subunit of 2 mg/mℓ was reacted with 500 μM-RITC for 0 to 120 minutes and then passed through a Sephadex G-25 column. The eluted protein fraction was then passed through a Sephadex G-100 column as shown in Figure 8.

Left Hand Axis n is the ratio of the concentration of bound RITC to the concentration of α-subunit.

FIGURE 9

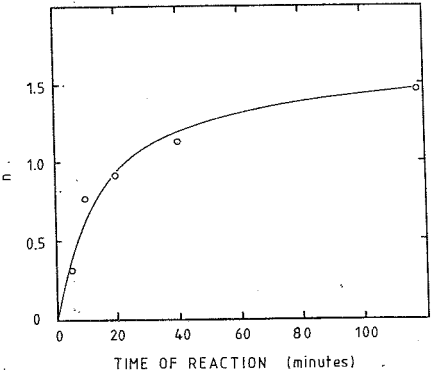

FIGURE 9

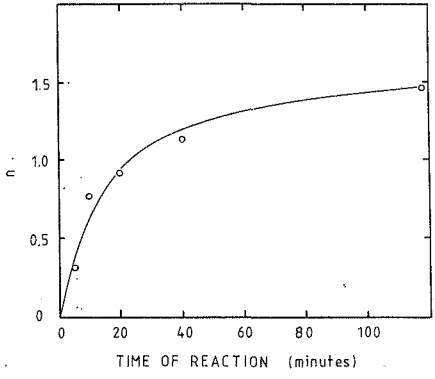

All experiments performed with RITC labelled α-subunit utilised α-subunit chromatographed on a Sephadex G-100 column.

3.4.2.2 Fluorescence Energy Transfer Experiments

Radiationless energy transfer from the protein bound FITC moeity to the protein bound RITC moeity would be expected to occur upon subunit assembly. This energy transfer would be indicated by a decreased fluorescence at the maximum emission wavelength of FITC (about 520 nm) and an increased fluorescence at the maximum emission wavelength of RITC (about 580 nm).

Difference fluorescence spectra were obtained for the assembly of the $\alpha_2 apo\beta_2$-complex with the α-subunit labelled with RITC and the β_2-subunit labelled with FITC. Figure 10 illustrates the decreased fluorescence at 520 nm due to fluorescence energy transfer. This fluorescence decrease was apparent within 20 seconds of mixing the labelled subunits and remained constant for up to 30 minutes (data not shown). As shown later in Section 3.5.3, subunit assembly involves slow reactions which are observable over periods of 5 to 20 minutes. Therefore this fluorescence energy transfer between RITC labelled α-subunit and FITC labelled β_2-subunit could not be used to monitor the slow reactions accompanying subunit assembly.

A second labelling system was investigated in order to ascertain *whether the slow reactions involved in the subunit assembly could* be observed under different conditions. The $\alpha_2 apo\beta_2$-complex was assembled with unlabelled $apo\beta_2$-subunit and on equimolar mixture of α-subunit labelled with FITC and α-subunit labelled with RITC.

This second labelling system has the advantage that the β_2-subunit maintains its maximum specific activity whereas in the former system reaction with FITC decreased the β_2-subunit activity. In addition, the α-subunit maintains its maximum specific activity when labelled either with FITC or with RITC (see Figure 7A).

The fluorescence difference spectrum obtained for this labelling system is shown in Figure 11. The fluorescence decrease observed at 520 nm was complete within 20 seconds of mixing the subunits and remained constant for up to 30 minutes. As discussed above, this labelling system could not be used to monitor the slow reactions accompanying subunit assembly. However, an important observation was made while recording emission spectra of RITC labelled α-subunit mixed with apoβ_2-subunit. A significant decrease of 28% of the intrinsic RITC fluorescence emission was observed over 15 minutes. This change in the fluorescence of the RITC bound to the α-subunit occurred upon assembly with apoβ_2-subunit irrespective of the presence of α-subunit labelled with FITC. Figure 12 illustrates the RITC fluorescence decrease accompanying subunit assembly.

The RITC probe provides a sensitive means of monitoring subunit assembly and has been used in stopped-flow experiments (see Section 3.5.3.2).

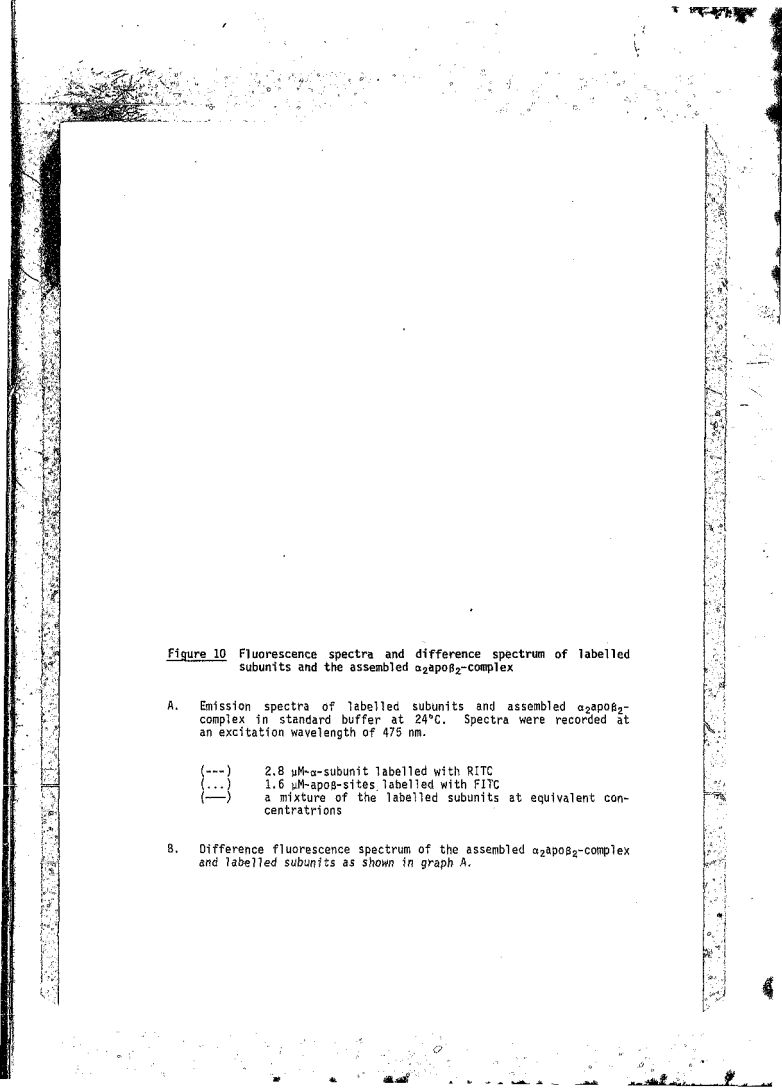

Figure 10 Fluorescence spectra and difference spectrum of labelled subunits and the assembled $\alpha_2 apo\beta_2$-complex

A. Emission spectra of labelled subunits and assembled $\alpha_2 apo\beta_2$-complex in standard buffer at 24°C. Spectra were recorded at an excitation wavelength of 475 nm.

(---) 2.8 μM-α-subunit labelled with RITC
(...) 1.6 μM-apoβ-sites labelled with FITC
(——) a mixture of the labelled subunits at equivalent concentrations

B. Difference fluorescence spectrum of the assembled $\alpha_2 apo\beta_2$-complex and labelled subunits as shown in graph A.

FIGURE 10

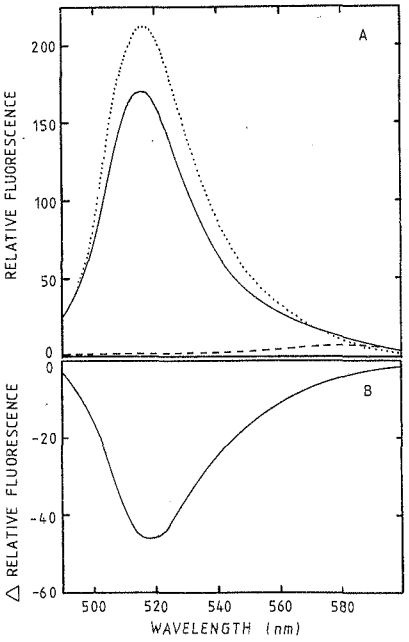
A
B
200
150
100
50
0
-20
-40
-60
RELATIVE FLUORESCENCE
Δ RELATIVE FLUORESCENCE
500
520
540
560
580
WAVELENGTH (nm)

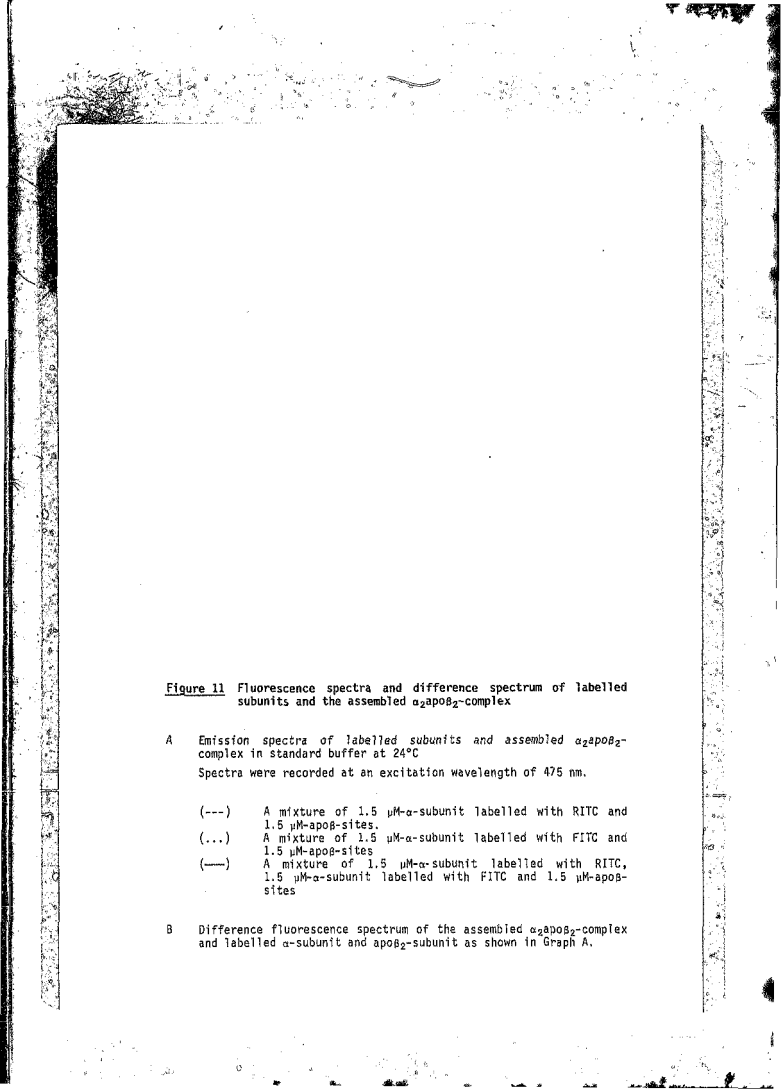

Figure 11 Fluorescence spectra and difference spectrum of labelled subunits and the assembled $\alpha_2 apo\beta_2$-complex

A *Emission spectra of labelled subunits and assembled* $\alpha_2 apo\beta_2$-complex in standard buffer at 24°C

Spectra were recorded at an excitation wavelength of 475 nm.

(---) A mixture of 1.5 µM-α-subunit labelled with RITC and 1.5 µM-apoβ-sites.

(...) A mixture of 1.5 µM-α-subunit labelled with FITC and 1.5 µM-apoβ-sites

(——) A mixture of 1.5 µM-α-subunit labelled with RITC, 1.5 µM-α-subunit labelled with FITC and 1.5 µM-apoβ-sites

B Difference fluorescence spectrum of the assembled $\alpha_2 apo\beta_2$-complex and labelled α-subunit and $apo\beta_2$-subunit as shown in Graph A.

FIGURE 11

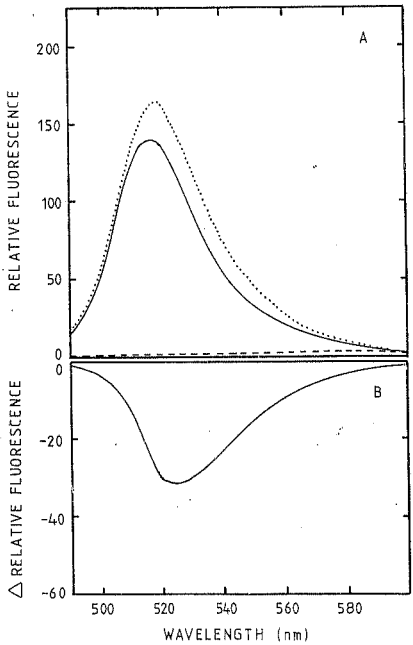
A
B
200
150
100
50
0
-20
-40
-60
500
520
540
560
580
RELATIVE FLUORESCENCE
△ RELATIVE FLUORESCENCE
WAVELENGTH (nm)

Figure 12 Fluorescence decrease of RITC bound to the α-subunit after addition of apoβ_2-subunit

The fluorescence emission of 1 μM-α-subunit labelled with RITC was monitored at 590 nm. After 2 minutes 2 μM-apoβ-sites was added and the fluorescence was observed for 18 minutes. The signal change represents a decrease of about 28% of the signal prior to addition of apoβ_2-subunit. The experiment was performed in standard buffer at 24°C and the excitation wavelength was 560 nm.

FIGURE 12

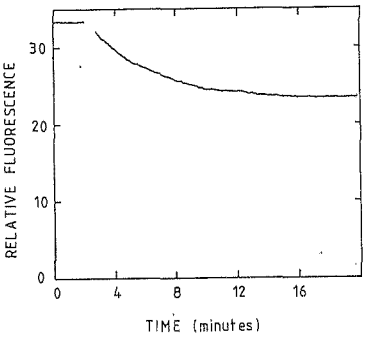

3.4.3 Probes Non-covalently Bound to Subunits

Although the covalently bound RITC probe proved useful in monitoring subunit assembly, large amplitudes are only obtained with reactions where the β_2-subunit concentration is in excess over the α-subunit concentration. Under conditions where the α-subunit concentration is in excess over the β_2-subunit concentration, the amplitudes obtained are lower. A different type of probe that exhibits large amplitudes even with α-subunit in excess, would therefore complement the RITC probe system. For this reason alternative probes were sought that would monitor subunit assembly by a mechanism different from that of the RITC probe.

Two probes that are non-covalently bound to the tryptophan synthase subunits were found which allow subunit assembly to be followed either by monitoring fluorescence or absorbance changes. Fluorescence changes accompanying subunit assembly were observed in the presence of the ANS probe while the BPB probe provided absorbance changes. However, before these probes could be used two possibilities had to be investigated. The first was whether the probes bind to the α-subunit, the β_2-subunit or to the $\alpha_2\beta_2$-complex and the second was whether the probes inhibit subunit assembly.

The results presented below derive from investigations into the binding and inhibitory properties of the ANS and BPB probes.

3.4.3.1 *The Binding of ANS to the Apoβ_2-Subunit by Equilibrium Dialysis*

Equilibrium dialysis was used to investigate the binding of ANS to the apoβ_2-subunit. A Scatchard plot for this binding is shown in Figure 13.

The non-linearity of the points in Figure 13 indicates the presence of two intrinisically different classes of binding sites on the apoβ_2-subunit for the ANS ligand. At low ligand concentrations the lower affinity sites do not play a significant role in the binding properties of the apoβ_2-subunit. The significant role played by the higher affinity sites was investigated by fluorescence and absorbance titrations in the presence of low ligand concentrations. The results of these investigations are described in the following section.

3.4.3.2 The Binding of the ANS and BPB Probes to Tryptophan Synthase Subunits

Fluorescence and absorbance spectral changes accompany the binding of ANS and BPB to the α-subunit, apoβ_2-subunit and the $\alpha_2$apoβ_2-complex respectively. Figures 14 and 15 represent typical spectral changes for the binding of the probes to the subunits.

Quantitative measurement of the binding of the ANS and BPB ligands by the higher affinity sites of the subunits was achieved by fluorescence and absorbance titrations respectively. The fluorescence enhancement resulting from ANS binding is shown in Figure 16 while the absorbance enhancement resulting from BPB binding is shown in Figure 17. The data was analysed by the method of Wilkinson (1961),

as described in Section 2.6.4, and the various binding parameters are collected in Table 5.

Titrations performed by adding ANS and BPB ligands to protein solutions result in high concentrations of the ligands with self quenching of ANS fluorescence and high absorbance of BPB solutions. Therefore the titrations were performed by adding protein to the ligand solutions. The former titration method results in saturation of protein binding sites with accurate determination of the number of sites occupied. The second titration method achieves saturation when all ligand is in a bound form and a high protein concentration exists. Under these conditions the maximum number of ligand molecules bound per protein molecule would be one. This titration method is weighted towards the determination of binding constants and not the number of sites. For this reason the values of n in Table 5 are only approximate and merely indicate trends in the binding behaviour of the proteins concerned.

An analysis of the ligand and subunit binding stoichiometries provides a possible mechanism whereby the ANS and BPB dyes provide signal changes which reflect subunit assembly (Table 6). The total number of moles of ligand bound to unassembled subunits in line 3 of Table 6 represents the maximum ligand binding prior to subunit assembly. Line 4 of Table 6 shows that assembled $\alpha_2\text{apo}\beta_2$-complex binds less ligand than the unassembled subunits. This implies that the assembly of subunits into the $\alpha_2\text{apo}\beta_2$-complex must result in the dissociation of a proportion of bound ligand. Since unbound ligand has lower fluorescence or absorbance than bound ligand (see Table 5), the dissociation of ligand results in part of the signal change observed

during subunit assembly. It is also possible that signal changes result from alterations in the intrinsic fluorescence and absorbance values of the respective ligands due to altered local environment during subunit assembly.

The kinetics of the binding of ANS and BPB dyes by the α-subunit, apoβ_2-subunit and the $\alpha_2$apoβ_2-complex was also investigated. This was necessary in order to ensure that the dye binding and dissociation is faster than subunit assembly. Under these conditions the signals derived from the probes would not merely reflect the dissociation of the probes from the subunits. On the contrary, the probes would reflect the subunit assembly. In addition the concentration at which the probes may be used must be such that inhibition of subunit assembly is kept at a minumum. The kinetic experiments that were performed are described in Section 3.5.2.

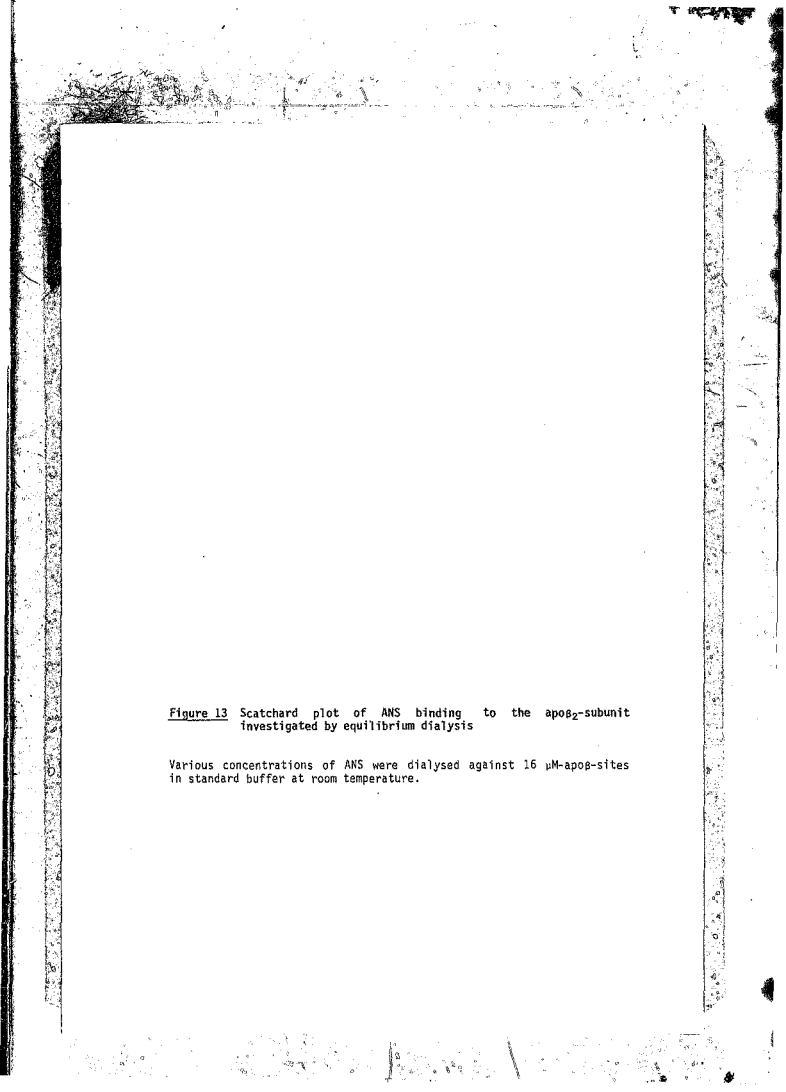

Figure 13 Scatchard plot of ANS binding to the apoβ_2-subunit investigated by equilibrium dialysis

Various concentrations of ANS were dialysed against 16 μM-apoβ-sites in standard buffer at room temperature.

FIGURE 13

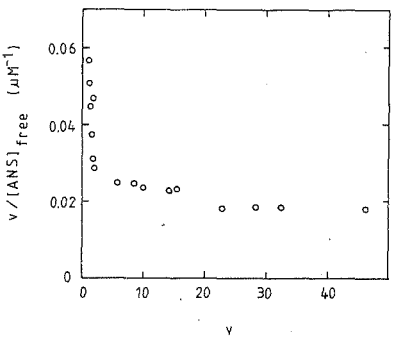

Figure 14 Fluorescence spectral changes accompanying ANS binding to the α-subunit

Lower Curves 20 μM-ANS in standard buffer at 24°C

Upper curves 20 μM-ANS in the presence of 14 μM-α-subunit in standard buffer at 24°C

(——) Excitation spectra recorded at an emission wavelength of 508 nm for ANS and 470 nm in the presence of α-subunit

(...) Emission spectra recorded at an excitation wavelength of 365 nm.

FIGURE 14

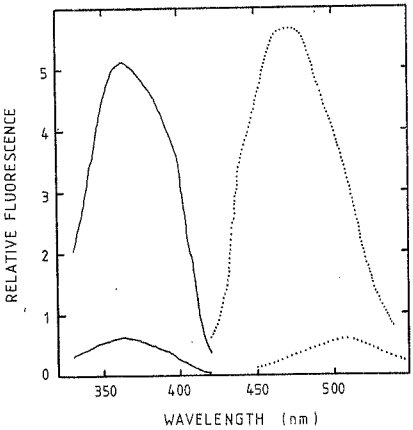
RELATIVE FLUORESCENCE
0
1
2
3
4
5
350
400
450
500
WAVELENGTH (nm)

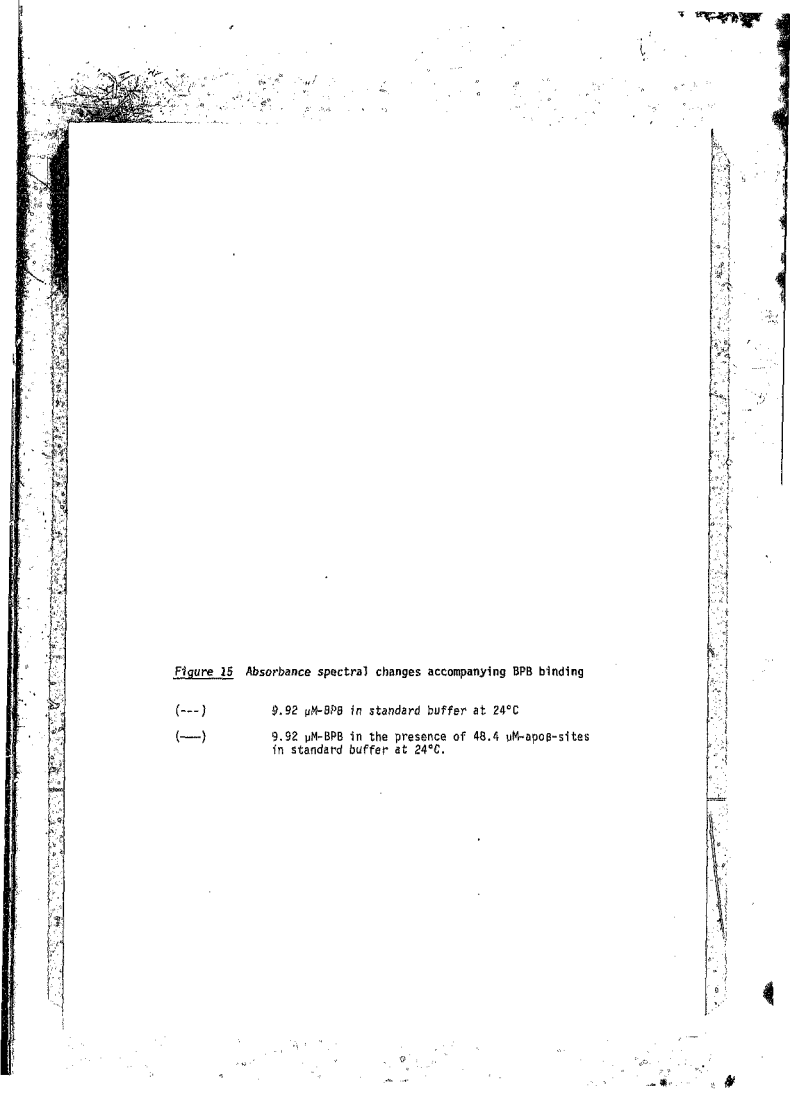

Figure 15 *Absorbance spectral changes accompanying BPB binding*

(---) *9.92 μM-BPB in standard buffer at 24°C*

(——) 9.92 μM-BPB in the presence of 48.4 μM-apoB-sites in standard buffer at 24°C.

FIGURE 15

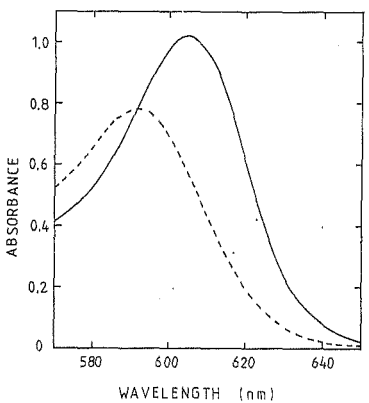

Figure 16 Fluorescence enhancement as ANS binds to protein

The fluorescence of 20 μM-ANS in standard buffer at 24°C was measured as the protein concentration increased. Excitation wavelength was 400 nm and the emission wavelength was 475 nm.

Horizontal lines on the right hand side represent the maximum fluorescence intensities for 20 μM-ANS bound to the proteins. Curves have been drawn with the parameters listed in Table 5.

(...) α-subunit

(---) apoβ$_2$-subunit

(——) $\alpha_2$apoL_2-complex.

FIGURE 16

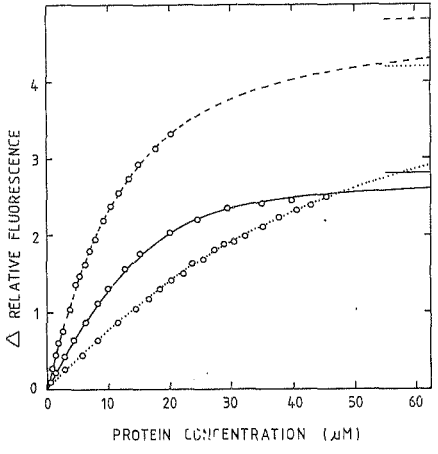
Δ RELATIVE FLUORESCENCE
0
1
2
3
4
0
10
20
30
40
50
60
PROTEIN CONCENTRATION (μM)

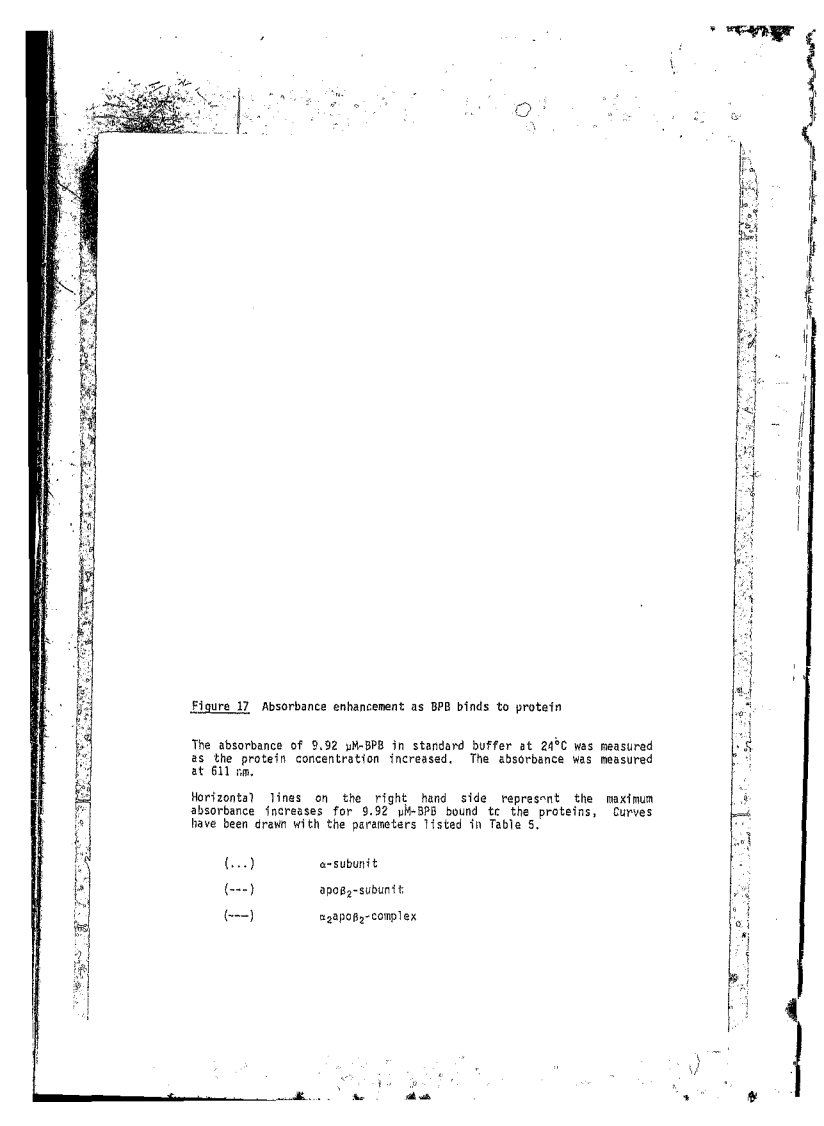

Figure 17 Absorbance enhancement as BPB binds to protein

The absorbance of 9.92 μM-BPB in standard buffer at 24°C was measured as the protein concentration increased. The absorbance was measured at 611 nm.

Horizontal lines on the right hand side represent the maximum absorbance increases for 9.92 μM-BPB bound to the proteins. Curves have been drawn with the parameters listed in Table 5.

(...) α-subunit

(---) apoβ$_2$-subunit

(---) α$_2$apoβ$_2$-complex

FIGURE 17

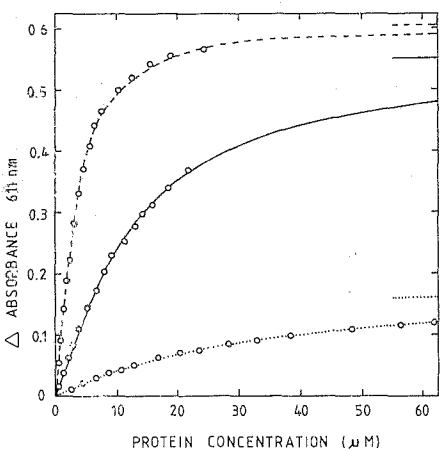
0.6
0.5
0.4
0.3
0.2
0.1
0
△ ABSORBANCE 611 nm
0
10
20
30
40
50
60
PROTEIN CONCENTRATION (μM)

TABLE 5 Binding Parameters for ANS and BPB binding to α-subunit, apo8_2-subunit and $\alpha_2$apo8_2-complex

n. The maximum number of moles of ligand bound per mole of protein

FI_{max} The maximum fluorescence intensities and absorbance changes
A_{max} resulting from ANS and BPB binding respectively.

TABLE 5

	ANS			BPB		
Protein	n	Association constant (K) (μM^{-1})	Fl_{max}	n	Association constant (K) (μM^{-1})	A_{max}
α-subunit	0.6	0.09	425	1	0.05	0.160
apoβ$_2$-subunit	2.3	0.07	480	2.3	0.41	0.610
α$_2$apoβ$_2$-complex	1.3	0.24	280	1.1	0.12	0.550

TABLE 6 *Analysis of ligand and protein binding stoichiometries*

The values of n have been taken from Table 5

TABLE 6

Line	Protein	n	
		ANS	BPB
1.	2 moles of α-subunit	1.2	2
2.	1 mole of apoβ_2-subunit	2.3	2.3
3.	Total ligand bound to 2 moles of α-subunit *and 1 mole of apoβ_2-subunit* prior to subunit assembly	3.5	4.3
4.	1 mole of $\alpha_2$apoβ_2-complex	1.3	1.1
5.	Ligand not bound to protein after assembly *of 1 mole of $\alpha_2$apoβ_2-complex*	2.2	3.2

3.5 Kinetics of Subunit-Dye Interactions and Subunit Assembly

3.5.1 Relaxation Times for Various Binding Mechanisms

In this section equations will be derived relating relaxation times to rate constants and reactant concentrations for a number of different binding mechanisms.

Single Step Mechanism

Consider the bimolecular reaction of species A and B to give species C as shown in Equation 11 (Bernasconi, 1976).

$$A + B \underset{k_{-1}}{\overset{k_{+1}}{\rightleftharpoons}} C \qquad (11)$$

The respective equilibrium concentrations of reactants and products at any time, t, are given by [A], [B] and [C]. If the system is quickly perturbed in such a way that the existing concentrations of reactants and products are no longer equilibrium concentrations, then the system will exhibit a relaxation to a new equilibrium position. The new equilibrium concentrations of reactants and products are then given by $[\bar{A}]$, $[\bar{B}]$ and $[\bar{C}]$ with the changes in concentrations defined by the following three equations.

$$[A] = [\bar{A}] + \Delta[A]$$
$$[B] = [\bar{B}] + \Delta[B]$$
$$[C] = [\bar{C}] + \Delta[C]$$

The rate of change of the concentration of product C in Equation 11 is given by

$$\frac{d[C]}{dt} = k_{+1}[A][B] - k_{-1}[C].$$

and the substitution of the above three equations results in

$$\frac{d[\bar{C}]}{dt} + \frac{d\Delta[C]}{dt} = k_{+1}[\bar{A}][\bar{B}] + k_{+1}([\bar{A}]\Delta[B] + [\bar{B}]\Delta[A]) + k_{+1}\,\Delta[A]\Delta[B] - k_{-1}[\bar{C}] - k_{-1}\Delta[C].$$

At the new equilibrium position

$$\frac{d[\bar{C}]}{dt} = 0 = k_{+1}[\bar{A}][\bar{B}] - k_{-1}[\bar{C}]$$

and substituting the preceding equation results in Equation 12.

$$\frac{d\Delta[C]}{dt} = k_{+1}([\bar{A}]\Delta[B] + [\bar{B}]\Delta[A]) + k_{+1}\,\Delta[A]\Delta[B] - k_{-1}\Delta[C] \qquad (12)$$

Relaxation kinetics requires the perturbations of concentrations to be small compared with total concentrations of species in order to linearize equations such as Equation 12. This implies that $\Delta[A]$, $\Delta[B] \ll [\bar{A}],[\bar{B}]$ and the $k_{+1}\,\Delta[A]\Delta[B]$ term can then be neglected in Equation 12.

For the stoichiometry of and for mass conservation in Equation 11

$$\Delta[A] = \Delta[B] \text{ and } \Delta[A] + \Delta[C] = 0.$$

Substitution of these equations into Equation 12 gives

$$\frac{d\Delta[C]}{dt} = -[k_{+1}([\bar{A}] + [\bar{B}]) + k_{-1}]\,\Delta[C]$$

and the integration of this differential equation gives Equation 13.

$$\Delta[C] = \Delta[C^\circ] \cdot \exp\left(-\left(k_{+1}\left([\bar{A}] + [\bar{B}]\right) + k_{-1}\right)t\right)$$
$$= \Delta[C^\circ] \exp(-t/\tau). \qquad (13)$$

The relaxation time (τ) in Equation 13 is defined as the time taken for the concentration of species C to decay to 1/e of the concentration of zero time ($[C^\circ]$) and is related to the equilibrium concentrations and rate constants as shown in Equation 14.

$$\tau^{-1} = k_{+1}\left([\bar{A}] + [\bar{B}]\right) + k_{-1} \qquad (14)$$

Experiments where reactants A and B are mixed to initiate reaction, cannot generally be analysed by relaxation kinetics because the changes in concentrations $\Delta[A]$ and $\Delta[B]$ are not small in comparison to $[\bar{A}]$ and $[\bar{B}]$. Therefore the $k_{+1}\Delta[A]\Delta[B]$ term cannot be neglected and Equation 12 cannot be linearized.

However, mixing experiments under pseudo-first order conditions requires that one of the reactants is in vast excess over the second reactant. Under these conditions $[A] >> [B] = \Delta[A]$, $\Delta[B]$ and the $k_{+1}\Delta[A]\Delta[B]$ term becomes small in comparison to the other terms of Equation 12. Neglecting this term from Equation 12 and integrating the resultant equation gives Equation 15.

$$\Delta[C] = \Delta[C^\circ] \exp(-[k_{+1}([\bar{A}]+[\bar{B}]) + k_{-1}]t) = \Delta[C^\circ]\exp(-k't) \quad (15)$$

The observed pseudo first order rate constant (k') is related to the equilibrium concentrations and rate constants as shown in Equation 16

$$k' = k_{+1}[A_o] + k_{-1} \tag{16}$$

Forward and reverse rate constants are obtained from the slopes and intercepts of linear plots of τ^{-1} or k' versus $[A_o]$ where $[A_o]$ is the original concentration of species A.

Multiple Binding Sites

If Mechanism 11 represents a binding reaction of species A and B, then Mechanism 17 represents the binding reaction with C replaced with species AB.

$$A + B \underset{k_{-1}}{\overset{k_{+1}}{\rightleftharpoons}} AB \tag{17}$$

If species B has N intrinsically identical binding sites for species A, the sequential binding of A to B is represented by Equation 18.

$$A + A_{(n-1)}B \longrightarrow A_nB \tag{18}$$

with dissociation constants given by

$$K_n = \frac{[\bar{A}]\ [A_{(n-1)}\bar{B}]}{[A_n\bar{B}]} \quad \text{where } n = 1,2,\ldots,N$$

The sequential dissociation constants in Equation 18 are related to the *intrinsic dissociation constant* (K) for the binding of A to each site on species B by the statistical factor in Equation 19.

$$K_n = \frac{n}{(N+1)-n} \times K \qquad (19)$$

where n = 1,2,...,N

For N binding sites on B, there are N possible reciprocal relaxation times relating to N binding steps. One of the N reciprocal relaxation times is given by Equation 20 which differs from Equation 14 in that the concentration of B is replaced by the concentration of unoccupied binding sites on B. The other reciprocal relaxation times are derived below.

$$k' = \tau^{-1} = k_{+1}([\bar{A}] + X[\bar{B}]) + k_{-1} \qquad (20)$$

where $X[\bar{B}] = \sum_{n=1}^{N} n\,[\overline{A_{(N-n)}B}]$

The intrinsic forward and reverse rate constants, related to the binding of A to binding sites on B, are obtained from the slopes and intercepts respectively of a linear plot of k' versus $([\bar{A}] + X[\bar{B}])$.

Two Step Mechanisms

Consider the bimolecular reaction of species A and B to give C which undergoes an unimolecular reaction to produce D as shown in Mechanism 21 (Bernasconi, 1976).

$$A + B \underset{k_{-1}}{\overset{k_{+1}}{\rightleftharpoons}} C \underset{k_{-2}}{\overset{k_{+2}}{\rightleftharpoons}} D \qquad (21)$$

The two possible reciprocal relaxation times for Mechanism 21 are coupled through species C which is common to both reactions.

The linearized rate equations for species C and D are given below.

$$\frac{d\Delta[C]}{dt} = k_{+1}([\bar{A}]+[\bar{B}])\,\Delta[A] + k_{-2}\Delta[D] - k_{+2}\Delta[C] - k_{-1}\Delta[C]$$

$$\frac{d\Delta[D]}{dt} = k_{+2}\Delta[C] - k_{-2}\,\Delta[D].$$

These two equations are combined with the conservation of mass requirement, $\Delta[A] + \Delta[D] + \Delta[C] = 0$, to give

$$\frac{-d\Delta[C]}{dt} = (k_{+1}([\bar{A}]+[\bar{B}]) + k_{+2} + k_{-1})\Delta[C] + (k_{+1}([\bar{A}]+[\bar{B}])-k_{-2})\Delta[D]$$

$$\frac{-d\Delta[D]}{dt} = -k_{+2}\Delta[C] + k_{-2}\,\Delta[D]$$

The two equations above may be solved simultaneously (Bernasconi, 1976) to give Solutions 22 and 23.

$$\tau_1^{-1} + \tau_2^{-1} = k_{+1}([\bar{A}]+[\bar{B}]) + k_{-1}+k_{+2}+k_{-2} \qquad (22)$$

$$\tau_1^{-1}\,\tau_2^{-1} = k_{+1}\,(k_{+2}+k_{-2})([\bar{A}]+[\bar{B}]) + k_{-1}k_{-2} \qquad (23)$$

If the bimolecular reaction of A and B is sufficiently faster than the unimolecular reaction of C to D, then the reciprocal relaxation time of the independent faster step is given by Equation 14.

The second reciprocal relaxation time is given by

$$\frac{\tau_1^{-1}\,\tau_2^{-1}}{\tau_1^{-1}} = \frac{k_{+1}\,(k_{+2}+k_{-2})([\bar{A}]+[\bar{B}]) + k_{-1}k_{-2}}{k_{+1}([\bar{A}]+[\bar{B}]) + k_{-1}}$$

which simplifies to Equation 24.

$$\tau_2^{-1} = \frac{k_{+2}([\bar{A}]+[\bar{B}])}{K_{-1}+([\bar{A}]+[\bar{B}])} + k_{-2} \qquad (24)$$

where $K_{-1} = k_{-1}/k_{+1}$

The hyperbolic plot of τ_2^{-1} versus $([\bar{A}]+[\bar{B}])$ may provide values for K_1, k_{+2} and k_{-2} if reciprocal relaxation times can be obtained over a sufficiently wide range of $[\bar{A}]$ and $[\bar{B}]$ concentrations:

$\tau_2^{-1} \simeq k_{-2}$ when $[\bar{A}]+[\bar{B}] \ll K_{-1}$

$\tau_2^{-1} \simeq k_{+2}+k_{-2}$ when $[\bar{A}]+[\bar{B}] \gg K_{-1}$

and K_{-1} is obtained from the slope of the graph of

$(\tau_2^{-1} - k_{-2})^{-1}$ versus $([\bar{A}]+[\bar{B}])^{-1}$.

The overall association constant for Mechanism 21 is given by

$$K = \frac{[\bar{C}] + [\bar{D}]}{[\bar{A}] \times [\bar{B}]}$$

and the two partial equilibrium constants are given by

$$K_1 = \frac{[\bar{C}]}{[\bar{A}]\times[\bar{B}]} \quad \text{and} \quad K_2 = k_{+2}/k_{-2} = \frac{[\bar{D}]}{[\bar{C}]}.$$

Combination of these three equations yields

$$K = \frac{[\bar{C}]}{[\bar{A}]\times[\bar{B}]} \; (1 + k_{+2}/k_{-2})$$

which simplifies to give Equation 25.

$$K = K_1 \left(\frac{k_{+2} + k_{-2}}{k_{-2}}\right) = K_1 (1 + K_2) \qquad (25)$$

A second example of two step mechanisms which will be considered here is that of two sequential bimolecular reactions as shown in Mechanism 26.

$$\begin{aligned} A + B &\underset{k_{-1}}{\overset{k_{+1}}{\rightleftharpoons}} C \\ C + D &\underset{k_{-2}}{\overset{k_{+2}}{\rightleftharpoons}} E \end{aligned} \qquad (26)$$

The linearized rate equations for species C and E are given below

$$\frac{d\Delta[C]}{dt} = k_{+1}([\bar{A}]+[\bar{B}])\Delta[A] + k_{-2}\Delta[E] - k_{-1}\Delta[C] - k_{+2}([\bar{C}]+[\bar{D}])\Delta[C]$$

$$\frac{d\Delta[E]}{dt} = k_{+2}([\bar{C}]+[\bar{D}])\Delta[C] - k_{-2}\Delta[E]$$

For conservation of mass $\Delta[A] + \Delta[C] + \Delta[E] = 0$, and the following two differential equations are obtained.

$$-\frac{d\Delta[C]}{dt} = [k_{+1}([\bar{A}]+[\bar{B}]) + k_{-1} + k_{+2}([\bar{C}]+[\bar{D}])]\Delta[C] + [k_{+1}([\bar{A}]+[\bar{B}]) - k_{-2}]\Delta[E]$$

$$-\frac{d\Delta[E]}{dt} = -k_{+2}([\bar{C}]+[\bar{D}])\Delta[C] + k_{-2}\Delta[E]$$

Solving these simultaneous equations gives solutions 27 and 28.

$$\tau_1^{-1} + \tau_2^{-1} = k_{+1}([\bar{A}]+[\bar{B}]) + k_{+2}([\bar{C}]+[\bar{D}]) + k_{-1} + k_{-2} \quad (27)$$

$$\tau_1^{-1}\tau_2^{-1} = k_{+1}k_{+2}([\bar{A}]+[\bar{B}])([\bar{C}]+[\bar{D}]) + k_{+1}k_{-2}([\bar{A}]+[\bar{B}]) + k_{-1}k_{-2} \quad (28)$$

A special case of Mechanism 26 is the binding of two monomers to identical sites on a dimer as shown in Mechanism 29.

$$A + B \underset{k_{-1}}{\overset{k_{+1}}{\rightleftharpoons}} AB + A \underset{k_{-2}}{\overset{k_{+2}}{\rightleftharpoons}} A_2B \quad (29)$$

Species C, D and E of Mechanism 26 have been replaced with AB, A and A_2B respectively. Equations 27 and 28 for Mechanism 26 are therefore modified to give the following two equations.

$$\tau_1^{-1} + \tau_2^{-1} = k_{+1}([\bar{A}]+[\bar{B}]) + k_{+2}([\overline{AB}]+[\bar{A}]) + k_{-1} + k_{-2}$$

$$\tau_1^{-1}\tau_2^{-1} = k_{+1}k_{+2}([\bar{A}]+[\bar{B}])([\overline{AB}]+[\bar{A}]) + k_{+1}k_{-2}([\bar{A}]+[\bar{B}]) + k_{-1}k_{-2}$$

When *the initial concentration of A is in vast excess over* the initial concentration of B ($[A_o] >> [B_o]$), the two equations above simplify to Equations 30 and 31

$$k_1' + k_2' = (k_{+1} + k_{+2})[A_o] + k_{-1} + k_{-2} \quad (30)$$

$$k_1'k_2' = k_{+1}k_{+2}[A_o]^2 + k_{+1}k_{-2}[A_o] + k_{-1}k_{-2} \quad (31)$$

3.5.2 Kinetics of Protein/Dye Interactions

The ANS and BPB dyes bind to each of the α-subunit, apoβ_2-subunit and $\alpha_2$apoβ_2-complex with differing affinities and stoichiometries. (See Table 6 for a summary of the dye binding stoichiometries).

During subunit assembly, the free dye concentrations will alter as will the ratios of dye bound to each of the three proteins involved. This redistribution of the dyes must occur at a faster rate than the subunit assembly reactions in order to utilize the dye absorbance or fluorescence changes to monitor the extent of subunit assembly. A second requirement for the use of *ANS and BPB as probes for the* subunit assembly is that the dyes must not inhibit the subunit assembly to any significant degree.

Kinetic studies of the binding of ANS and BPB by the α-subunit, apoβ_2-subunit and $\alpha_2$apoβ_2-complex were performed in order to ensure that the protein-dye interactions do not occur in the same time period *as the subunit assembly reactions. The results of these studies are* presented below. Inhibition of subunit assembly by ANS was also investigated and the results are given in Section 3.5.2.3.

3.5.2.1 Kinetics of BPB Interactions with Tryptophan Synthase and its Subunits

The binding of the BPB ligand to the α-subunit, apoβ$_2$-subunit and the α$_2$apoβ$_2$-complex was studied in the pressure-jump apparatus.

All three proteins exhibited an exponential increase in absorbance which was complete within 15 seconds following a pressure release of 10 to 20 MPa. Figure 18 presents a typical relaxation curve for the apoβ$_2$-subunit. Pressure-jump experiments with only BPB in standard buffer resulted in a small amplitude absorbance decrease which was complete within 5 ms. The initial decrease in absorbance observed in Figure 18 was also observed with α-subunit and α$_2$apoβ$_2$-complex and is therefore independent of the binding of BPB to the proteins.

Figure 19 shows the linear increase of reciprocal relaxation times with protein concentrations in the presence of 5 μM-BPB. This concentration dependence is consistent with a binding mechanism such as that given in Equation 32.

$$P + n\ BPB \rightleftharpoons P(BPB)_n \qquad (32)$$

where P represents the α-subunit, apoβ$_2$-subunit or the α$_2$apoβ$_2$-complex. and n represents the number of moles of BPB bound per mole of protein.

The reciprocal relaxation time concentration dependence is given by Equation 20 (see Section 3.5.1 for the derivation of Equation 20).

$$\tau^{-1} = k_{+1}([\bar{BPB}] + X[\bar{P}]) + k_{-1} \quad (20)$$

where $X[\bar{P}] = \sum_{n=1}^{N} n[\overline{P(BPB)_{(N-n)}}]$

The data points in Figure 19 have been fitted to Equation 20 by an iterative procedure of fitting a least squares line through the points and calculating the appropriate dissociation constants. The free protein site and free BPB concentrations were calculated from the total concentrations and the calculated dissociation constants. The parameters obtained from these experiments are given in Table 7.

The association constants obtained from kinetic experiments (K_{+1}) are in agreement with those obtained from equilibrium measurements except for the apoβ_2-subunit (see Table 7). This disagreement implies that a more complex mechanism than that given in Equation 32 governs the binding of BPB to the apoβ_2-subunit. For the purposes of this investigation the mechanism for apoβ_2-subunit binding BPB was not required. The important conclusion is that the forward and reverse rates are much faster than the rates of subunit assembly (see Section 3.5.3.1).

The free BPB may then be considered to be in equilibrium with the protein bound BPB during the course of subunit assembly.

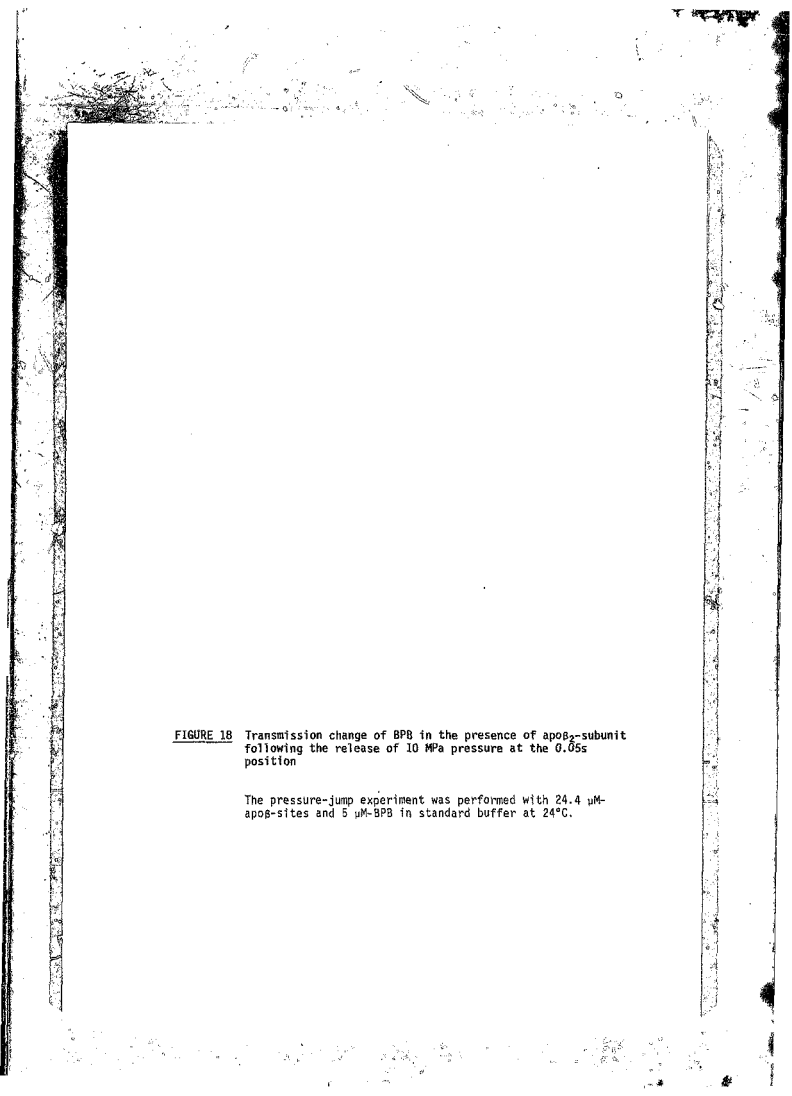

FIGURE 18 Transmission change of BPB in the presence of apoβ_2-subunit following the release of 10 MPa pressure at the 0.05s position

The pressure-jump experiment was performed with 24.4 μM-apoβ-sites and 5 μM-BPB in standard buffer at 24°C.

FIGURE 18

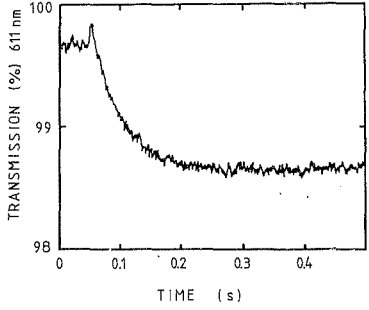

Figure 19 Concentration dependence of the reciprocal relaxation times for the interaction of BPB with the α-subunit, apoβ_2-subunit and $\alpha_2$apoβ_2-complex

The data was obtained from pressure-jump experiments in which the concentrations of the respective proteins were varied in standard buffer containing 5 μM-BPB.

Solid lines were drawn as described in the text.

A: α-subunit

B: apoβ_2-subunit

C: $\alpha_2$apoβ_2-complex.

FIGURE 19

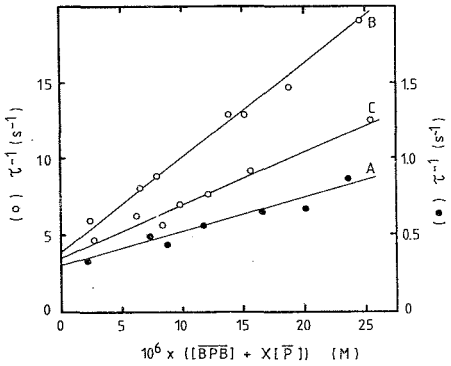

FIGURE 19

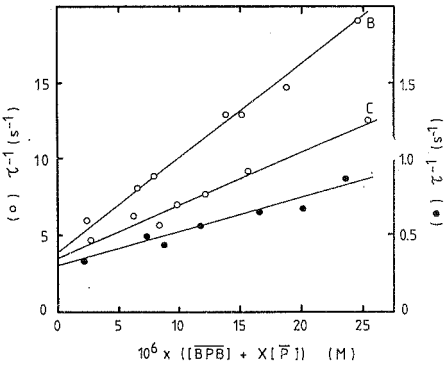
B
C
(o) τ^{-1} (s^{-1})
(•) τ^{-1} (s^{-1})
0
5
10
15
20
25
1.5
1.0
0.5
10^6 x ([$\overline{BPB}$] + X[$\overline{P}$]) (M)

TABLE 7 Kinetic parameters and association constants for the binding of BPB to the α-subunit, apoβ_2-subunit and α_2^Sapoβ_2-complex of tryptophan synthase

(a) $K_{+1} = k_{+1}/k_{-1}$ = slope/intercept

(b) The association constants from Table 5 are included for comparison.

TABLE 7

Protein	10^{-6} x slope($M^{-1}s^{-1}$)	Intercept (s^{-1})	10^{-6} x slope/intercept(M^{-1})	10^{-6} x K_{+1}(M^{-1})[a]	10^{-6} x $K(M^{-1})$[b]
α	0.022	0.30	0.073	0.073	0.05
$\alpha_2 apoB_2$	0.35	3.4	0.10	0.10	0.12
$apoB_2$	0.62	3.9	0.16		0.41

3.5.2.2 The Kinetics of ANS Interactions with Tryptophan Synthase and its Subunits

The kinetics of ANS binding to the α-subunit, apoβ_2-subunit and $\alpha_2$apoβ_2-complex was studied in the stopped-flow apparatus. No reactions were observed when 100 μM-ANS was mixed with α-subunit or with the $\alpha_2$apoβ_2-complex. This implies that the binding of ANS to these proteins is complete within the dead time of the intrument.

Mixing experiments with the apoβ_2-subunit showed a rapid increase in fluorescence followed by a slower increase as shown in Figure 20. No further fluorescence changes were observed up to a period of 5 minutes.

The important conclusion here is that no reactions take place in the same time period as that of subunit assembly (see Section 3.5.3.1).

3.5.2.3 Effect of ANS Concentration on the Kinetics of Subunit Assembly

High ANS concentrations were found to inhibit the subunit assembly whereas low ANS concentrations did not provide large enough fluorescence signals for monitoring subunit assembly. For these reasons the effect of ANS concentration on the kinetics of subunit assembly was studied to find the most suitable ANS concentration for monitoring subunit assembly and with minimal inhibition.

The RITC dye requires an excitation wavelength of 567 nm which is beyond the excitation spectrum of ANS (see Fig 14 in Section 3.4.3.2).

Therefore if ANS is present it does not interfere with the fluorescence signal derived from the RITC dye. Subunit assembly in the presence of low ANS concentrations could therefore be monitored by mixing RITC labelled α-*subunit with excess* β_2-*subunit*.

A linear relationship between the observed rate constant, k_1', and $[ANS_o]$ was achieved by plotting the data on a logarithmic scale as shown in Figure 20A. A straight line has been fitted to the data of Figure 20A and is described by Equation 33.

$$\log_e (60xk_1') = -(3.1x10^{-3})[ANS_o] + 7x10^{-2} \qquad (33)$$

At ANS concentrations below 50 μM, the decrease of the observed rate constant was within 14% of the value without ANS. The reaction amplitudes at this ANS concentration were sufficiently large and therefore all experiments in the presence of ANS were performed with 50 μM-ANS.

Figure 20 Fluorescence change following the mixing of ANS and apoβ_2-subunit in a stopped-flow instrument

The final concentration of ANS was 50 μM and that of the apoβ-protomer was 4 μM. The experiment was performed in standard buffer at room temperature with an excitation wavelength of 400 nm. The emission was monitored through a GG435 filter.

FIGURE 20

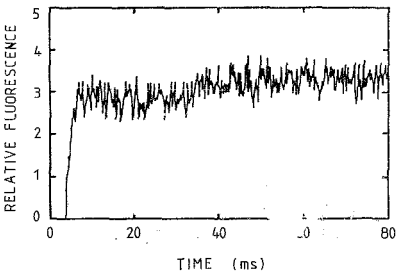

FIGURE 20

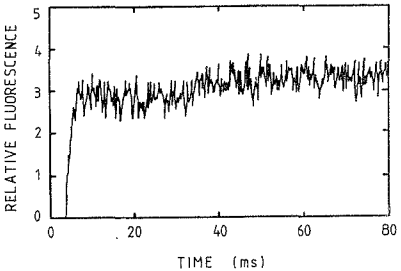

Figure 20A **Effect of ANS concentration on the observed rate constant for the assembly of tryptophan synthase subunits.**

The experiments were performed by mixing RITC labelled α-subunit with excess β_2-subunit in the presence of various ANS concentrations in standard buffer at room temperature. Final concentrations were 0.6 μM-α-subunit and 6 μM-β_1-sites. The excitation wavelength was 567 nm and the emission was observed through an OG 590 filter. The equation of the line fitted to the data is given by Equation 37.

FIGURE 20A

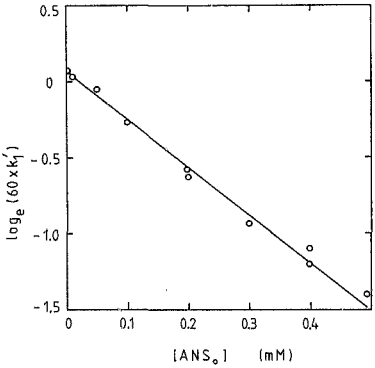

3.5.3 Kinetics of Subunit Assembly

The kinetics of subunit assembly was investigated in the stopped-flow apparatus with the ANS and RITC fluorescence probes. In the presence of ANS, the reaction amplitudes obtained with $[\alpha_o] > [\beta_{2o}]$ were larger than with $[\beta_{2o}] > [\alpha_o]$. In contrast the α-subunit bound RITC probe provided larger reaction amplitudes with $[\beta_{2o}] > [\alpha_o]$ than with $[\alpha_o] > [\beta_{2o}]$. Because of these phenomena, subunit assembly was first investigated in the presence of ANS with $[\alpha_o] > [\beta_{2o}]$.

3.5.3.1 Subunit Assembly in the Presence of ANS and with $[\alpha_o] >> [\beta_{2o}]$

Figures 21 and 22 present typical time courses for the fluorescence change after mixing apoβ$_2$-subunit with excess α-subunit. The deviation of fluorescence in Figure 22 from its final equilibrium value can be fitted to a single exponential given by : $\Delta F_t = \Delta F_3^\circ \exp(-k_3't)$. However the curve shown in Figure 21 requires the fitting of the sum of two exponentials given by : $\Delta F_t = \Delta F_1^\circ \exp(-k_1't) + \Delta F_2^\circ \exp(-k_2't)$.

As shown in Figure 23A, k_1' increases linearly with increasing α-subunit concentration thereby indicating a binding reaction. In Figure 23B, k_2' approaches a plateau value of 3.25×10^{-2} s^{-1} and indicates an isomerisation step subsequent to a binding step. In Figure 23C, the k_3' value of 1.1×10^{-3} s^{-1} appears independent of α-subunit concentration over the range of concentrations used in these experiments. This concentration independence is consistent with an isomerisation step.

The data of Figure 23A is consistent with Mechanism 18 with the concentration dependence of k_1' given by Equation 20 (for convenience these equations are rewritten below).

$$A + A_{(n-1)} \longrightarrow A_nB \quad (n = 1,2,\ldots,N) \tag{18}$$

$$k_1' = k_{+1}([\bar{A}] + X[\bar{B}]) + k_{-1}$$

$$\text{where } X[\bar{B}] = \sum_{n=1}^{N} n\,[\overline{A_{(N-n)}B}] \tag{20}$$

Under pseudo first order conditions of $[\alpha_0] >> [\beta_{20}]$, Equations 18 and 20 can be modified to give Equations 18A and 20A.

$$\alpha + \alpha_{(n-1)}\beta_2 \longrightarrow \alpha_n\beta_2 \quad (n = 1,2) \tag{18A}$$

$$k_1' = k_{+1}[\alpha_0] + k_{-1} \tag{20A}$$

A straight line fit to the data of Figure 23A provides the rate constants given in Table 8.

The data in Figure 23B is consistent with Mechanism 21, with the concentration dependence of k_2' given by Equation 24.

$$A + B \underset{k_{-1}}{\overset{k_{+1}}{\rightleftharpoons}} C \underset{k_{-2}}{\overset{k_{+2}}{\rightleftharpoons}} D \tag{21}$$

$$k_2' = \frac{k_{+2}([\bar{A}] + [\bar{B}])}{K_{-1} + ([\bar{A}] + [\bar{B}])} + k_{-2} \tag{24}$$

where $K_{-1} = k_{-1}/k_{+1}$

Under pseudo first order conditions of $[\alpha_0] >> [\beta_{20}]$ Equations 21 and 24 may be modified to give Equations 21A and 24A.

$$A + A_{(n-1)}B \rightleftharpoons A_nB \quad (n = 1,2,\ldots,N) \tag{18}$$

$$k_1' = k_{+1}\,([\bar{A}] + X[\bar{B}]) + k_{-1}$$

$$\text{where } X[\bar{B}] = \sum_{n=1}^{N} n\,[\overline{A_{(N-n)}B}] \tag{20}$$

Under pseudo first order conditions of $[\alpha_0] >> [\beta_{20}]$, Equations 18 and 20 can be modified to give Equations 18A and 20A.

$$\alpha + \alpha_{(n-1)}\beta_2 \rightleftharpoons \alpha_n\beta_2 \quad (n = 1,2) \tag{18A}$$

$$k_1' = k_{+1}[\alpha_0] + k_{-1} \tag{20A}$$

A straight line fit to the data of Figure 23A provides the rate constants given in Table 8.

The data in Figure 23B is consistent with Mechanism 21, with the concentration dependence of k_2' given by Equation 24.

$$A + B \underset{k_{-1}}{\overset{k_{+1}}{\rightleftharpoons}} C \underset{k_{-2}}{\overset{k_{+2}}{\rightleftharpoons}} D \tag{21}$$

$$k_2' = \frac{k_{+2}\,([\bar{A}] + [\bar{B}])}{K_{-1} + ([\bar{A}] + [\bar{B}])} + k_{-2} \tag{24}$$

where $K_{-1} = k_{-1}/k_{+1}$

Under pseudo first order conditions of $[\alpha_0] >> [\beta_{20}]$ Equations 21 and 24 may be modified to give Equations 21A and 24A.

$$\alpha + \alpha_{(n-1)}\beta_2 \rightleftharpoons \alpha_n\beta_2 \underset{k_{-2}}{\overset{k_{+2}}{\rightleftharpoons}} \alpha_n\beta_2^* \qquad (21A)$$

where (n = 1,2)

and $\alpha_n\beta_2^*$ is an isomer of $\alpha_n\beta_2$

$$k_2' = \frac{k_{+2}\,[\alpha_0]}{K_{-1}+[\alpha_0]} + k_{-2} \qquad (24A)$$

The relevant kinetic parameters are obtained from Figure 23B by the method of Wilkinson (1961) and are given in Table 8.

Mechanism 21A requires that the K_{-1} value obtained from Figure 23B must equal the k_{-1}/k_{+1} value calculated for *Figure 23A (see Table 8)*. Since K_{-1} is nearly an order of maghitude larger than k_{-1}/k_{+1}, the assembly mechanism must be more complex than that given in Equations 18A and 21A.

Mechanisms 18A and 21A assume that the α-subunit binding to the $\alpha_1\beta_2$-complex is equivalent to the α-subunit binding to the β_2-subunit. It is possible that the discrepancy between K_{-1} and k_{-1}/k_{+1} in Table 8 may be due to differences in the binding of the first and second α-subunits to the β_2-subunit. For this reason the binding of only one α-subunit to the β_2-subunit was investigated under the conditions of $[\beta_{2_0}] > [\alpha_0]$. These conditions required the use of the α-subunit bound RITC probe and is described in the following section.

Figure 21 Fluorescence change after mixing apoβ_2-subunit with excess α-subunit in the stopped-flow apparatus.

Final concentrations were 20.0 μM-α-subunit, 1.10 μM-apoβ-sites and 50 μM-ANS in standard buffer. The experiment was performed at room temperature with an excitation wavelength of 400 nm. The emission was monitored through a GG435 filter.

All protein solutions for stopped-flow experiments contained 50 μM-ANS in order to prevent re-equilibration of ANS with the proteins after mixing.

FIGURE 21

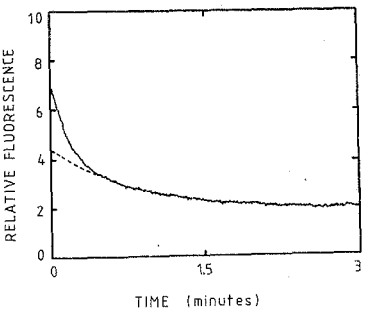

Figure 22 Fluorescence change after 5 minutes from the time of mixing apoβ_2-subunit with excess α-subunit in the stopped-flow apparatus

The experimental conditions were those given in Figure 21.

FIGURE 22

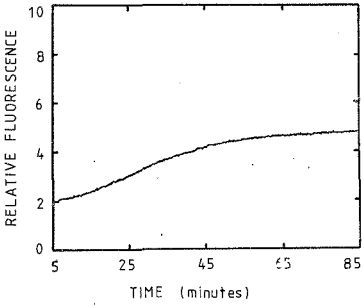

Figure 23 *Concentration dependence* of the observed rate constants on the α-subunit concentration

The final concentration of ANS was 50 μM and the $[\alpha_o]/[\beta_{1o}]$ ratio was between 18 and 20. The experiments were performed in standard buffer at room temperature with an excitation wavelength of 400 nm. The emission was monitored through a GG435 filter.

A: Dependence of k_1' on $[\alpha_o]$

B: Dependence of k_2' on $[\alpha_o]$

C: Dependence of k_3' on $[\alpha_o]$

FIGURE 23A

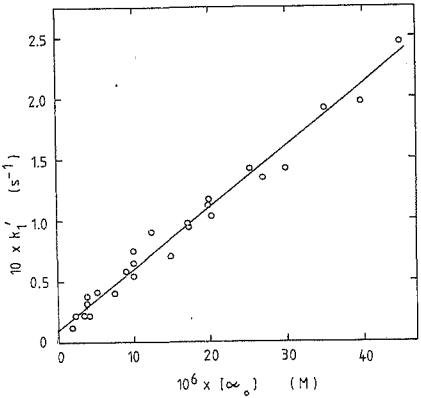

FIGURE 23B

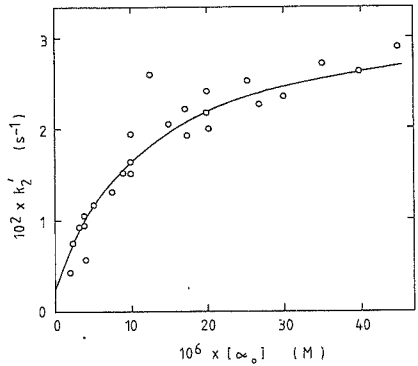

FIGURE 23C

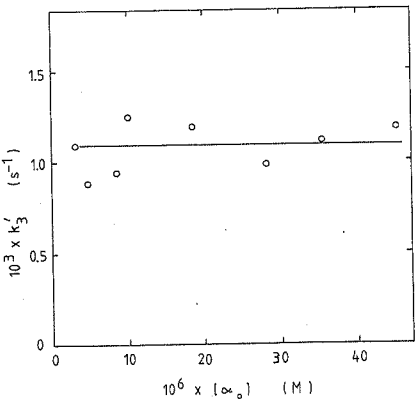

TABLE 8 Kinetic parameters for the assembly of tryptophan synthase subunits in the presence of AMS when $[\alpha_0] >> [\beta_{20}]$

The parameters are obtained from the curves in Figure 23 for Mechanisms 18A and 21A.

TABLE 8

Figures	Kinetic Parameter	Values
Figure 23A	k_{+1}	$5.1 \times 10^{8} M^{-1} s^{-1}$
	k_{-1}	$7 \times 10^{-3} s^{-1}$
	k_{-1}/k_{+1}	1.4×10^{-6} M
Figure 23B	k_{+2}	$3.0 \times 10^{-2} s^{-1}$
	k_{-2}	$2.5 \times 10^{-3} s^{-1}$
	K_{-1}	12×10^{-6} M
Figure 23C	k_3'	$1.1 \times 10^{-3} s^{-1}$

3.5.3.2 Subunit Assembly Monitored with the RITC Probe and with $[\beta_1\text{-sites}_0] >> [\alpha_0]$

Figures 24 and 25 present typical time courses for the fluorescence change after mixing RITC labelled α-subunit with excess β_2-subunit. The deviation of fluorescence in Figure 25 from its final equilibrium value can be fitted to a single exponential given by : $\Delta F_t = \Delta F_\infty^2 \exp(-k_4' t)$. The curve shown in Figure 24 can also be fitted to a single exponential given by : $\Delta F_t = \Delta F_1^\circ \exp(-k_1' t)$.

The linear increase of k_1' with the concentration of apoβ_1-sites$_0$ in Figure 26A indicates a binding reaction consistent with Mechanism 11 with the concentration dependence of k_1' given by Equation 16. In Figure 26B, the k_4' value of 8.5×10^{-4} s^{-1} appears independent of $[\beta_1\text{-sites}_0]$ over the range of concentrations used in these experiments. This behaviour indicates an isomerisation reaction consistent with Mechanism 21 with the concentration dependence of k_4' given by Equation 24.

Under pseudo first order conditions of $[\beta_1\text{-sites}_0] >> [\alpha_0]$, Equations 11, 16, 21 and 24 can be rewritten to give Equations 11B, 16B, 21B, and 24B.

$$\alpha + \beta_1 \underset{k_{-1}}{\overset{k_{+1}}{\rightleftharpoons}} \alpha\beta_1 \qquad (11B)$$

$$k_1' = k_{+1} [\beta_1\text{-sites}_0] + k_{-1} \qquad (16B)$$

$$\alpha+\beta_1 \underset{k_{-1}}{\overset{k_{+1}}{\rightleftharpoons}} \alpha\beta_1 \underset{k_{-4}}{\overset{k_{+4}}{\rightleftharpoons}} \alpha\beta_1^* \qquad (21B)$$

where $\alpha\beta_1^*$ is an isomer of $\alpha\beta_1$

$$k_4' = \frac{k_{+4}\,[\beta_1\text{-sites}_0]}{K_{-1}+[\beta_1\text{-sites}_0]} + k_{-4} \qquad (24B)$$

A straight line fit to the data of Figure 26A provides the kinetic parameters given in Table 9. The k_4' values in Figure 26B could not be obtained at β_1-site concentrations below 3 μM because the reaction amplitudes were too low. For this reason the K_{-1} value could not be obtained from Figure 26B but is indeed less than 3 μM.

There are two important differences between the experiments performed with the ANS probe and the RITC probe. Firstly, the k_{+1} value of 2.4×10^3 M^{-1} s^{-1} for the RITC probe (see Table 9) and the k_{+1} value of 5.1×10^3 M^{-1} s^{-1} for the ANS probe (see Table 8) differ by a factor of two. Secondly, the sum of two exponential curves obtained with the ANS probe (see Figure 21) was not observed with the RITC probe. These two differeces could be ascribed either to the different fluorescence probes used in the experiments or the different subunit concentratrations with which the experiments were performed.

In order to eliminate the possibility that these two differences are due to the fluorescence probes, the subunit assembly was investigated in the presence of ANS under the conditions of $[\beta_1\text{-sites}_0] >> [\alpha_0]$.

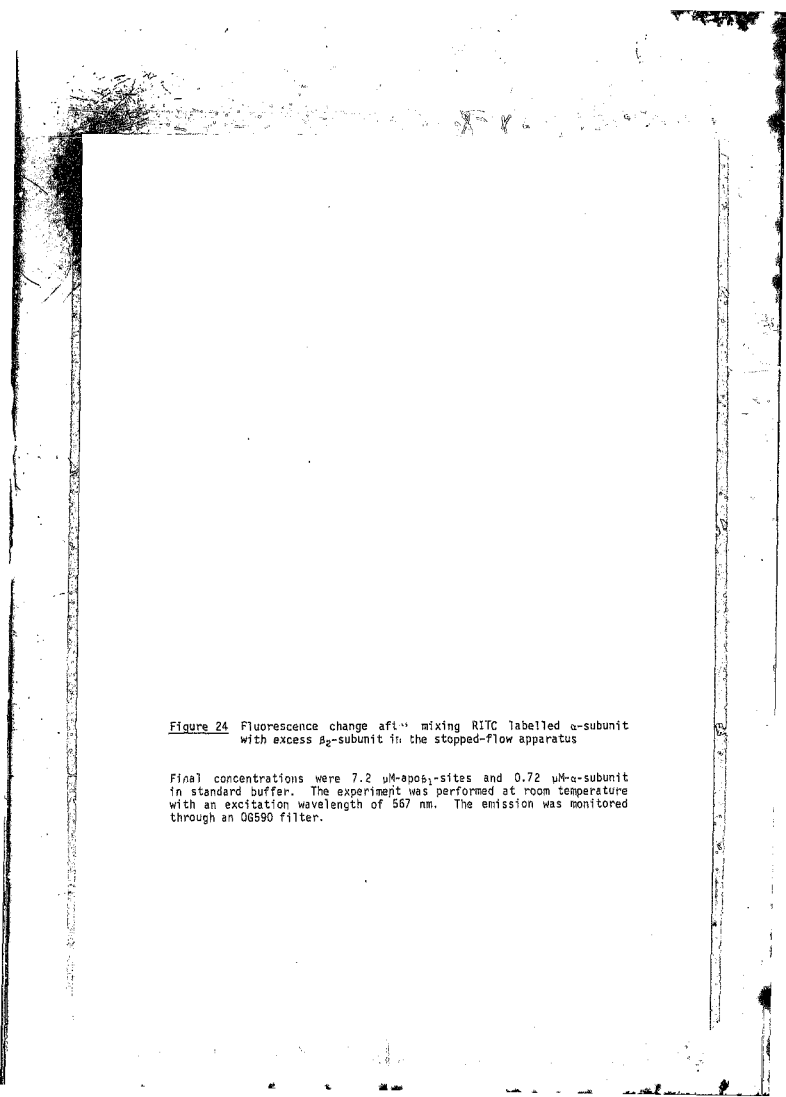

Figure 24 Fluorescence change after mixing RITC labelled α-subunit with excess β_2-subunit in the stopped-flow apparatus

Final concentrations were 7.2 μM-apoβ_1-sites and 0.72 μM-α-subunit in standard buffer. The experiment was performed at room temperature with an excitation wavelength of 567 nm. The emission was monitored through an OG590 filter.

FIGURE 24

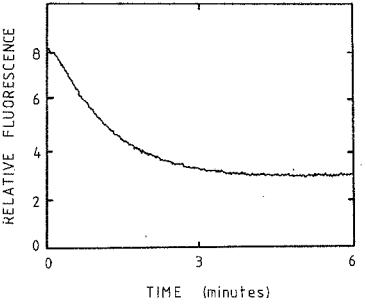

Figure 25 Fluorescence change after mixing RITC labelled α-subunit with excess β_2-subunit in the stopped-flow apparatus

The experimental conditions were those given in Figure 24.

FIGURE 25

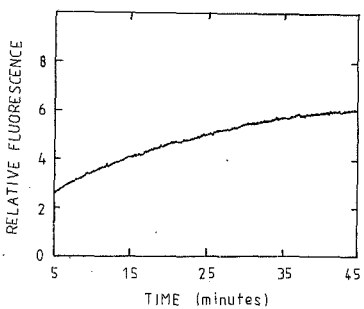

Figure 26 Concentration dependence of the observed rate constants on the apoβ_1-sites concentration

The $[\beta_1\text{-sites}_0]/[\alpha_0]$ ratio of 10 was used for all experiments. The reactions were performed in standard buffer at room temperature with an excitation wavelength of 567 nm. The emission was monitored through an OG 590 filter.

A. Dependence of k_1' on $[\beta_1\text{-sites}_0]$

B. Dependence of k_4' on $[\beta_1\text{-sites}_0]$.

FIGURE 26A

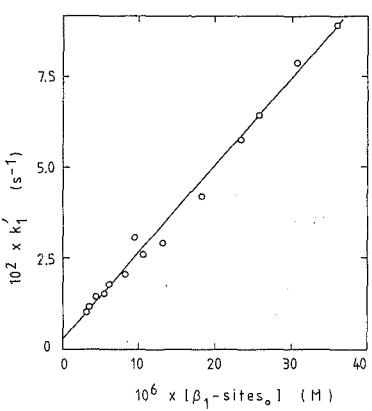
7.5
5.0
2.5
0
0
10
20
30
40
$10^2 \times k_1'$ (s^{-1})
$10^6 \times [\beta_1\text{-sites}_o]$ (M)

FIGURE 26B

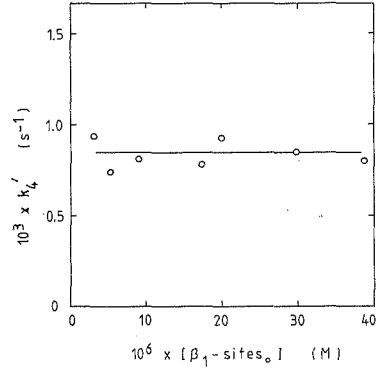
1.5
1.0
0.5
0
0
10
20
30
40
$10^3 \times k_4'$ (s^{-1})
$10^6 \times [\beta_1\text{-sites}_o]$ (M)

TABLE 9 Kinetic parameters for the assembly of tryptophan synthase subunits under the conditions of $[\beta_1\text{-sites}_0] >> [\alpha_0]$

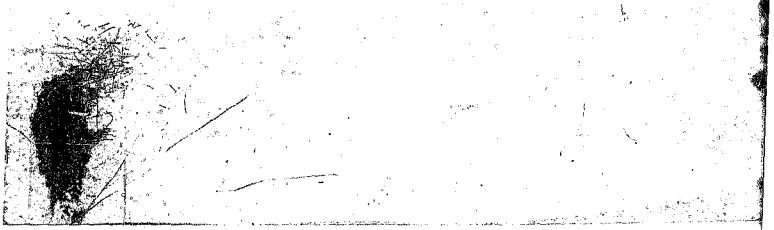

TABLE 9

Figure	Probe	k_{+1} $(M^{-1}s^{-1})$	k_{-1} (s^{-1})	k_{-1}/k_{+1} (M)	k_h' (s^{-1})	K_{-1} (M)
26A	RITC	2.4×10^3	2.9×10^{-3}	1.2×10^{-6}		
28	ANS	1.8×10^3	2.4×10^{-3}	1.3×10^{-6}		
26B	RITC				0.85×10^{-3}	$<3 \times 10^{-6}$

3.5.3.3 Subunit Assembly in the Presence of ANS and with $[\beta_1\text{-sites}_0] >> [\alpha_0]$

As mentioned earlier, the reaction amplitudes are small when $[\beta_1\text{-sites}_0] > [\alpha_0]$ in the presence of ANS. However, the amplitudes were large enough to obtain reliable data for the fast reaction corresponding to k_1' in Figure 24.

Figure 27 presents a typical time course for the change of fluorescence after mixing α-subunit with excess β_2-subunit in the presence of ANS. The curve has been fitted with an exponential given by $\Delta F_t = \Delta F^\circ \exp(-k_1't)$. Figure 28 shows the linear increase of k_1' with $[\beta_1\text{-sites}_0]$ which is consistent with Mechanism 11B and Equation 168. A straight line fit to the data of Figure 28 provides the kinetic parameters given in Table 9.

The kinetic parameters for the subunit assembly with the ANS and the RITC probes are similar. This similarity together with the observation that a reaction corresponding to k_2' (see Figure 21) is absent, implies that the subunit assembly can be monitored with either the ANS or RITC probe. The discrepancy between the subunit assembly mechanisms in the presence of ANS with $[\alpha_0] >> [\beta_{20}]$ and with the RITC probe with $[\beta_1\text{-sites}_0] >> [\alpha_0]$ can be attributed to the different subunit concentrations used in the experiments.

In the case of $[\beta_1\text{-sites}_0] >> [\alpha_0]$, only a single α-subunit binds to each β_2-subunit whereas with $[\alpha_0] >> [\beta_{20}]$, the $\alpha_2\beta_2$-complex is formed. It is this binding of two α-subunits to each β_2-subunit which must account for the observation of k_2' in Figure 21 and the factor of two difference in the k_{+1} values given in Tables 8 and 9.

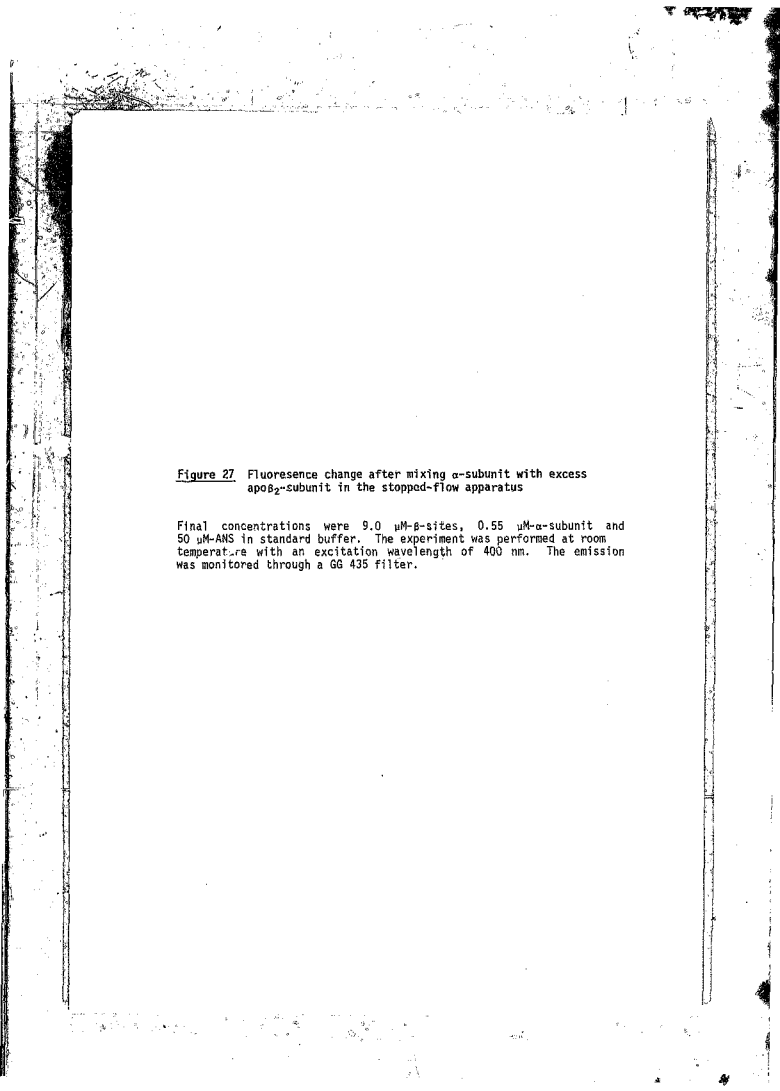

Figure 27 Fluoresence change after mixing α-subunit with excess apoβ$_2$-subunit in the stopped-flow apparatus

Final concentrations were 9.0 μM-β-sites, 0.55 μM-α-subunit and 50 μM-ANS in standard buffer. The experiment was performed at room temperature with an excitation wavelength of 400 nm. The emission was monitored through a GG 435 filter.

FIGURE 27

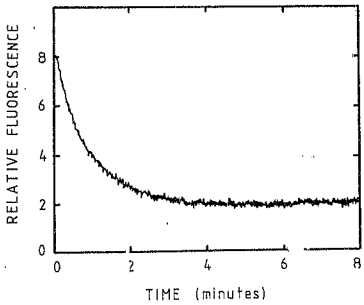

Figure 28 Concentration dependence of the observed rate constant on the apoβ_1-sites concentration

The [β_1-sites$_0$]/[α_0] ratio of 16 was used for all experiments. The reactions were performed in standard buffer at room temperature with an excitation wavelength of 400 nm. The emission was monitored through a GG 435 filter.

FIGURE 28

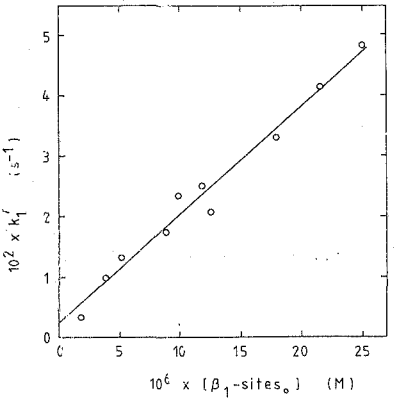
5
4
3
2
1
0
0
5
10
15
20
25
$10^2 \times k_1'$ (s^{-1})
$10^6 \times [\beta_1\text{-sites}_o]$ (M)

At this stage the data of Figures 23A and 23B must be reconsidered. The ratios of k_1'/k_2' are less than an order of magnitude and therefore the two observed rate constants should be treated as coupled. The appropriate plots would be $(k_1' + k_2')$ and $(k_1'k_2')$plotted against $[\alpha_0]$. This was not originally done because separate plots for k_1' and k_2', such as in *Figures 23A and 23B*, would give reasonable estimates for the respective rate constants. This is because the k_1'/k_2' ratios are close to an order of magnitude at high α-subunit concentrations.

For the reasons given above, the data from the experiments performed in the presence of ANS, with $[\alpha_0] >> [\beta_{2_0}]$, was replotted according to the method for coupled observed rate constants.

3.5.3.4 *Treatment for Coupled Observed Rate Constants*

Plots of $(k_1'+k_2')$ and $(k_1'k_2')$ versus $[\alpha_0]$ are given in *Figure 29*. For the data to be consistent with a mechanism such as that given in Equation 21, $(k_1'k_2')$ must be linearly dependent upon $[\alpha_0]$ as described in Equation 23 (see Section 3.5.1). Inspection of Figure 29B shows that the data points are non-linear. Therefore alternative mechanisms were sought which are consistent with a non-linear dependence of $(k_1'k_2')$ on $[\alpha_0]$.

Mechanism 18 assumes that both apoβ_2-subunit sites are intrinsically identical and that no α-subunit interactions occur in the $\alpha_2\beta_2$-complex. However, if the binding of the first α-subunit were to alter the affinity of the $\alpha_1\beta_2$-complex for the second α-subunit, then the binding would be consistent with Mechanism 34.

Figure 29 Concentration dependence of the sum of observed rate constants and the product of observed rate constants on the α-subunit concentration.

The final concentratin of ANS was 50 μM and the $[\alpha_o]/[\beta_{1o}]$ ratio was between 18 and 20. The experiments were performed in standard buffer at room temperature with an excitation wavelength of 400 nm. The emission was monitored through a GG 435 filter.

A: Dependence of $k_1' + k_2'$ on $[\alpha_o]$

B: Dependence of $k_1'k_2'$ on $[\alpha_o]$

FIGURE 29A

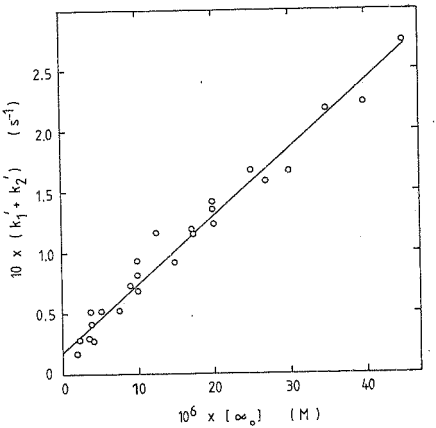

FIGURE 29B

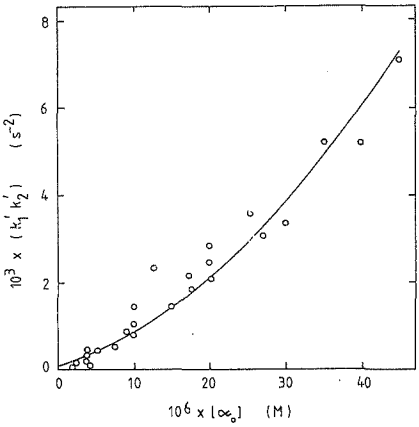

$$\alpha + \beta_2 \underset{k_{-1}}{\overset{k_{+1}}{\rightleftharpoons}} \alpha\beta_2^{\circ} \qquad (34)$$

$$\alpha + \alpha\beta_2^{\circ} \underset{k_{-2}}{\overset{k_{+2}}{\rightleftharpoons}} \alpha_2\beta_2$$

In Mechanism 34 the affinities for α-subunit of the β_2-subunit and the $\alpha\beta_2^{\circ}$-complex are different due to α-subunit interactions in the $\alpha_2\beta_2$-complex.

Mechanism 34 is described by the general mechanism of Equation 29 with A replaced with α-subunit, B replaced with β_2-subunit, AB replaced with $\alpha\beta_2^{\circ}$-complex and A_2B replaced with $\alpha_2\beta_2$-complex. Equations 35 and 36 are obtained from Equations 30 and 31 by altering the parameters to suit the conditions applicable to Mechanism 34.

$$k_1' + k_2' = (k_{+1} + k_{+2})\,[\alpha_o] + k_{-1} + k_{-2} \qquad (35)$$

$$k_j'k_2' = k_{+1}k_{+2}\,[\alpha_o]^2 + k_{+1}k_{-2}\,[\alpha_o] + k_{-1}k_{-2} \qquad (36)$$

The data in Figures 29A and 29B has been analysed by the fitting of a least squares line and a least squares parabola respectively. The least squares parameters are given in Table 10 while the rate constants for Mechanism 34 are given in Table 11.

3.5.4 Summary of Tryptophan Synthase Subunit Assembly.

Non-cooperative or possibly negatively cooperative subunit assembly in phosphate buffer occurs by Mechanism 38. The averaged rate constants for Mechanism 38 are given in Table 12.

TABLE 10 Least squares parameters for the assembly of tryptophan synthase subunits by Mechanism 34

The experiments were performed in the presence of ANS and with $[\alpha_0] >> [\beta_{20}]$.

(a) Equation of line is $k_1' + k_2' = m[\alpha_0] + c$

(b) Equation of parabola is $k_1' k_2' = a[\alpha_0]^2 + b[\alpha_0] + c$

TABLE 10

Figure	m	a	b	c
29A[a]	$5.61 \times 10^{3} M^{-1} s^{-1}$			$1.9 \times 10^{-2} s^{-1}$
29B[b]		$2.5 \times 10^{6} M^{-2} s^{-2}$	$49 M^{-1} s^{-2}$	$7.7 \times 10^{-5} s^{-2}$

TABLE 10

Figure	m	a	b	c
29A[a]	$5.61 \times 10^{3} M^{-1} s^{-1}$			$1.9 \times 10^{-2} s^{-1}$
29B[b]		$2.5 \times 10^{6} M^{-2} s^{-2}$	$49 M^{-1} s^{-2}$	$7.7 \times 10^{-5} s^{-2}$

TABLE 11 Kinetic constants for the assembly of tryptophan synthase subunits by Mechanism 34

The experiments were performed in the presence of ANS with $[\alpha_0] >> [\beta_{2_0}]$.

(a) $K_{-1} \approx k_{-1}/k_{+1}$

(b) $K_{-2} \approx k_{-2}/k_{+2}$

TABLE 11

Constant	Value
k_{+1}	$4.8 \times 10^{3}\ M^{-1}\ s^{-1}$
k_{-1}	$8.7 \times 10^{-3}\ s^{-1}$
K_{-1}[a]	$1.8 \times 10^{-6}\ M$
k_{+2}	$0.6 \times 10^{3}\ M^{-1}\ s^{-1}$
k_{-2}	$10.0 \times 10^{-3}\ s^{-1}$
K_{-2}[b]	$17 \times 10^{-6}\ M$

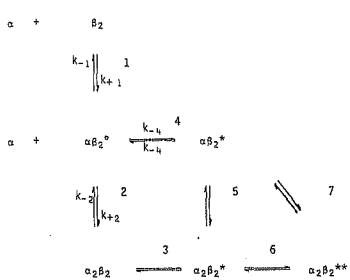

where $\alpha\beta_2$* and $\alpha_2\beta_2$* are isomers of $\alpha\beta_2$° and $\alpha_2\beta_2$ respectively and $\alpha_2\beta_2$** is a second isomer of $\alpha_2\beta_2$.

Assembly of subunits to form the intermediate $\alpha_1\beta_2$-complex can be monitored when $[\beta_1\text{-sites}_0] >> [\alpha_0]$. Data for the concentration dependence of k_1' was obtained with both the RITC and ANS probes whereas k_4' was only observed with the RITC probe. The concentration independence of k_4' suggests that an isomerisation of the $\alpha\beta_2$°-complex occurs forming the $\alpha\beta_2$*-complex (see Reaction (4) in Mechanism 3A).

Subunit assembly under the conditions of $[\alpha_0] >> [\beta_{20}]$ results in the $\alpha_2\beta_2$-complex with two coupled observed rate constants, k_1' and k_2'. The observed concentration independence of k_3' suggests that an isomerisation of the $\alpha_2\beta_2$-complex takes place.

The β_2-subunit may be represented as being composed of two separate domains, $\beta\beta$, one of which binds the first α-subunit to give the $\alpha\beta\beta$-

complex. Isomerisation of this complex can occur in either of two ways. Either the whole $\alpha\beta\beta$-complex isomerises to give a $\alpha\overset{\ddagger}{\beta}\overset{\ddagger}{\beta}$-complex or only one domain isomerises to give a $\alpha\overset{*}{\beta}\beta$-complex. In the former case, binding of a second α-subunit gives the $\alpha\overset{\ddagger}{\beta}\overset{\ddagger}{\beta}\alpha$-complex via Reaction (7) of Mechanism 38. In the latter case, binding of a second α-subunit would give the intermediate $\alpha\overset{*}{\beta}\beta\alpha$-complex which undergoes a further isomerisation to give the final $\alpha\overset{\ddagger}{\beta}\overset{\ddagger}{\beta}\alpha$-complex. This occurs via Reactions (5) and (6) of Mechanism 38.

Reactions (4), (3) and (6) of Mechanism 38 all represent similar isomerisation reactions and their observed rate constants are not expected to be vastly different. This accounts for the observation that the k_4' value for Reaction (4) is 77% of the k_3' value (see Tables 8 and 9). However, with the available data, it cannot be decided whether k_3' refers to only Reaction (3) or to an average of the rate constants for Reactions (3) and (6) of Mechanism 38. Therefore, the existence of intermediate $\alpha_2\beta_2{}^*$-complex is uncertain.

If the α-subunit concentration is in vast excess over the apoβ_2-subunit concentration then the equilibrium ratios of $\alpha_2\beta_2$ to its isomers may be estimated.

The mechanisms for the binding of two α-subunits to identical sites on the apoβ_2-subunit are given below.

$$\alpha + \beta_2 \rightleftharpoons \alpha\beta_2 \qquad \text{(a)}$$

$$\alpha + \alpha\beta_2 \rightleftharpoons \alpha_2\beta_2 \qquad \text{(b)}$$

$$2\alpha + \beta_2 \rightleftharpoons \alpha_2\beta_2 \qquad \text{(d)}$$

The intrinsic site dissociation constants (K_a and K_b) are related to the overall dissociation constant (K_d) by the following equations.

$$K_d = \frac{[\alpha]^2 \times [\beta_2]}{[\alpha_2\beta_2]} = \frac{[\alpha] \times [\beta_2]}{[\alpha\beta_2]} \times \frac{[\alpha] \times [\alpha\beta_2]}{[\alpha_2\beta_2]}$$

$$K_d = K_a \times K_b$$

$$K_d = (0.93)^2 \text{ (see Table 4)}$$

However for Mechanism 38 assembly is given by the following condensed mechanism.

$$2\alpha + \beta_2 \rightleftharpoons \alpha_2\beta_2 \rightleftharpoons \alpha_2\beta_2^{\ddagger}$$

where $\alpha_2\beta_2^{\ddagger}$ represents isomers of $\alpha_2\beta_2$.

The overall dissociation constant is given by

$$K_d = \frac{[\text{unbound subunits}]}{[\text{bound forms}]}$$

and the equilibrium constant for bound forms is given by

$$K_I \quad \frac{(\alpha_2\beta_2)}{[\alpha_2\beta_2^{\ddagger}]}$$

Therefore

$$K_d = \frac{[\alpha]^2 \times [\beta_2]}{[\alpha_2\beta_2] + [\alpha_2\beta_2^{\ddagger}]}$$

and substitution of the preceding equation, $K_d = (0.93)^2$ and K_{-1}, K_{-2} values from Table 12 gives

$$(0.93)^2 = \frac{1.6 \times 17}{(1 + \frac{1}{K_I})}$$

$$K_I = 0.03$$

At equilibrium the predominant form of bound complex is therefore $\alpha_2\beta_2^4$.

TABLE 12 Rate constants for the assembly of tryptophan synthase subunits by Mechanism 38

The rate constants have been taken from Tables 8, 9 and 11 and have been averaged where possible.

(a) $K_{-1} = k_{-1}/k_{+1}$

(b) $K_{-2} = k_{-2}/k_{+2}$

TABLE 12

Constant	Value
k_{+1}	3.0 x 10^3 M^{-1} s^{-1}
k_{-1}	4.7 x 10^{-3} s^{-1}
K_{-1}[a]	1.6 x 10^{-6} M
k_{+2}	0.6 x 10^3 M^{-1} s^{-1}
k_{-2}	10.0 x 10^{-3} s^{-1}
K_{-2}[b]	17 x 10^{-6} M
k_3'	1.1 x 10^{-3} s^{-1}
k_4'	0.85 x 10^{-3} s^{-1}

4. DISCUSSION

4.1 Purification of Tryptophan Synthase Subunits

The study of the assembly kinetics of α-subunit with β_2-subunit, requires α-subunit and β_2-subunit which was, at first, prepared from *E. coli* strains Trp B8 and TrpA2/F'A2 respectively. These purified subunits possessed specific activities between 50% and 60% of the maximum activities reported by Bartholmes *et al.* (1976). Higher specific activities could not be obtained using the spectrophotometric assay method of Higgins *et al.* (1979) nor could higher activities be obtained by reduction of oxidised subunit thiol groups, necessary for activity, as described by Hogberg-Raibaud & Goldberg (1977).

Single peaks were obtained by electrophoresis of the subunits on SDS polyacrylamide gels (see Figure 2), indicating that the low subunit specific activities are not due to impure subunit preparations but, rather, low enzyme activities. The possibility of the *E. coli* mutant strains Trp B8 and TrpA2/F'A2 producing low activity subunits existed and therefore an alternative mutant strain, Trp R-ΔLD102/F'ΔLD102, was obtained. Purification of subunits from this strain was also advantageous since both subunits could be obtained from the same strain minimising the quantity of bacterial growth required to produce a specific quantity of purified subunits.

Tschopp & Kirschner (1980) used this strain to produce both α-subunit and β_2-subunit. Precipitation of the β_2-subunit at pH 4.5 yielded free α-subunit and heat denaturation of the α-subunit yielded free β_2-subunit. In this study a non-destructive method of separating the subunits was used in order to conserve purified protein and to limit exposure of the proteins to the extreme conditions of pH 4.5 and temperatures of over 60°C. Instead removal of PLP and dissociation of the $\alpha_2$apoβ_2-complex was performed following the method of Miles & Moriguchi (1977) which involved filtration on a Sephadex G-100 column.

After these attempts at purifying both α-subunits and β_2-subunits from a single different strain of bacteria, the specific activities were similar to those obtained previously from *E. coli* Trp B8 and TrpA2/F'A2. It therefore remains uncertain why the subunits prepared here have lowered specific activities. Before proceeding with the kinetic experiments these low activity subunits were compared to those prepared with high activity with respect to PLP and α-subunit binding as described in Sections 3.2 and 3.3. The results of these binding experiments indicated that the low specific activity subunits displayed similar binding properties to high specific activity subunits. In view of these similarities kinetic experiments were then performed without further attempts at purifying high specific activity subunits.

4.2 Stability of the apo-Tryptophan Synthase Complex

Miles & Moriguchi (1977) achieved dissociation of the $\alpha_2 apo\beta_2$-complex by filtration on a Sephadex G-100 column. However Bartholmes & Teuscher (1979) could not detect any significant dissociation of the $\alpha_2 apo\beta_2$-complex on a Sephadex G-100 column. These, seemingly contradictory results may be resolved by considering the buffers used in the two experiments. Miles & Moriguchi (1977) used bicine whereas Bartholmes & Teuscher (1979) used pyrophosphate buffer implying that the stability of the apo-complex may depend upon the solvent buffer.

Binding experiments of α-subunits and $apo\beta_2$-subunits in various solvents are described in Section 3.3 and confirm the greater stability of the $\alpha_2 apo\beta_2$-complex in pyrophosphate as compared to that in bicine buffer. However the $\alpha_2 apo\beta_2$-complex has even greater stability in phosphate buffer and the binding process is transformed to a non-cooperative and possibly even a negatively cooperative mechanism from a cooperative mechanism in pyrophosphate buffer. This alteration of mechanism influences the overall assembly process of tryptophan synthase as discussed in the following section.

4.3 Assembly of the Tryptophan Synthase Complex

The mechanism for the overall assembly of tryptophan synthase is given below.

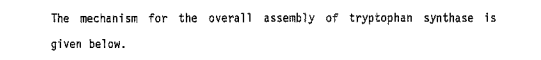

Bartholmes *et al.* (1976) have shown that reaction (1) to (2) is cooperative and reaction (3) to (4) is non-cooperative. Furthermore they have predicted that either reaction (1) to (3) is cooperative (and reaction (2) to (4) is then non-cooperative) or reaction (2) to (4) is negatively cooperative (and reaction (1) to (3) is then non-cooperative).

The results of Bartholmes & Teuscher (1979) have verified the first of the two alternatives viz. that reaction (1) to (3) is cooperative. However the results given in Section 3.3 show that reaction (1) to (3) is cooperative only in pyrophosphate but non-cooperative in phosphate with reaction (2) to (4) then negatively cooperative. The possibility that reaction (1) to (3) is negatively cooperative cannot, however, be ignored.

For the kinetic analysis of the non-cooperative binding of 2 α-subunits to a β_2-dimer, the β_2-dimer may be treated as consisting of two independent β-sites. This simplification allows for easier kinetic analysis than for the case of negative cooperativity in which the binding of the first α-subunit results in a decreased affinity for the second α-subunit.

Because of the simplified kinetic analysis it was decided that the first tryptophan synthase assembly reaction to be investigated would be the *non-cooperative assembly of* $\alpha_2 apo\beta_2$-complex *in phosphate* buffer. The difficulties of monitoring the kinetics of assembly of $\alpha_2 apo\beta_2$-complex are discussed in the next section.

4.4 Monitoring the Assembly of the Tryptophan Synthase Complex

The hundred-fold enhancement of α-subunit activity and thirty-fold enhancement of holoβ_2-subunit activity when incorporated into the tryptophan synthase complex suggests that conformational alterations of the subunits occur during assembly. It is these conformational alterations which can be observed by following the kinetics of assembly.

In the case of $\alpha_2$holoβ_2-complex the PLP cofactor serves as a means of monitoring the extent of reaction since PLP absorbs in the 400-430 nm region of the spectrum. This region is far removed from the ultraviolet region (280 nm) in which intrinsic protein absorption occurs and therefore simplifies the design of the kinetic experiments. *Increasing the ratio of* α-subunit concentration to the holoβ_2-subunit concentration does not affect the signal change observed at 420 nm and therefore a high signal to noise ratio is obtained.

In the case of the $\alpha_2$apoβ_2-complex the assembly must be followed in the region of intrinsic protein absorption (280 nm). Increasing the ratio of the α-subunit concentration to that of the apoβ_2-subunit concentration increases the background absorption of the excess α-subunit and therefore decreases the signal to noise ratio. The experiments recorded in Section 3.4.1 indicate that the absorbance changes at 280 nm arising from subunit assembly are indeed small. For this reason fluorescence and absorbance probes were investigated which would allow the subunit assembly to be monitored with high signal to noise ratios.

4.5 Probes for Monitoring Assembly of $\alpha_2 apo\beta_2$-Complex

In order to monitor the binding of α-subunits to the $apo\beta_2$-subunit, probes were required which either reflected the α-subunit to β_2-subunit interprotein distances or alterations of the local environments of the probes due to the proximity of the subunits. These requirements ensure that the probe used reflects not only the binding reactions of the subunits but also any later conformational changes of the $\alpha_2 apo\beta_2$-complex. However a probe which only reflects conformation changes of proteins would now allow faster earlier binding reactions to be monitored.

It was initially decided to attempt monitoring the α-subunit to β_2-subunit interprotein distance utilising fluorescence energy transfer measurements. Suitable fluorescence probes were found in a review by Fairclough & Cantor (1978) but the procedure involved completely coating the surface of the proteins with bound probe. This would probably interfere with the assembly of the subunits because of the high charges on the subunits resulting from the high loading of the probes. Lower loading of the subunits with the probes would not coat the surfaces uniformly and therefore not yield absolute interprotein distances but only relative distances between probe molecules. As this is sufficient for monitoring subunit assembly the FITC and RITC probes were used with limited loading of the subunits below two probes per subunit protomer.

The results given in Section 3.4.2.1 illustrate the successful labelling of tryptophan synthase subunits with FITC and RITC. However, only limited fluorescence energy transfer was observed (see Section 3.4.2.2). The observed intrinsic fluorescence changes of the RITC

probe when bound to α-subunit reflected the binding of α-subunit to the β_2-subunit and this system was used to study tryptophan synthase assembly under the conditions of $[\beta_2] >> [\alpha]$.

A second type of probe was then required in order to monitor tryptophan synthase assembly when $[\alpha] >> [\beta_2]$. Dicamelli *et al.* (1973) concluded that hydrophobic bonding plays a role in the binding of the subunits. It was therefore anticipated that a fluorescence probe, such as ANS, which binds to hydrophobic regions on membranes would also bind to the hydrophobic regions on the tryptophan synthase subunits. After assembly the excess ANS would be excluded from the resultant $\alpha_2 apo\beta_2$-complex thereby giving rise to fluorescence signal changes. In fact this was found to occur with more ANS being bound to free $apo\beta_2$-subunit than to free α-subunit. Such a distribution of ANS allowed this probe to be used when $[\alpha] >> [\beta_2]$ and complemented the experiments with RITC. Only low ANS concentrations were used because high ANS concentrations decreased subunit assembly (see Section 3.5.2.3).

In addition, an absorbance probe, BPB, was also found to monitor subunit assembly in a similar manner to the ANS fluorescence probe. The data from these experiments have not been presented since similar results are obtained with either probe.

An approach similar to that presented here could be used to investigate the binding of any proteins which only absorb in the ultraviolet region of the spectrum. The criterion is that ANS binds loosely to the hydrophobic regions of the proteins concerned and is partially excluded from the bound protein complex.

Seifert *et al.* (1984) have employed similar fluorescence titrations to those in Section 3.4.3.2 to estimate the number of ANS binding sites per apoβ_2-dimer and the corresponding dissociation constant. Their results show that n ≥ 10 ANS molecules are bound per apoβ_2-dimer with a dissociation constant ≥ 0.6 mM. The results obtained here indicate the presence of 2 to 3 high affinity ANS binding sites per apoβ_2-dimer with a dissociation constant of 0.014 mM (see Table 5). One possible reason for the lower number of binding sites and lower dissociation constants obtained here is the presence of phosphate buffer. Seifert *et al.* (1984) employed 0.1 M triethanolamine·HCl buffer thereby implying that the phosphate anion affects the ligand binding properties of the apoβ_2-subunit. Indeed, Table 4 shows that the affinity of the apoβ_2-subunit for binding α-subunit is 100 fold greater in phosphate than in bicine buffer.

4.6 Assembly of the $\alpha_2apo\beta_2$-complex

4.6.1 Mechanism of Assembly

In the presence of PLP, assembly of the $\alpha_2holo\beta_2$-complex is negatively cooperative and the weaker binding of the second α-subunit is possibly due to steric hinderance (Lane *et al.*, 1984). However, the large distances measured between α-subunits in the $\alpha_2holo\beta_2$-complex indicate that steric hinderance is unlikely to account for the presence of negative cooperativity (Ibel *et al.*, 1985).

Mechanism 38 for assembly of the $\alpha_2apo\beta_2$-complex is similar to the mechanism given for the $\alpha_2holo\beta_2$-complex (Lane *et al.*, 1984) with respect to the weaker binding of the second α-subunit and the subsequent isomerisation reactions. Comparison of these two mechanisms shows that the "on" and "off" rate constants for the binding of the first α-subunit, via reaction (1) of Mechanism 38, are both approximately 10^3 fold lower than for the $holo\beta_2$-subunit. This decrease in rate is reasonable since the transformation of $apo\beta_2$-subunit to $holo\beta_2$-subunit occurs with positive cooperativity and involves gross conformational changes (Bartholmes *et al.*, 1980).

The effect of this conformational change is to raise the activation energy for the transition state involved in the binding of the α-subunit to $apo\beta_2$-subunit. It is possible that the higher activation energy may result from the α-subunit binding sites being more accessible on the $holo\beta_2$-subunit than on the $apo\beta_2$-subunit.

Since the apoβ_2-subunit and the holoβ_2-subunit exist in different conformational states the conclusions drawn from the measured distances between α-subunits in the $\alpha_2$holoβ_2-complex do not necessarily apply to the $\alpha_2$apoβ_2-complex. Furthermore the distances between α-subunits in the final equilibrium state of $\alpha_2$holoβ_2-complex bear little significance to the distances in the $\alpha_2\beta_2$-intermediate prior to isomerisation reactions (3) and (6) of Mechanism 38. Therefore it is possible that for Mechanism 38, $K_{-2}$is greater than K_{-1} due to steric hinderance in the $\alpha_2\beta_2$-intermediate. For this reason the '0'-superscript for the $\alpha_2\beta_2^0$-intermediate has been included in Mechanism 38 and implies that while the conformation of the $\beta_2$subunit is unaltered, the value of K_{-2} is larger than K_{-1}.

The equilibrium dialysis experiments in Section 3.3 are not conclusive regarding the presence or absence of negative cooperativity. The dissociation constant (K_d = 0.93 μM) has been determined for the assembly of the $\alpha_2$apoβ_2-complex, in phosphate buffer, for a non-cooperative mechanism. As discussed above the first and second α-subunits have different kinetic dissociation constants ($K_{-2} > K_{-1}$) which might arise from steric hinderance. This suggests that the binding mechanism might be negatively cooperative. The value of $K_d \approx 0.93$ μM then probably represents an approximate value for the binding of the second α-subunit. In order to estimate the thermodynamic dissociation constant for the first α-subunit, binding data would have to be obtained at very low α-subunit concentrations. This could not be achieved by equilibrium dialysis as described in Section 3.3 since the α-subunit concentrations were measured by enzyme activity assays and the concentrations are already close to the assay's limit of detection. Therefore a definite conclusion regarding the presence of negative cooperativity cannot be made with the available equilibrium data.

The kinetic data in Table 12 implies the presence of two alternatives. Either the assembly mechanism exhibits negative cooperativity or the mechanism is non-cooperative with steric hinderance occurring only in the $\alpha_2\beta_2$-intermediate. Therefore the overall conformations of the apoβ_2-subunit and the final equilibrium $\alpha_2$apoβ_2-complex are similar with steric hinderance altering the binding affinity of the $\alpha_1\beta_2$*-intermediate for the second α-subunit. Under these conditions non-cooperativity could occur even though steric hinderance may be present.

4.6.2 Conformational Changes of the β_2-Subunit

Tschopp & Kirschner (1980b) have compared the cooperative binding of pyridoxine-phosphate (an analogue of PLP) to the apoβ_2-subunit with the non-cooperative binding to the $\alpha_2$apoβ_2-complex. They concluded that the α-subunit stabilises a conformation of the β_2-subunit which resembles the 'R' conformation of the apoβ_2-subunit. This implies that the binding of the α-subunit to the apoβ_2-subunit induces a conformational change of the β_2-subunit which probably corresponds to the proposed isomerisation reartions in Mechanism 38.

The effect of the holoβ_2-subunit conformational change, induced by α-subunit binding, has been indirectly observed by comparison of the reactivities of the holoβ_2-subunit and the $\alpha_2$holoβ_2-complex towards reaction with trypsin. In the case of holoβ_2-subunit, reaction with trypsin results in nicking of the β_2-subunit (Högberg-Raibaud & Goldberg, 1977).

However, the holoβ_2-subunit remains intact when the $\alpha_2$holoβ_2-complex is reacted with trypsin (Miles & Higgins, 1978). It is not known whether this protection of the β_2-subunit, afforded by the α-subunit, occurs in the case of apoβ_2-subunit. Such experiments to compare the reactivities of the apoβ_2-subunit and the $\alpha_2$apoβ_2-complex towards reaction with trypsin would indicate whether the conformation of the apoβ_2-subunit, stabilised by α-subunit binding, resembles the conformation of the holoβ_2-subunit or the β_2-subunit in the $\alpha_2$holoβ_2-complex. These experiments would verify whether the PLP cofactor and α-subunit induce similar conformational changes in the apoβ_2-subunit.

4.7 Structure and Function of the $\alpha_2apo\beta_2$-complex

The $\alpha_2holo\beta_2$-complex catalyses the condensation of indole and L-serine to give L-tryptophan (Reaction 2 in Table 1) and the hydrolysis of indoleglycerol-phosphate to give indole and glyceraldehyde-3-phosphate (Reaction 1 in Table I).

Bartholmes *et al.* (1980) have mixed PLP with $\alpha_2apo\beta_2$-complex and observed a binding step followed by two consecutive isomerisation reactions. In addition the authors have demonstrated that full enzyme activity for the β_2-subunit partial reaction (Reaction 2 in Table I) is generated during the second isomerisation reaction.

However it is not known whether the full enzyme activity for the *α-subunit partial reaction (Reaction 1 in Table I)* is *generated* in the same isomerisation reaction as for the β_2-subunit partial reaction or in the isomerisation reactions of Mechansim 38 leading to the formation of the $\alpha_2apo\beta_2$-complex. In the former case, where the activities for both the α-subunit and β_2-subunit partial reactions increase during the same isomerisation step, this isomerisation must involve the reorientation of all four subunits of the $\alpha_2apo\beta_2$-complex. In the latter case, where the activity of the α-subunit partial reaction is maintained constant during the increase in activity of the β_2-subunit partial reaction, the isomerisation observed by Bartholmes *et al.* (1980) must involve a change located mainly within the β_2-subunit section of the $\alpha_2holo\beta_2$-complex. Differentiation of these two possibilities could be achieved by measuring the rate of increase of activity of the α-subunit partial reaction during the assembly of α-subunit with $apo\beta_2$-subunit or during the binding of PLP to the $\alpha_2apo\beta_2$-complex.

While this study has been concerned with the assembly of the $\alpha_2$apoβ_2-complex, a similar experimental approach has been used to study the assembly of the $\alpha_2$holoβ_2-complex.

Lane *et al.* (1984) have shown that binding of α-subunit to holoβ_2-subunit results in an initial αβ-complex which subsequently isomerises to a final αβ*-complex. In addition full α-subunit and β_2-subunit activities are achieved in the isomerisation process indicating synchronous changes of both α- and β-protomers.

REFERENCES

Adachi, O. & Miles, E.W. (1974) J. Biol. Chem. 249, 5430-5434.

Adachi, O. Kohn, L.D. & Miles, E.W. (1974) J. Biol. Chem. 249, 7756-7763.

Bagshaw, C.R., Eccleston, J.F., Trentham, D.R., Yates, D.W. & Goody, R.S. (1972) Cold Spring Harbour Sympos. on Quantit. Biol. 37, 127-135.

Balk, H., Frank, A., Bartholmes, P. & Jaenicke, R. (1981a) Eur. J. Biochem. 121, 105-112.

Balk, H., Merkl, I. & Bartholmes, P. (1981b) Biochemistry 20, 6391-6395.

Bartholmes, P. & Teuscher, B. (1979) Eur. J. Biochem. 95, 323-326

Bartholmes, P., Kirschner, K. & Gschwind, H.P. (1976) Biochemistry 15, 4712-4717.

Bartholmes, P., Balk, H. & Kirschner, K. (1980) Biochemistry 19, 4527-4533.

Becker, J.S. Oliver, J.M. & Berlin, R.D. (1975) Nature (London) 254, 152-154.

Bernasconi, C.F. (1976) Relaxation kinetics, Academic Press, New York, San Francisco, London.

Crawford, I.P. (1975) in Subunit Enzymes, Biochemistry and Functions (Ebner, K.E., ed.), pp 223-239, M. Dekker, New York.

Creighton, T.E. & Yanofsky, C. (1966) J. Biol. Chem. 241, 980-990.

Daniel, E. & Weber, G. (1966) Biochemistry, 6, 1893-1900.

Davis, J.S. (1981a) Biochem. J. 197, 301-308.

Davis, J.S. (1981b) Biochem. J. 197, 309-314.

Davis, J.S. & Gutfreund, H. (1976) FEBS Lett. 72, 199-207.

Dicamelli, R.F., Balbinder, E. & Lebowitz, J. (1973) Arch. Biochem. Biophys. 155, 315-324.

DiJeso, F. (1968) J. Biol. Chem. 243, 2022-2023.

Dodd, G.H. & Radda, G.K. (1969) Biochem. J. 114, 407-417.

Faeder, E.J. & Hammes, G.G. (1970) Biochemistry 9, 4043-4049.

Fairclough, R.H. & Cantor, C.R. (1978) Methods in Enzymology 48, 347-379, Academic Press, New York.

Fluri, R., Jackson, L.E., Lee, W.E. & Crawford, I.P. (1971) J. Biol. Chem. 246, 6620-6624.

Freedberg, W.B. & Hardman, J.K. (1971) J. Biol. Chem. 246, 1449-1456.

Gennis, L.S., Gennis, R.B. & Cantor, C.R. (1972) Biochemistry 11, 2517-2524.

Groha, C., Bartholmes, P. & Jaenicke, R. (1978) Eur. J. Biochem. 92, 437-441.

Hardman, J.K. & Yanofsky, C. (1966) J. Biol. Chem. 240, 725-732.

Hathaway, G.M. (1972) *J. Biol. Chem.* 247, 1440-1444.

Henning, U., Helinski, D.R., Chao, F.C. & Yanofsky, C. (1962) J. Biol. Chem. 237, 1523-1530.

Higgins, W., Fairwell, T. & Miles, E.W. (1979) Biochemistry 18, 4827-4835.

Högberg-Raibaud, A. & Goldberg, M.E. (1977) Biochemistry 16, 4014-4020.

Ibel, K., May, R.P., Kirschner, K., Lane, A.N., Szadkowski, H., Dauvergne, M.T. & Zulauf, M. (1985) Eur. J. Biochem. 151, 505-514.

Jackson, D.A. & Yanofsky, C. (1969) J. Biol. Chem. 244, 4526-4538.

Kasprzak, A.A. & Kochman, M. (1981) J. Biol. Chem. 256, 6127-6133.

Kirschner, K. & Wiskocil, R.L. (1972) FEBS 8th Meeting, Amsterdam Vol 29, 71-93.

Kirschner, K., eischet, W. & Wiskocil, R.L. (1975) in Protein-Ligand Interactions (Sund, H. & Blauer, G., eds.) pp 27-44, Walter de Gruyter & Co., Berlin.
Kirschner, K., Wiskocil, R.L., Foehn, M. & Rezeau, L. (1975) Eur. J. Biochem 60, 513-523.
Lane, A.N. & Kirschner, K. (1981) Eur. J. Biochem. 120, 379-387.
Lane, A.N. & Kirschner, K. (1983a) Eur. J. Biochem. 129, 561-570.
Lane, A.N. & Kirschner, K. (1983b) Eur. J. Biochem. 129, 571-582.
Lane, A.N. & Kirschner, K. (1983c) Eur. J. Biochem. 129, 575-684.
Lane, A.N., Paul, C.H. & Kirschner, K. (1984) EMBO J. 3, 279-287.
Lowry, O.H., Rosebrough, N.J., Farr, A.C. & Randall, R.J. (1951) J. Biol. Chem. 193, 265-275.
Matthews, C.R. & Crisanti, M.M. (1981) Biochemistry 20, 784-792.
Miles, E.W. (1970) J. Biol. Chem. 245, 6016-6025.
Miles, E.W. (1979) Adv. Enzymol. Relat. Areas Mol. Biol. 49, 127-186.
Miles, E.W. & Higgins, W. (1978) J. Biol. Chem. 253, 6266-6269.
Miles, E.W. & Moriguchi, M. (1977) J. Biol. Chem. 252, 6594-6599.
Miles, E.W., Yutani, K. & Ogasahara, K. (1982) Biochemistry 21, 2586-2592.
Seifert, T., Bartholmes, P. & Jaenicke, R. (1984) Z. Naturforsch. C. Biosci. 39C, 1008-1011.
Storvick, C.A., Benson, E.M., Edwards, M.A. & Woodring, M.J. (1964) in Meth. of Biochem. Anal. (Glick, D., ed) 12, 214-216, Interscience, New York, London, Sydney.
Stryer, L. (1965) J. Mol. Biol. 13, 482-495.
Tonomura, B., Nakatani, H., Ohnishi, M., Yamaguchi-Ito, J. & Hiromi, K. (1978) Anal. Biochem. 84, 370-383.
Tschopp, J. & Kirschner, K. (1980a) Biochemistry 19, 4514-4521.
Tschopp, J. & Kirschner, K. (1980b) Biochemistry 19, 4521-4527.
Wang, Y.L. & Taylor, D.L. (1981) Cell 27, 429-436.
Weber, K. & Osborn, M. (1969) J. Biol. Chem. 244, 4406-4412.
Weischet, W.O Kirschner, K. (1976a) Eur. J. Biochem. 64, 313-320.
Weischet, W.O Kirschner, K. (1976b) Eur. J. Biochem 65, 375-385.
Wiesinger, H., Bartholmes, P. & Hinz, H.J. (1979) Biochemistry 18, 1979-1984.
Wilhelm, P., Pilz, I., Lane, A.N. & Kirschner, K. (1982) Eur. J. Biochem. 129, 51-56.
Wilkinson, G.N. (1961) Biochem. J. 80, 324-332.
Wilson, D.A. & Crawford, I.P. (1955) J. Biol. Chem. 240, 4801-4808.
Yanofsky, C. & Crawford, I.P. (1972) in The Enzymes 3rd ed. (Boyer, P.D., ed) Vol. VII, pp 1-31, Academic Press, New York.
Yanofsky, C., Platt, T., Crawford, I.P., Nichols, B.P., Christie, G.E., Horowitz, H., van Cleemput, M. & Wu, A.M. (1981) Nucleic Acids Res. 9, 6647-6668.
Yutani, K., Ogasahara, K. & Sugino, Y. (1980) J. Mol. Biol. 144, 455-465.
Zalkin, M.M., Boulot, G. & Goldberg, M.E. (1980) Eur. J. Immunol. 10, 16-21.